ABSTRACT

WU, TONG. Cobalt Mediated Cyclotrimerization of Alkyne and Isocyanate to Form 2-Pyridones; New Linkage Chemistry for RNA Mediated Nanoparticle Growth on Gold Surface. (Under the direction of Professor Bruce E. Eaton).

Cobalt (I) mediated cyclotrimerization is a powerful synthesis methodology to construct six member carbocyclic and heterocyclic aromatic rings. A new cobalt (I) catalyst, Cp^{CF3}CoCOD, was synthesized successfully. The X-ray crystal structure analysis revealed special structure features, which could be feasible to the associative Cp ring slippage mechanism. Examination of cyclotrimerization of alkyne showed Cp^{CF3}CoCOD was a very active catalyst. Kinetic data indicated that the reaction rate shows a first order dependence on the concentration of alkyne.

Cyclotrimerization between alkyne and isocyanate has been investigated with new cobalt catalyst, Cp^{CF3}CoCOD. It was found that 2-pyridones could be formed under mild experimental conditions with excellent yield and chemospecificity. The yield and product distribution depends greatly on the substituents of alkyne and isocyanate. Cylcotrimerizing diyne and isocynante gave moderate to good yields. The yield of diyne conversion to 2-pyridones was controlled by the Thorpe – Ingold effect. An associative Cp ring slippage mechanism has been proposed for cyclotrimerization of alkyne and isocyanate.

In order to maintain RNA's folded structure to afford shape-controlled nanoparticles, it was of interest to test a linker to connect RNA to the gold surface. Two linker strategies were examined to achieve this goal. One strategy assembles linker onto gold surface firstly, and then 5'-phosphorothioate-modified RNA will introduce to couple with the

linker. The other strategy uses chemical or enzymatic methods to bind the linker with RNA molecules firstly; then, Linker and RNA molecule were introduced onto gold surface as a single molecule. The synthetic routes for both linkers were established. Gold slides were prepared according to these strategies and were examined by SEM. In both cases, well-shaped hexagonal Pd nanoparticles were observed. The second strategy provided cleaner background. SEM images also showed that particle density appeared dependence on RNA concentration.

Cobalt Mediated Cyclotrimerization of Alkyne and Isocyanate to Form 2-Pyridones; New Linkage Chemistry for RNA Mediated Nanoparticle Growth on Gold Surface

by

Tong Wu

A dissertation submitted to the Graduate Faculty of
North Carolina State University
in partial fulfillment of the
requirement for the Degree of
Doctor of Philosophy

Chemistry

Raleigh

2006

Approved By:

Bruce E. Eaton Chair of Advisory Committee	Daniel L. Feldheim
T. Brent Gunnoe	Bruce M. Novak

DEDICATION

I would like to dedicate this work to my parents, Fenghua Dai and Xueshun Wu, and my beloved wife, Kangqin Chen

Thank you for all the love, understanding, support and encouragement

Without you, I could do nothing.

BIOGRAPHY

The author, Tong Wu, was born in Nanjing, China on February 16th, 1976. His interest towards chemistry started from high school. All the demo experiments with color change and fire flame excited him to try to understand what is behind these experiments. After graduating from high school in 1994, he attended Nanjing University and chose chemistry as his major. Just like every college student, he learned a lot; not just in chemistry. He also met his wife, Kangqing Chen in college. After wonderful four years, he was honored a B. S. Degree in Chemistry in 1998. In the same year, he was accepted as a master student in Department of Chemistry, Nanjing University. He worked under the direction of Professor Yi Pan with the project to construct new organic luminescence device. In order to learn in the forefront of chemistry, he came to United States in August 2000 and attended North Carolina State University as a Ph. D. student in organic chemistry. His joined in Dr. Eaton's research group and worked area relative to cobalt mediated cyclotrimerization and RNA mediated nanoparticle growth.

ACKNOWLEDGEMENTS

First of all, I wish to send my tremendous gratitude to my advisor, Dr. Bruce Eaton, for his incredible guidance, training, and influence. He helps me to absorb knowledge from different scientific areas and teaches me to solve the problem like a chemist. His positive attitude towards unknown scientific mysteries always encourages me to overcome the frustrations in the experiments. I would also like to thank my committee members Dr. Daniel Feldheim, Dr. Brent Gunnoe, Dr. Bruce Novak and my old committee member, Dr. Binghe Wang. I will present a special thanks to Dr. Feldheim for joining my committee after Dr. Wang moved GSU.

I have many colleagues want to thank here. First, I have to thank Dr. Lina Gugliotti. She taught me every single biochemistry experiment related to my project by hand. Without her help I could not have finished the RNA project. I also need to thank Dr. Dage Liu in Feldheim, who helped me to prepare gold slides and take SEM images at Duke University.

I have to thank everyone in Eaton research group and Feldheim group, present ones and old ones, Carly Carter, Marta Cerruti, Dana Didonato, Magda Dolska, Ben Holley, Rich Latta, Jon Vaught, and Jie Zhao. Their help and care made my life and my research program interesting and easier. At the same time, I need thank the discussions and suggestions coming from my friends, Gonglu Tian, Jubo Zhang and Jun Yan.

Finally, I want to give thanks to my entire friends at North Carolina State University, in United States, and in China for their great help and support.

TABLE OF CONTENTS

CHAPTER THREE

NEW LINKAGE CHEMISTRY FOR RNA MEDIATED NANOPARTICLE GROWTH ON GOLD SURFACE

CHAPTER FOUR

GENERAL EXPERIMENTAL PROCEDURE AND ANALYTICAL DATA

LIST OF SCHEMES

CHAPTER ONE

CHAPTER TWO

LIST OF FIGURES

CHAPTER ONE

CHAPTER TWO

LIST OF TABLES

CHAPTER ONE

SYNTHESIS AND CHARACTERIZATION OF NEW COBALT (I) CATALYSTS FOR THE CYCLOTRIMERIZATION REACTION

1. History of Cobalt(I)-mediated Cyclotrimerization

Carbocyclic and heterocyclic aromatic rings are central to many biologically active, pharmaceuticals and polymer molecules. Numerous synthetic methods have been developed to form different varieties of ring structures. Among them, [2 + 2 + 2] cyclotrimerization (**Scheme 1-1**) of either alkynes, or alkynes with other unsaturated heteroatom molecule is a very ideal and atom-economic method for the construction of substituted carbocylic and heterocyclic aromatic rings.

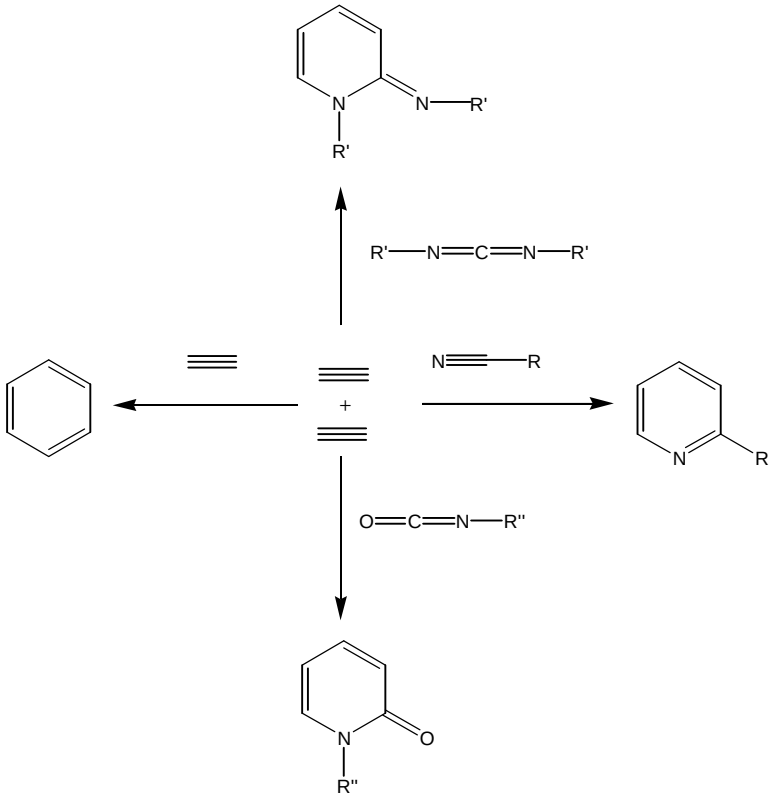

Scheme 1-1. Examples for [2 + 2 + 2] cyclotrimerization

The biggest advantage of this method is that this transformation enables the assembly of compounds with a high degree of complexity from rather simple starting materials in one step. Also, the different substituted groups on alkynes and other unsaturated heteroatom

molecules could provide the possibility of generating a diverse array of carbocylic and heterocyclic aromatic ring derivatives.

Although these [2 + 2 + 2] cyclotrimerization reactions are symmetry allowed in principle[1] and the π bonds conversion to σ bonds is a remarkable exothermic process, the pure thermal [2 + 2 + 2] cyclotrimerization examples are rare. This fact is probably due to the large entropic barriers coming from the requirement of bringing and orientating the three molecules together in the reaction. It has been estimated that the activation barrier of transforming three acetylene molecules into a benzene ring is about 60 – 80 Kcal/mol[2]. Overcoming this energy barrier requires the reaction temperature to exceed 400 °C[3]. It is possible to low the activation energy barrier of [2 + 2 + 2] cyclotrimerization by using transition metal catalysts. Metal catalysts could coordinate the reaction molecules in a stepwise process, so that the entropic barriers of each step are much lower than the origin entropic barrier.

In 1948, *Reppe et al.*[4] described the first example of alkyne cyclotrimerizaiton, which was catalyzed by low-valent nickel complex, $Ni(COD)_2$. Subsequently, transition metal catalyzed [2 + 2 + 2] cyclotrimerization became a powerful and widely used method for the synthesis of different interesting molecules with carbocylic and heterocyclic aromatic rings as the core structure. A wide array of transition metal catalysts, such as cobalt[5], nickel[6, 7], chromium[8], rhodium[9], iridium[9], titanium[7, 10], palladium[11], ruthenium[12], tantalum[13] and zirconium[14], have been employed in this kind of reaction with varying degrees of success.

But the number of practically useful catalysts for [2 + 2 + 2] cyclotrimerization is rather small. Among them, the cobalt catalysts are the complexes of the most utility for the preparation of pyridine from alkynes and nitriles, the cobalt catalysts are the only choice,

since this type of transformation has not been reported or gave less satisfactory results[15] for other catalysts.

Nickel catalysts, $Ni(COD)_2$ or Ni(COD)(COT) in most reports, are also reactive catalyst for cyclotrimerization. The reaction of alkynes and acetylene seems to be a quite general method for the formation of benzene ring, and the facile introduction of chiral ligands to the catalyst system is another notable feature of the nickel catalyzed reaction[7a]. But the activity of the nickel catalysts seems to be lower compared to that of cobalt or rhodium catalysts, since most disubstituted alkynes did not react with diynes in the presence of Ni catalysts[16]. At the same time, the Ni catalysts are less stable than cobalt or rhodium catalysts, which give the nickel catalysts a narrow tolerance of different substituents.

Unlike with cobalt complexes, acetylene generally gives linear dimers product instead of benzene ring from rhodium complexes[17]. However, Grigg and Stevenson's work[18] showed that Wilkinson's catalyst ($RhCl(PPh_3)_3$) was an effective catalyst for the construction of substituted benzene rings in a partial intramolecular cyclotrimerization manner. Although this rhodium catalyst could offer improved selectivity compared to existing cobalt catalysts since it induces less side reaction, like dimerization of the diyne and homotrimerization of monoalkyne, this catalyst system has certain limitation. It appears that this catalyst could only be applied to reactions of 1,6-heptadiyne with other unhindered terminal monoalkynes.

In 1998, a zirconium catalyst, Cp_2ZrCl_2, was reported by Takahashi group[14]. Multi-substituted benzene derivatives were synthesized regioselectively with middle to high yields. However, regardless the excellent regioselectivity, this method requires the use of stoichiometric amount of zirconium catalyst to prepare zirconocyclopentadienes in situ, which is the intermediate coming from Cp_2ZrCl_2 and two alkyne molecules. And the addition

of the third alkyne to form the benzene ring needs the present of one or two equivalents copper or Nickel salt. All these facts make this catalyst less suitable for practical synthesis.

Though some other metal complexes have shown catalytic activities in the cyclotrimeriztion transformation, the synthetic usefulness of these catalysts remains to be examined, and the general method to construct the Carbocyclic and heterocyclic aromatic rings still needs to be established.

To summarize, till now, low-valent cobalt (I) catalysts are still one of the most successful complexes to accomplish [2 + 2 + 2] cyclotrimerization (Scheme 1-2).

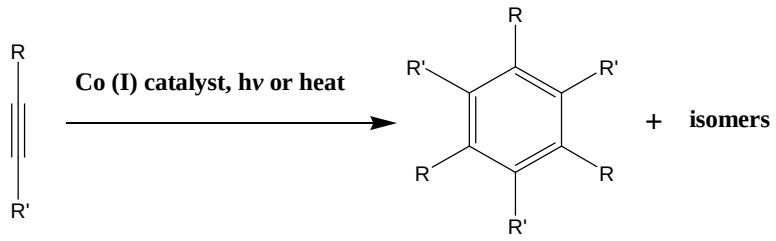

Scheme 1-2. Cyclotrimerization of one non-symmetric alkyne

The cobalt (I)-catalyzed cyclotrimerization of three alkynes has been applied in the elegant syntheses of various synthetically challenging molecules, including antitumor anthracycline aglycones[19], the protoberberine skeleton[20], and ($\pm$) estrone[21](Figure 1-1).

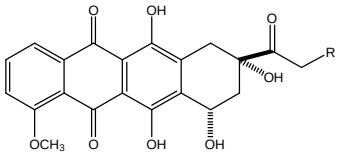

Anthracycline Aglycone

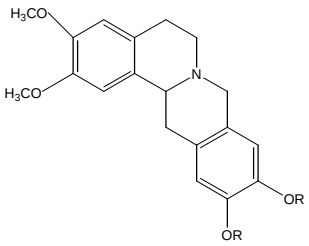

Protoberberine Skeleton

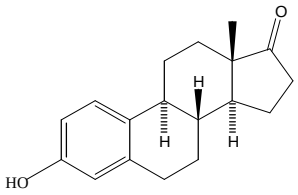

(±)-estrone

Figure 1-1. Molecules assembled by cobalt(I)-catalyzed cyclotrimerization

An important class of aromatics get to be made easily by [2 + 2 + 2] cyclotrimerization are pyridine and its derivatives. These are technically important fine chemicals. Their manufacture by synthetic methods has increased rapidly since 1950[22]. In 1973, *Wakatsuki* and *Yamazaki*[23] first report the successful synthesis of substituted pyridines by acetylene heterocyclization with nitriles in the presence of Co-containing complex catalysts. Thereafter, numerous researches focused on this kind of transformation, and variations of substituted pyridines were constructed, including, i-naphthyridine[24], 2-azaanthracene skeleton[25] and vitamin B_6[26] (Scheme 1-3).

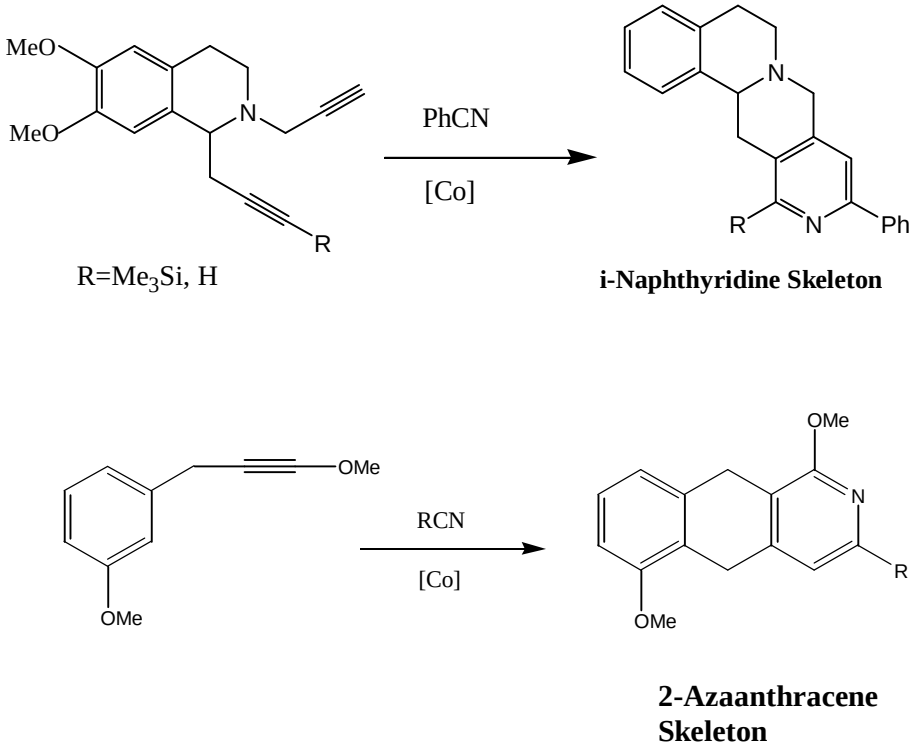

Scheme 1-3. Pyridine based complexes assembled by cobalt(I)-catalyzed cyclotrimerization

2. Proposed Mechanism

Since the catalytic procedure involves several intermediates, the general mechanism of [2 + 2 + 2] cyclotrimerization has got to be completely understood. Some previous mechanistic investigations[27, 28] have proposed that the formation of cobaltacyclopentadienes was the key step of that cobalt catalyzed transformation.

A general proposed mechanism of $CpCoL_2$ (L = olefin, PPh_3, CO) catalyzed cyclotrimerization to form substituted benzene and pyridine is shown in Scheme 1-4. Initially, a first and then a second alkyne moieties sequentially displace two ligands on the metal to form the intermediate **C**, following that, oxidative coupling gives the coordinatively unsaturated cobaltacyclopentadiene. This intermediate complex may then coordinate with a third alkyne molecule or a nitrile molecule to give the alkyne/nitrile-coordinated cobaltacycle(either intermediate **D** or **E**). Insertion of this coordinated alkyne or nitrile into one of the Co-C σ-bonds forming the cobaltacycloheptatriene, which subsequently undergoes reductive elimination to form benzene or pyridine complex. Releasing arene or pyridine and coordination of a pair of alkyne molecules regenerates alkyne-coordinated cobalt species to complete the whole catalytic cycle.

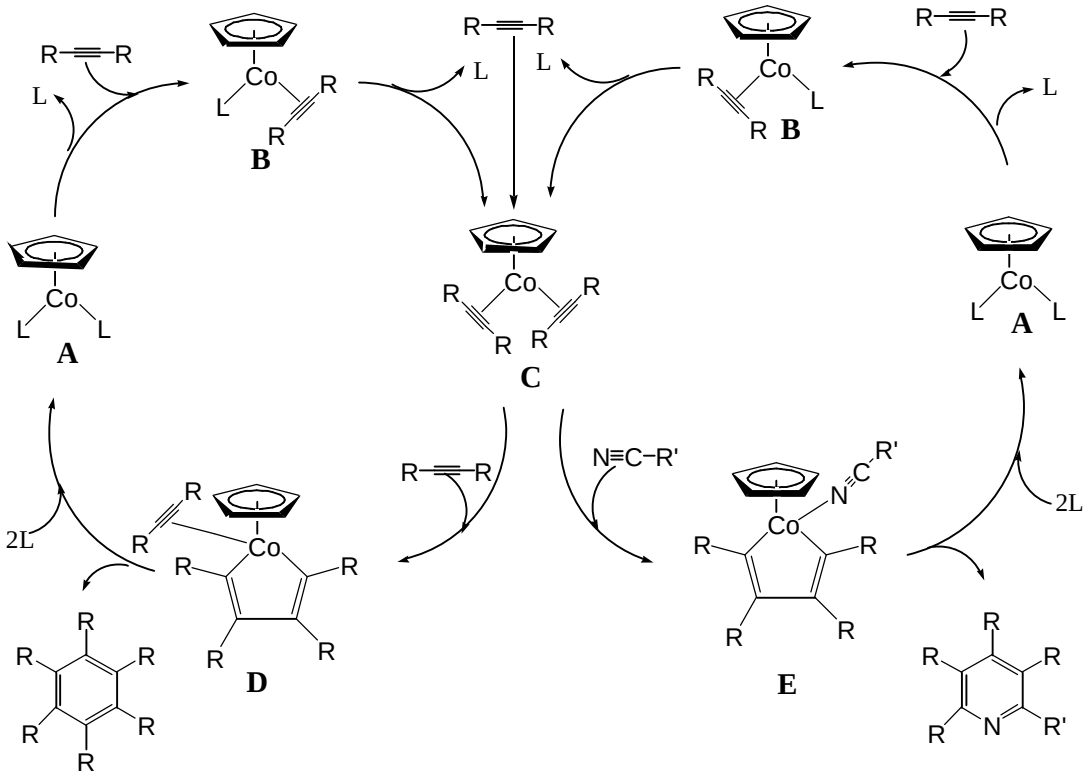

Scheme 1-4. Proposed mechanism of cobalt (I) catalyzed cyclotrimerization to form substituted benzenes and pyridines

Due to the lack of direct structural evidence to support the formation of cobaltacycloheptatriene intermediate **F**, another possible pathway for the addition reaction of the third alkyne also could be followed (Scheme 1-5). When the third alkyne molecule is close to the metal center, a Diels-Alder cycloaddition could happen between unsaturated cobaltacyclopentadiene and the third alkyne to form the intermediate **G. G** also could undergo a reductive elimination step to reform the active catalyst and release the final product. Similarly, the nitrile molecule could undergo a heteromolecule Diels-Alder cycloaddition to generate pyridine ring structures.

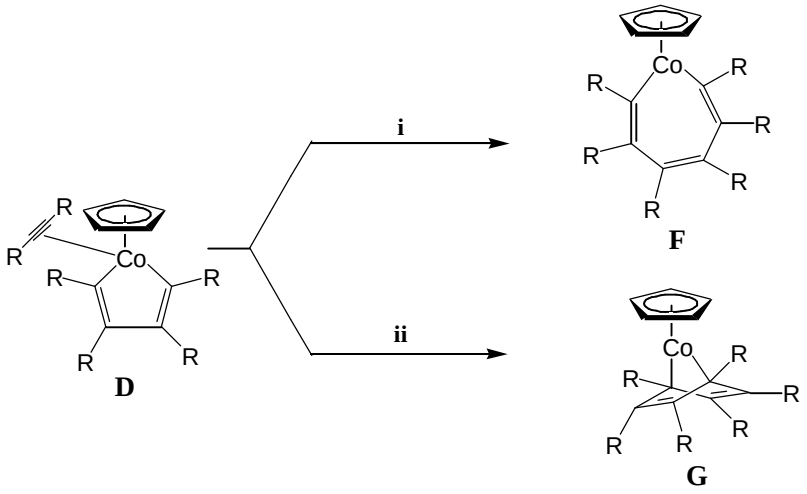

Scheme 1-5. Two possible pathways for the addition of the third alkyne molecule

i. Insertion. **ii.** Diels-Alder cycloaddition

3. Rationale for Cp Modification

Although the various cobalt (I) catalysts have performed several remarkable syntheses, they still have some inherent limitations. Current catalysts have relatively low activity. In most cases, extremely harsh reaction conditions are needed to carry out the reaction, such as photochemical initiation[29-32], high reaction temperature, refluxing aprotic solvents[33-35], and long reaction times[36], which can cause the decomposition of the catalysts to lead to a poor turnover number[20, 29, 33, 37]. These harsh reaction conditions narrow the variation of the substrates. Normally, protection and deprotection steps are necessary right before and after the cyclotrimerization, which leads to a decrease of overall yields[38, 39]. So, there is still a need to develop more effective catalysts to catalyze cyclcotrimerizaiton under mild reaction conditions.

Casey *et al.*[40-42] have proposed that the electron withdrawing substituent group on the Cp ring would make the Cp ring more electron deficient than an unsubstituted Cp ring. The electron deficiency of the Cp ring may then render the metal more electrophilic by decreasing its electron density and facilitating the transfer of an electron pair into the Cp ring, thereby creating a vacant orbital on the metal for nucleophilic attack from an external ligand.

This theory could be explained more clearly by examining a molecular orbital diagram of $CpCo(CO)_2$ (shown in figure 1-2).

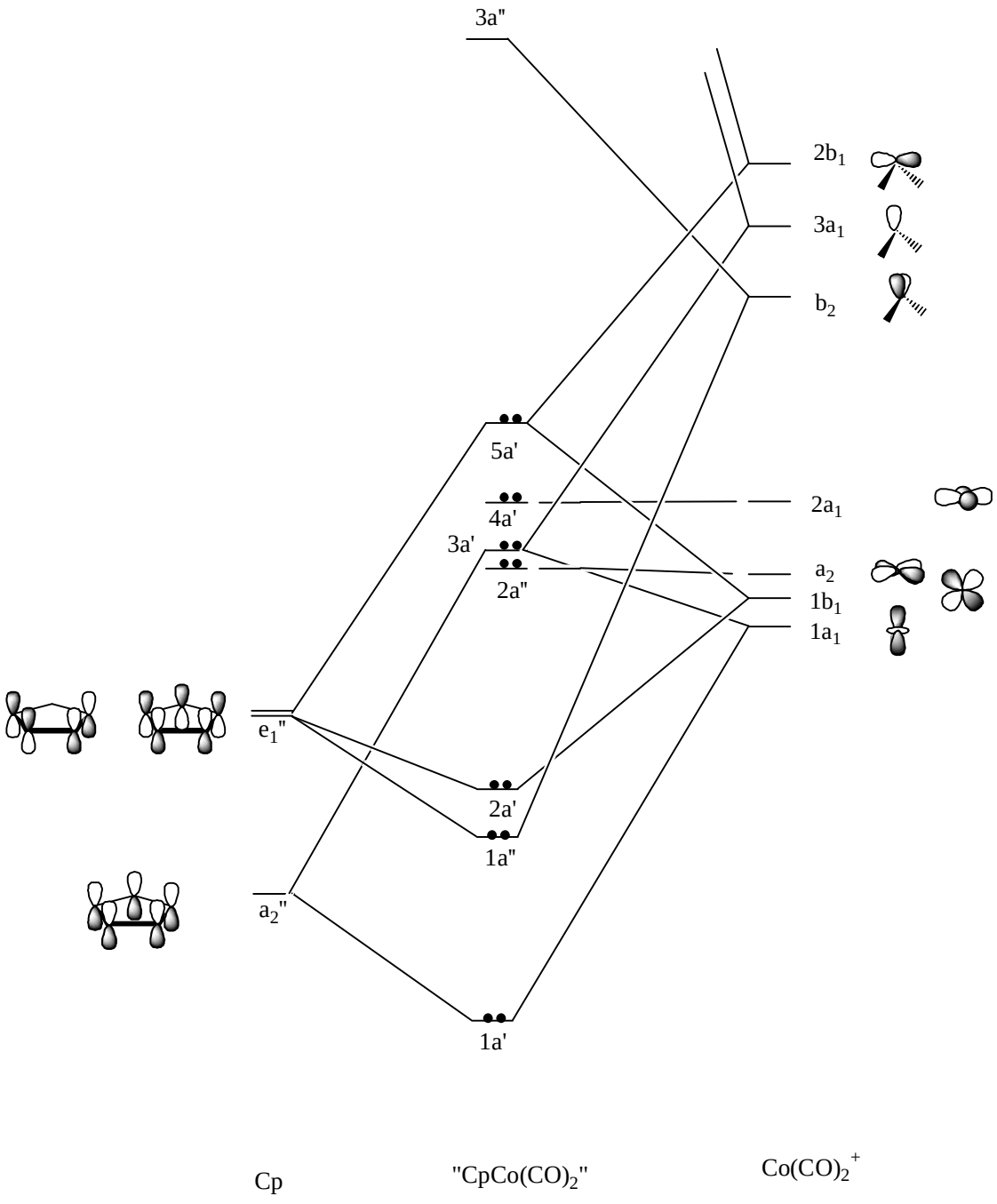

Figure 1-2. Approximate MO digram for $CpCo(CO)_2$[43]. The order of the MO's, particularly the antibonding orbitals, is subject to scrutiny but the pattern is generally accepted. The relative energies of the orbitals are only meant to be qualitative.

It is clear that $CpCo(CO)_2$ has 18 valence electrons. If $CpCo(CO)_2$ coordinates an additional ligand without first losing a CO or undergoing Cp ring slippage to open up a vacant coordination site, a 20 valence electrons species would be formed , which is normally energetically unfavorable. Therefore, it is likely that either ligand dissociation or slippage to generate active catalyst species is necessary. At the same time, the highest occupied molecular orbital (HOMO) is 5a', which does is a moderately high-energy antibonding orbital. So, losing a pair of electrons on the 5a' to diminish this antibonding is energetically favorable for $CpCo(CO)_2$ as well as other 18-electron CpCo catalysts where an analogous situation occurs.

An electron-withdrawing group on the Cp ring could lower the energies of the bonding orbitals, at the same time, the energies of the antibonding orbital 5a' would be increased, which makes the pair of electrons located on 5a' easy to be removed. So, due to the energy increase of the 5a' orbital, slippage of the Cp ring from η^5 to η^3 would remove two electrons from the 5a' orbital.

4. **Development of Modified CpCo Catalysts**

Following the discovery of the cobalt(I) catalyzed cyclotrimerization to form carbocyclic and heterocyclic aromatic rings, further studies were undertaken aimed at developing a highly efficient cobalt catalyst. As discussed before, one of the practical ways of designing the new catalysts is to introduce electron withdrawing substituents into the cyclopentadienyl ring.

Bönnemann and his coworkers[44] reported many modifications of the cyclopentadienyl ring to make new cobalt catalysts, which are shown in figure 1-3.

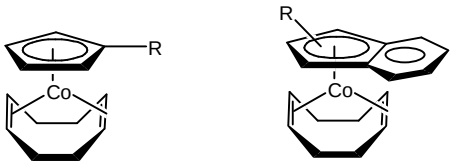

R = Cl, Br, I
HCO
CH_3CO
CH_3CHOH

$H_2C=C(CH_3)$
C_2H_5CO
CH_3OCO
HOOC
PhNHCO
CpFeCp-CO
Ph_3C
Ph_2P
$Ph_2P(s)$
t-Bu
Me_3Si

R = 2-$(CH_3)_2N$
1-CH_3
1-C_2H_5
1-*t*-Bu
2-Ph
1-Me_3Si

Figure 1-3. Some mono-substituted Cp and indenyl cobalt catalysts

Although no catalyst for alkyne cyclotrimerization was reported. Their work on the cocyclotrimerization of alkynes and nitrile showed that the yield and regioselectivity of this kind of reaction were very sensitive to the structural modification of the catalysts. Generally, with the same substituted Cp ring, COD-complexes were more active than dicarbonyl complexes. The regioselectivity of these catalysts was the same for substituted Cp ring Co catalysts, it changed immediately when the structure of Cp ring was varied. But the relationship between regioselectivity and structure of Cp ring is unclear yet.

Some disubstituted and multiple-substituted Cp rings have been used to synthesize new cobalt catalysts, such as pentamethylcyclopentadienyl ring, 1,2-Me_3Si substituted cyclopentadienyl ring etc. Also, η^5-Fluorenyl ring and η^6-borininato derivatives were used to displace the cyclopentadienyl ring to form the new catalysts in some publications[45-50].

Some new catalysts with mono-substituted Cp rings do have been shown to be better catalytic property than the traditional Co catalyst. For example, the *di-tert*-butylphosphanylethylcyclopentadienylcobalt(I) chelate compound[51] (figure 1-4) could catalyze the [2 + 2 + 2] cyclotrimerization of terminal alkynes in water/ethanol mixture at room temperature without photo activation.

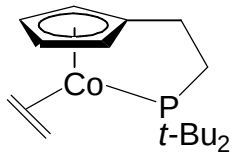

Figure 1-4. *di-tert*-butylphosphanylethylcyclopentadienylcobalt(I) chelate compound

Recently, a new catalyst $Cp^{\$}CoCOD$[52, 53] (Figure 1-5) has been developed which catalyzed cyclotrimerization of alkynes or alkynes with nitrile molecules under mild reaction conditions in aqueous media with good yields.

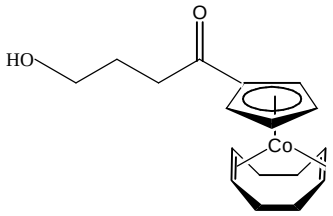

Figure 1-5. Structure of $Cp^{\$}CoCOD$

In comparison with the old catalysts, like $CpCo(CO)_2$, $Cp^{\$}CoCOD$ has some advantages, which are indicated in the following table (Table 1-1).

Table 1-1. Comparison of Cobalt Catalysts for Cyclotrimerization

	$CpCo(CO)_2$	$Cp^{\$}CoCOD$
Reaction conditions	Irradiation or high temperature, high pressure	Pure thermal condition
Catalytst loading	High, frequently stoichiometric	Low, 2.5-10 mol%
Reaction medium	Aprotic solvent	Aqueous or aprotic solvent
Functional groups tolerated	Need to protect function groups before reaction	Tolerates many function groups
Benzene side-product in the alkyne- nitrile cyclotrimerization	Considerable	Only trace of benzene side product detected
Excess nitrile needed in the reaction	Yes.	No.

A double isotopical labeling crossover experiment[53] (shown in Scheme 1-6) verified that no dissociation of COD happened in the catalytic cycle. Consistent with this result, an alternative mechanism with ligand slippage was proposed[52] (Scheme 1-7). An advantage of ligand slippage over ligand dissociation for generation of active catalysts may be the ability

to avoid coordination with other unsaturated species, which might cause the formation of inactive sequences.

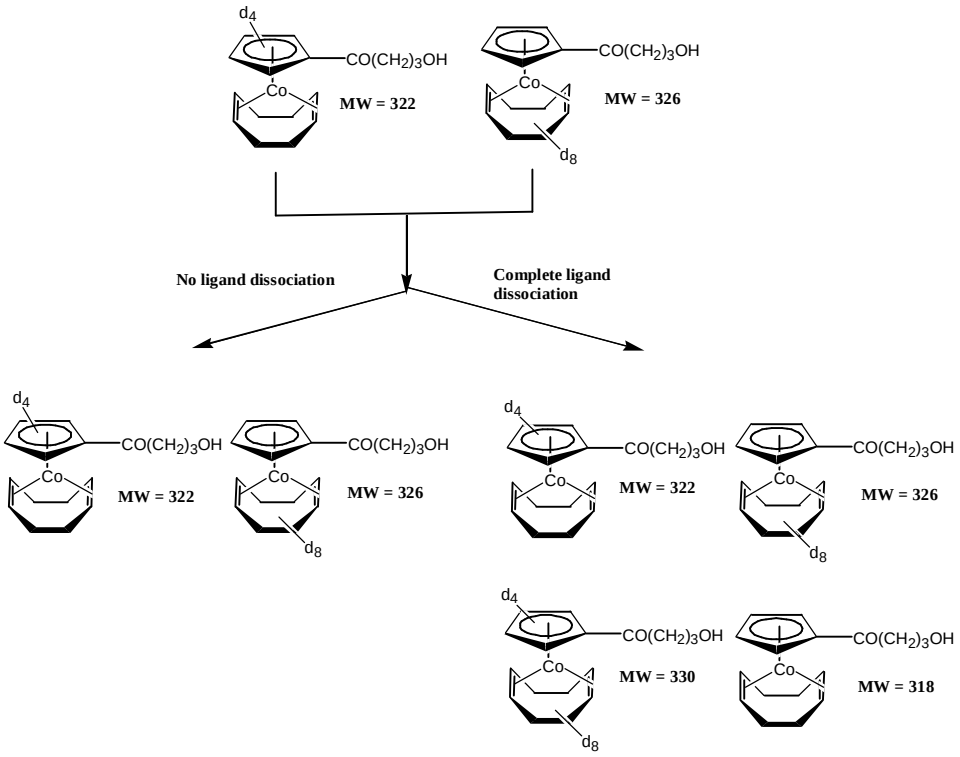

Scheme 1-6. Double isotopic crossover experiment

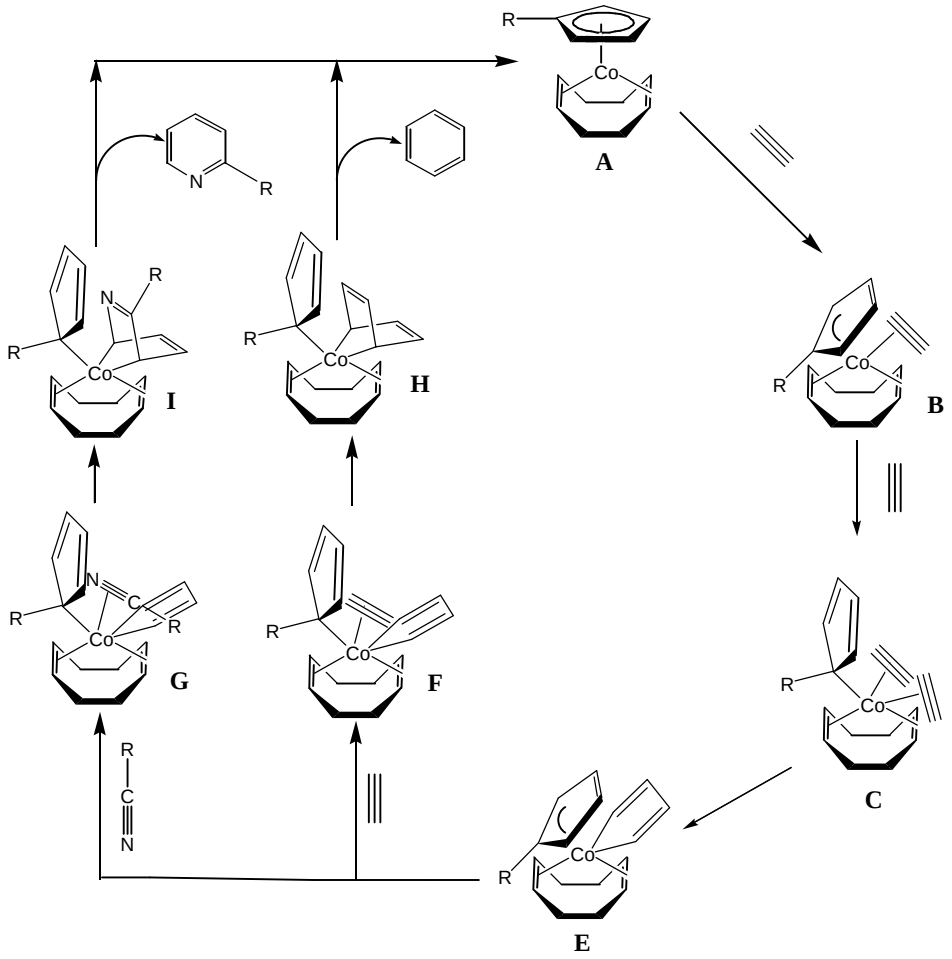

Scheme 1-7. Proposed Mechanism of $Cp^{\$}CoCOD$ catalyzed cyclotrimerization to form substituted benzene (R= $C(O)CH_2CH_2CH_2OH$)

In the proposed cyclotrimerization mechanism, the substituted Cp ring of $Cp^{\$}CoCOD$ would slip from η^5 to η^3 coordination, forming the vacant coordination site for the first alkyne to give intermediate **B**. A second alkyne could enter the coordination sphere of the cobalt by further Cp slippage form η^3 to η^1. Shown as intermediate **C**. Oxidative coupling of these two alkyne ligands forms the cobaltapentadiene with Cp slippage back from η^1 to η^3 (intermediate **D)**. Subsequently, the third alkyne or nitrile bound with metal center

(intermediate **E** or **F**) was followed by the Cp ring slippage from η^3 to η^1 again. The third alkyne or nitrile undergoes Diels-Alder addition to form the intermediate 7-cobaltanorbornadiene complex **H** or **I** (or perhaps simple migratory insertion to yield the cobaltaheptatriene complex). Reductive elimination of the 7-cobaltanorbornadiene complex would give the product, and slippage of the Cp ring from η^1 to η^5 would regenerate the resting state of the catalyst.

The exciting experimental results, that came from $Cp^{\$}CoCOD$ catalyzed cyclotrimerization encouraged us to further investigate this kind of catalyst modification.

5. Synthesis of New Cyclopentadienylcobalt(I) Catalysts for Cyclotrimerization Reactions

A general synthetic route was reported by ***Raush*** and coworkers[54], which synthesized mono-substituted cyclopentadienylsodium via reaction of cyclopentadienylsodium with some rather simple-structured esters. However, the ability of cyclopentadienylsodium reacting with more complex ester structures has not been examined.

The initial effort to synthesize Cp rings substituted with two adjacent carbonyl groups therefore started from cyclopentadienylsodium and methyl pyruvate (scheme 1-8).

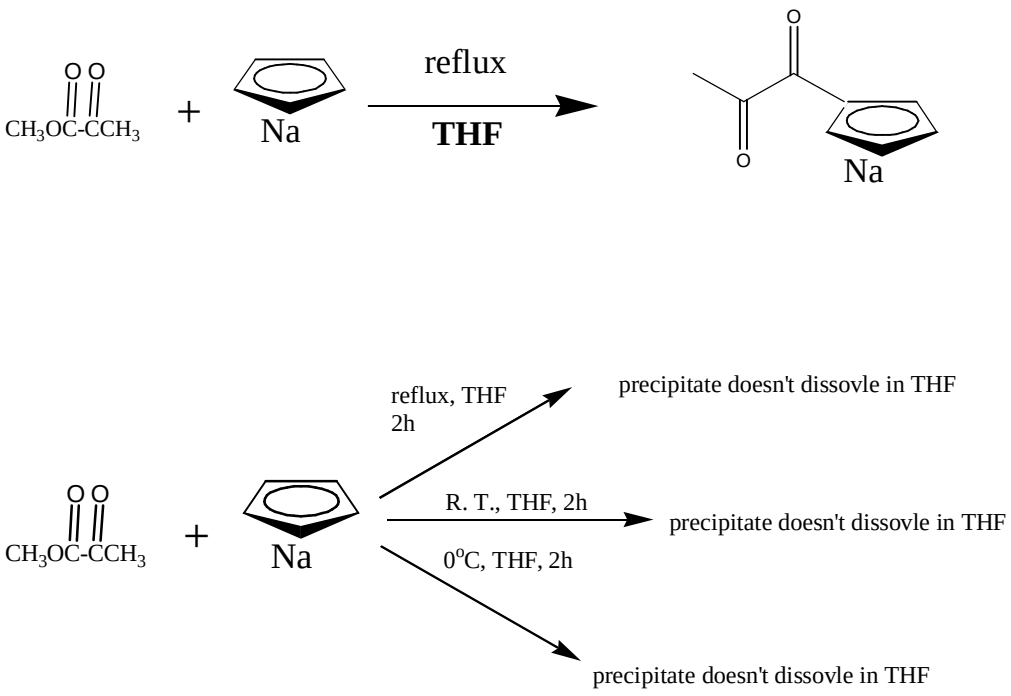

Scheme 1-8. Attempted synthesis of two adjacent carbonyls substituted CpNa

It was originally thought that only the ester carbonyl group could undergo the nucleophilic attack of sodiumcyclopentadienide (NaCp) to give the expected product. The first attempt is adding methyl pyruvate/THF solution into a freshly prepared sodiumcyclopentadienide/THF solution and refluxing the mixture. But only a dark brown precipitate formed during refluxing. Workup of the remaining THF solution did not yield any compounds containing cyclopentadiene protons. Considering the ester group of methyl pyruvate was much more active than the normal isolated ester group, the reaction was carried out again at lower temperature. Unfortunately, the desired product was never obtained either at room temperature or at 0˚C.

It was then realized that the ketone carbonyl of the methyl pyruvate also may act as an electrophile, which could undergo enolization very easily. What type of side reaction that

cause the precipitate was not clear yet, since the precipitate could not dissolve in any organic solvents. But it was obvious that the reaction of sodiumcyclopentadienide and methyl pyruvate was not a viable option for constructing substituted sodiumcyclopentadienide ring.

In order to reduce the side reactions, dimethyl oxolate was used instead of methyl pyruvate. In this case, the secondary carbonyl group could not undergo any enolization reaction (Scheme 1-9). After several attempts, a synthetic route has been built up. A solution of freshly prepared sodiumcyclopentadienide in THF was treated with a solution of dimethyl oxolate in THF. After stirred for 6h, the reaction mixture was precipitated in sparged hexanes, yielding a white powder, which was characterized to be $NaCp^{\%}$.

A solution of $NaCp^{\%}$ in THF was then added to a dry benzene solution of $Co(PPh_3)_3Cl$ and COD. The reaction mixture immediately turned into wine-red color (Scheme 1-10).

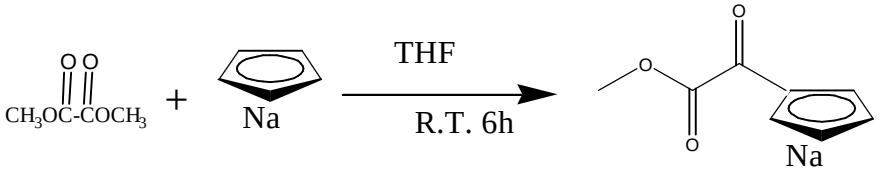

Scheme 1-9. Synthetic Route of $NaCp^{\%}$

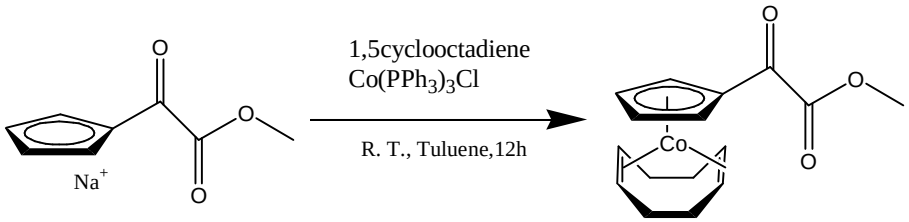

Scheme 1-10. Synthetic Route of $Cp^{\%}CoCOD$

Unfortunately, when using chromatography to purify the $Cp^{\%}CoCOD$, it decomposed on the column. If using less active alumina gel, the catalyst and PPh_3 could not be separated completely. Therefore the modification of sodiumcyclopentadienide with adjacent carbonyls was abandoned.

Considering the $CpCoL_2$ molecular orbital diagram, the electron-withdrawing group substituted on the Cp ring would increase the energy of antibond orbital (5a'), which facilitates the slippage of Cp ring, and the 5a' orbital has a higher energy if the substituted group is more electron attractive. Trifluoromethyl group is one of the most electron attractive groups. So, if we could connect the trifluoromethyl group with a carbonyl group, Theoretically, it may make the slippage of Cp ring easier than the normal ester or ketone substituted CpCoCOD catalyst. Another reason to design this kind of structure is that we could use ^{19}FNMR to monitor the catalyst behavior in the catalytic reaction very easily.

The first attempt of the synthesis of trifluoromethyl acetyl sodiumcyclopentadienide involved ethyl trifluoroacetate reacting with freshly prepared sodiumcyclopentadienide(scheme 1-11). Considering that the carbonyl group of ethyl trifluoroacetate was more active than the normal carbonyl group, the reaction mixture stirred at room temperature for only 6h. After the completion of the reaction, the general workup procedure was employed to collect the pale-yellow powder successfully. The NMR data showed the yellow powder was the product we expected.

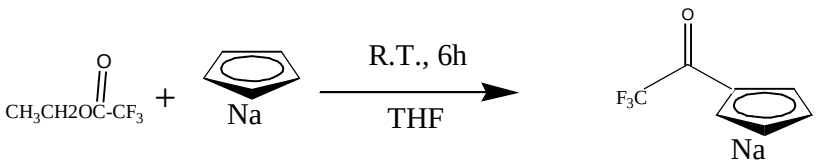

Scheme 1-11. Synthetic Route of $NaCp^{CF3}$

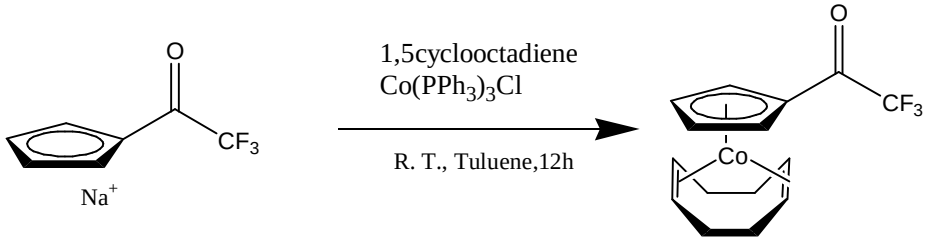

Scheme 1-12. Synthetic Route of $Cp^{CF3}CoCOD$

A solution of $NaCp^{CF3}$ in THF was added to a solution of $Co(PPh_3)_3Cl$ and COD in dry benzene, the reaction mixture turned red immediately (Scheme 1-12). The problem of separating the catalyst with PPh_3 still existed. During the chromatographic separation step, the eluent containing the catalyst and PPh_3 was collected. Fortunately, the catalyst and PPh_3 could be precipitated out separately. The eluent was stored at -20°C over night. The catalyst crystals were collected and recrystallized with THF/pentane to obtain pure catalyst, $Cp^{CF3}CoCOD$.

The crystals of Cp^{CF3}CoCOD were of sufficient size and quality that an X-ray structure was obtained, which gave us a chance to take a closer look at the structure of the Cp^{CF3}CoCOD. The refined structure is shown in Figure 1-6 (50% probability).

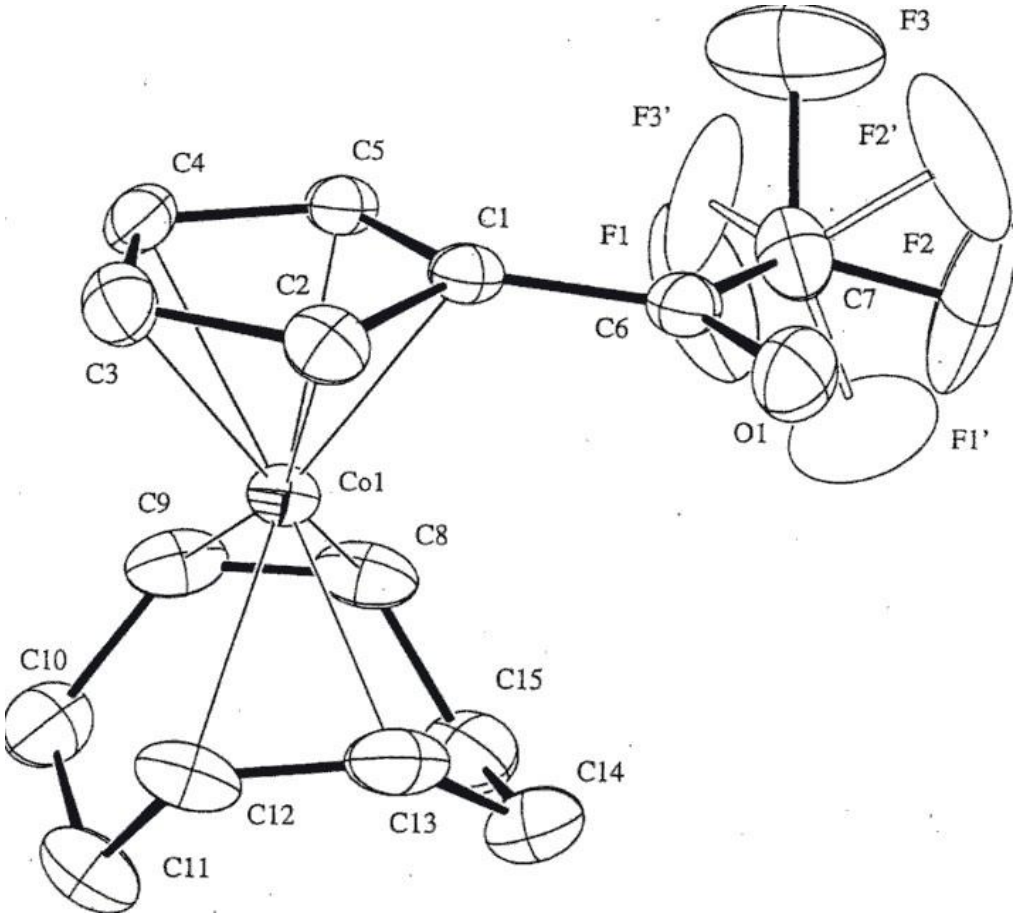

Figure 1-6. X-ray crystallography structure of Cp^{CF3}CoCOD

Table 1-2. Selected bond lengths (Å) for Cp^{CF3}CoCOD

Co1 – C1	2.082(2)	C1 – C2	1.435(4)
Co1 – C2	2.070(3)	C1 – C5	1.441(3)
Co1 – C3	2.143(3)	C2 – C3	1.409(4)
Co1 – C4	2.137(3)	C3 – C4	1.407(4)
Co1 – C5	2.072(2)	C4 – C5	1.419(4)
Co1 – C8	2.036(3)		
Co1 – C9	2.040(3)	C1 – C6	1.439(4)
Co1 – C12	2.059(3)	C8 – C9	1.397(5)
Co1 – C13	2.036(3)	C12 – C 13	1.392(5)

Table 1-3. Selected bond angles (˚) for Cp^{CF3}CoCOD

C1 - Co1 – C2	40.45(10)	C1 – C2 – C3	109.3(2)
C2 – Co1 – C3	39.01(10)	C2 – C3 – C4	107.8(2)
C3 – Co1 – C4	38.38(10)	C3 – C4 – C5	108.8(2)
C4 – Co1 – C5	39.37(10)	C1 – C5 – C4	108.1(2)
C1 – Co1 – C5	40.60(9)	C2 – C1 – C5	105.9(2)
C8 – Co1 – C13	84.57(12)		
C13 – Co1 – C12	39.75(13)	C1 – C6 – O1	124.4(2)
C9 – Co1 – C12	83.57(11)	C7 – C6 – O1	116.1(2)
C8 – Co1 – C9	40.10(14)	C2 – C1 – C6	123.2(2)

Table 1-2 and 1-3 show some select bond lengths and angles, respectively, for $Cp^{CF3}CoCOD$.

The space group of the $Cp^{CF3}CoCOD$ is P 21/N. Although, there is very little data on crystal structures of modified CpCo catalysts[55-58], making it hard to compare and constrast structural differences and similarities of these catalysts, a closer examination of the structure of $Cp^{CF3}CoCOD$ reveals several interesting aspects:

1). The bond length of C1 – C6 is 1.439(4) Å, which is close to the bond length of double bonds, indicating that some conjugation of the Cp ring and carbonyl group occurs. This spectroscopic feature reveals that the carbonyl group in the catalyst may not only act as a simple electron withdrawing group, but also lowers the energy of η^3 and η^1 Cp ring configuration through a conjugation effect.

2) The bond lengths of Co1 to C1 through Co1 to C5 are not uniform: the metal atom is not located at the center of the Cp ring. The bond length of Co1 – C3 is 2.143(3) and the bond length of Co1 –C4 is 2.137(3). Obviously, these two bonds are longer than the other three bonds, and the cobalt center is close to C1, C2, and C5. This feature indicates some slippage of the Cp ring, which would facilitate the transformation form η^5-Cp ring to η^3-Cp. At the same time, these two bonds are also longer than the bonds of Co1 –C8, Co1 –C9, Co1 –C12 and Co1 –C13. This suggests that breaking these two bonds may be easier than breaking the bonds between Co center and COD. So, the ring slippage should be easier than the loss of COD. These structural characteristics are consistent with the previous proposed Cp ring slippage mechanism.

3) Compared to other structural data of substituted Cp rings, the trifluoromethyl carbonyl substituted Cp ring shows some special aspects. The summary of bond angles of C1

– C2 – C3, C2 – C3 – C4, C3 – C4 – C5, C4 – C5 – C1 and C5 – C1 – C2 is 539.9°, which indicates a planar Cp ring. But the angle of C5 – C1 – C2 is 105.9(2)°. It is more than 2 degree smaller than the rest angles of Cp ring. The bond length of C1 – C2 is 1.435(4) and the bond length of C1 – C5 is 1.441(3). Both bonds are longer than the other three bonds of the Cp ring. All these features shows the electrons are not delocalized on the Cp ring evenly.

Considering all the special aspects of $Cp^{CF3}CoCOD$ catalyst, a possible conjugate structure was proposed as figure 1-7.

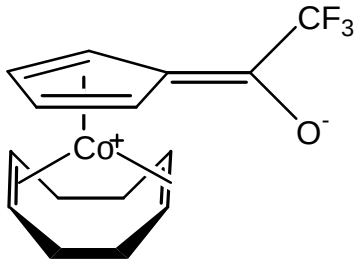

Figure 1-7. A possible conjugate structure of $Cp^{CF3}CoCOD$

It is a coordinatively unsaturated 16e complex. In this structure, cobalt center binds with the cyclopentadiene by a η^4 pattern, which should be easier to slip to a η^1 coordination pattern. The positive charge on the cobalt will help the binding of electron-rich alkyne molecules, which maybe can make the catalyst more active.

6. Kinetic Investigation of $Cp^{CF3}CoCOD$ mediated cyclotrimerization

Previous research[59] has shown that cyclotrimerization of 1,4-dimethoxy-2-butyne is an extremely slow reaction. In order to determine how ative the $Cp^{CF3}CoCOD$ catalyst was, a reaction was set up to catalyze 1,4-dimethoxy-2-butyne cyclotrimerization with $Cp^{CF3}CoCOD$(Scheme 1-13) at 85˚C. The reaction was monitored by ^{1}HNMR.

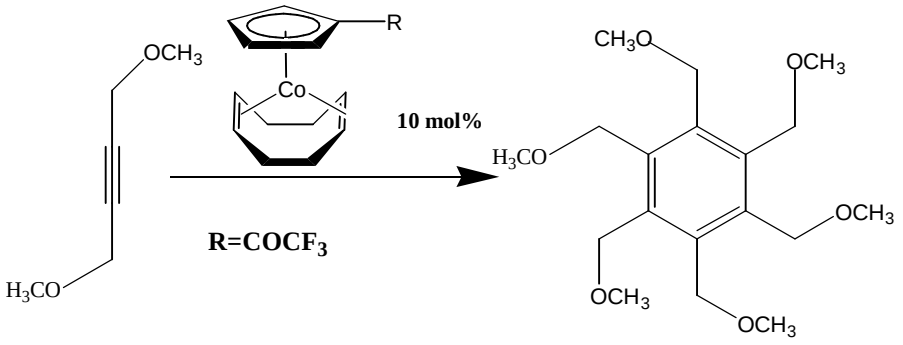

Scheme 1-13. Proposed cyclotrimerization reaction of 1,4-dimethoxy-2-butyne with $Cp^{CF3}CoCOD$ as the catalyst

The first attempt was performing this reaction in the 70% D_2O/MeOD-d_3 medium. Unfortunately, the $Cp^{CF3}CoCOD$ catalyst could not exist in the aqueous solution, although it is stable in the MeOH. Our explanation was that the carbonyl group in the catalyst was especially active, which would undergo nucleophilic attack by D_2O to yield inactive species.

The second attempt alternated the reaction mediate from 70% D_2O/MeOD-d_3 to THF-d_8. The reaction was monitored by ^{1}HNMR and ^{19}FNMR. The kinetic data were collected over three half-life periods. Within experimental error, a first order rate dependence of

alkyne concentration was observed. The kinetic plot (Figure 1-8) showed the pseudo-first order rate to be $2x10^{-6}$ sec^{-1}.

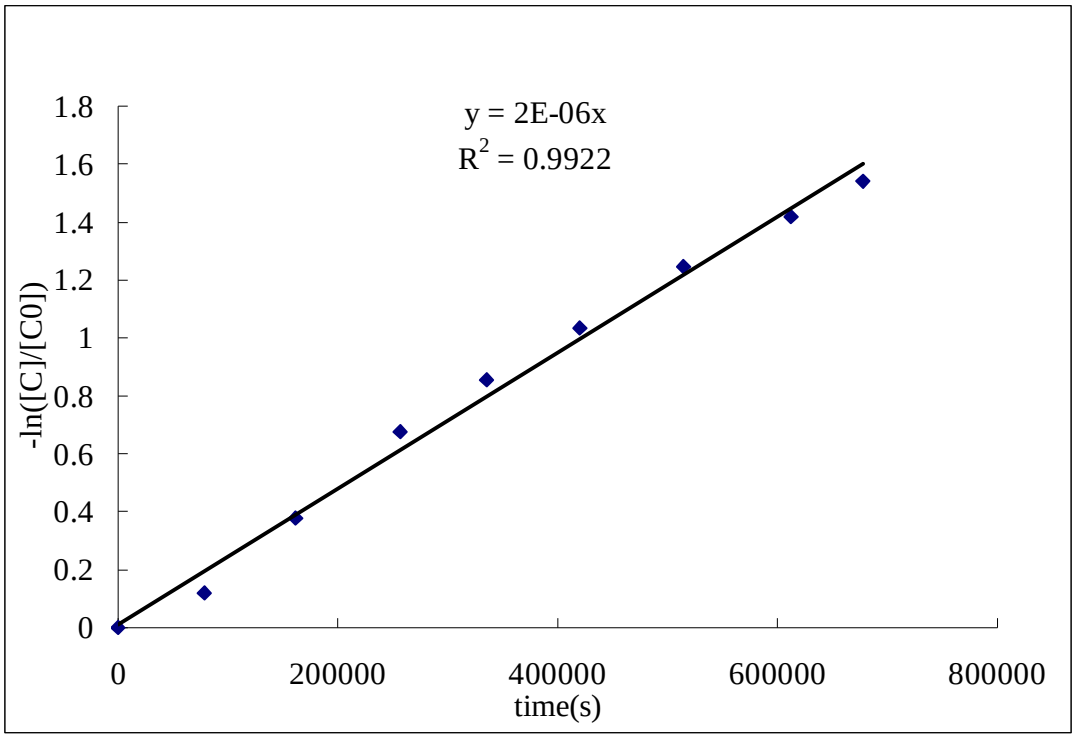

Figure 1-8. First order plot of cyclotrimerization of 1,4-dimethoxy-2-butyne with Cp^{CF3}CoCOD as the catalyst at 85˚C. Pseudo-first order rate: $2x10^{-6}$ sec^{-1}.

At the same time, the cyclotrimerization of 1,4-dimethoxy-2-butyne, with $Cp^{\$}$CoCOD as the catalyst, at the identical reaction conditions showed the pseudo-first order rate to be $3x10^{-7}$ sec^{-1} (figure 1-9).

$Cp^{\$}$CoCOD catalyst exhibited a rate almost 10 times slower than that of Cp^{CF3}CoCOD. These rates verified that Cp^{CF3}CoCOD was a more effective catalyst than the $Cp^{\$}$CoCOD.

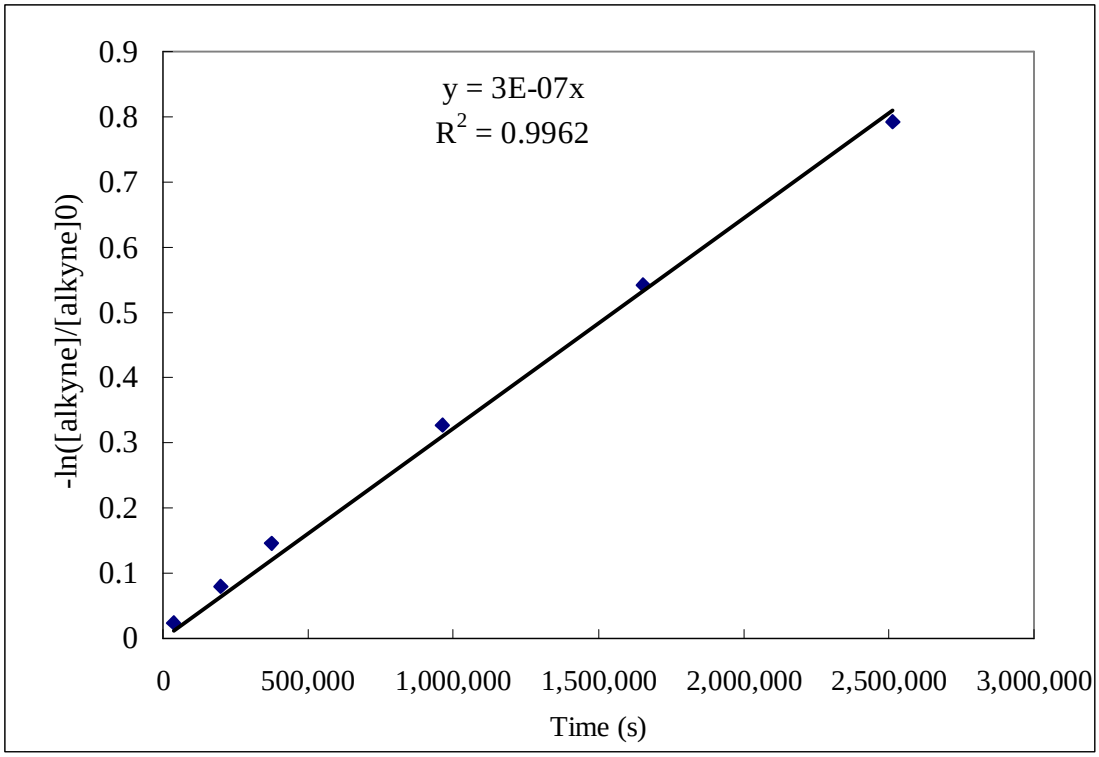

Figure 1-9. First order plot of cyclotrimerization of 1,4-dimethoxy-2-butyne with $Cp^{\$}CoCOD$ as the catalyst at 85˚C. Pseudo-first order rate: $3x10^{-7}$ sec^{-1}.

The second reaction attempt increased the temperature from 85˚C to 100˚C. The kinetic data were collected over three half-life periods. Within experimental error, the data were fitted to a first order kinetic plot (Figure 1-10) showing that the pseudo-first order rate to be $8x10^{-6}$ sec^{-1}.

Increasing the reaction temperature from 85˚C to 100˚C caused a 4-fold increase in the reaction rate of the cyclotrimerization.

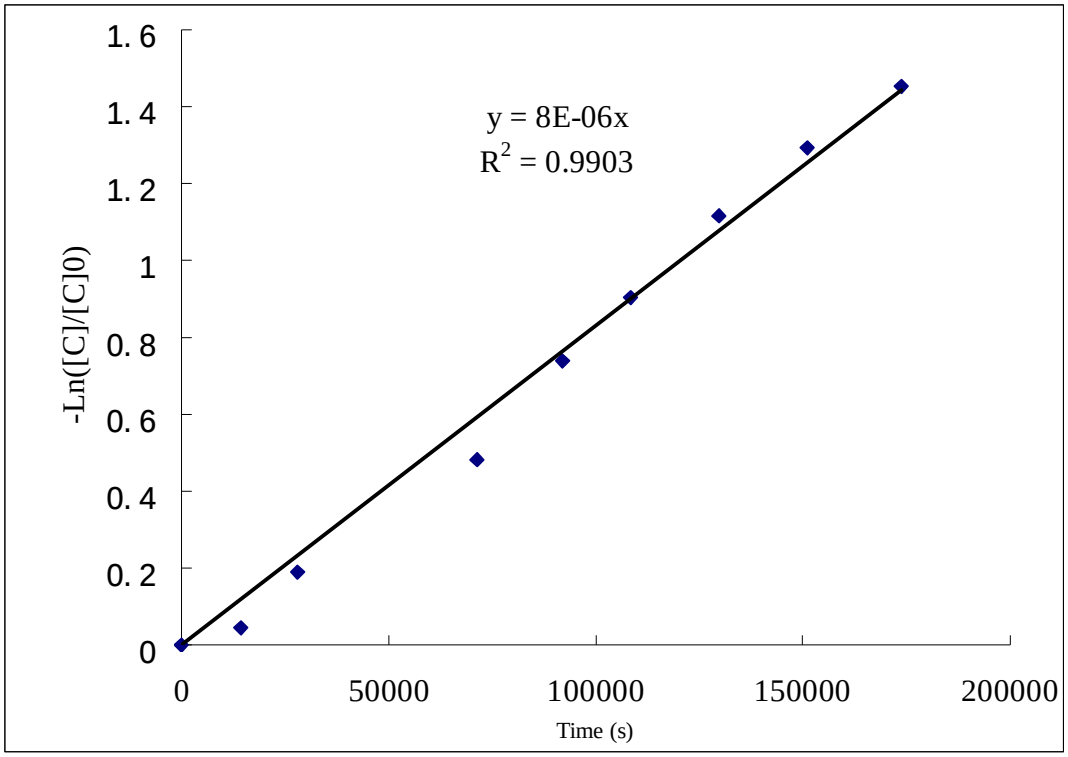

Figure 1-10. First order plot of cyclotrimerization of 1,4-dimethoxy-2-butyne with $Cp^{CF3}CoCOD$ as the catalyst at 100˚C. Pseudo-first order rate: $8x10^{-6}$ sec^{-1}.

Attempts to capture the Cp ring slippage intermediate were not successful. Excess diphenyl acetylene was heated with $Cp^{CF3}CoCOD$ in anhydrous THF-d_8 in a sealed NMR tube at 85°C and the reaction was monitored by ^{1}HNMR. No reaction happened after one week and no decomposition of catalyst was observed. Increase the reaction temperature to 100 °C and the reaction mixture was heated about one month, we observed a new pair of Cp ring proton signals on the NMR spectra. And a new signal that was assigned to free COD protons was presented. Unfortunately, the efforts to separate the new complexes failed and decomposed on the alumina column.

7. Conclusions

In summary, a new cobalt (I) catalyst Cp^{CF3}CoCOD was synthesized successfully. The X-ray crystal structure analysis revealed special structure features, which could be feasible to the associative Cp ring slippage mechanism.

The examination of cyclotrimerization of 1,4-dimethoxy-2-butyne with both Cp^{CF3}CoCOD and $Cp^{\$}$CoCOD catalysts showed Cp^{CF3}CoCOD was a much more active catalyst than $Cp^{\$}$CoCOD. It verified our hypothesis that a stronger electron-withdrawing group on the Cp ring would make the cobalt catalyst more active for the cyclotrimerization.

Kinetic data indicated that the reaction rate shows a pseudo-first order dependence on the concentration of alkyne.

8. References

1) (a) Woodward, R. B.; Hoffmann, R. *Angew. Chem.* **1969**, *81*, 797; (b) Woodward, R. B.; Hoffmann, R. *The Conservation of Orbital Symmetry*, Academic Press; New York, 1970

2) (a) Houk, K. N.; Gandour, R. W.; Rondan, N. G.; Paquette, L.A. *J. Am. Chem. Soc.* **1979**, *101*, 6797. (b) Bach, R. D.; Wolber, G. J.; Schlegel, H. B. *J. Am. Chem. Soc.* **1985**, *107*, 2837

3) Badger, G. M.; Lewis, G. E.; Napier, I. M. *J. Am. Chem. Soc.* **1960**, 2825

4) Peppe, W.; Schlichting, O.; Klager, K.; Toepel, T. *Justus Liebigs Ann. Chem.* **1948**, *560*, 3.

5) (a) Lecker, S. H., Nguyen, N. H.; Vollhardt, K. P. C. *J. Am. Chem. Soc.* **1986**, *108*, 856. (b) Halterman, R. L.; Vollhardt, K. P. C. *Organometallics* **1988**, *7*, 883. (c) Schwager, H.; Spyroudis, S.; Vollhardt, K. P. C. *J. Organomet. Chem.* **1990**, *382*, 191. (d) Cruciani, P.; Aubert, C.; Malacria, M. *J. Org. Chem.* **1995**, *60*, 2664 (e) Bönnemann, H.; Brijoux, W. *Heterocycl. Chem.* **1990**, *48*, 177 and references cited there.

6) (a) Whitesides, G. M.; Ehmann, W. J. *J. Am. Chem. Soc.* **1969**, *91*, 3800. (b) Jolly, P. W.; Wilke, G. *The organic chemistry of Nickel*; wiley: New York, 1975; Vol. 2, p94. (c) Smith, E. H.; Bhatarah, P. *J. Chem. Soc., Perkin Trans. 1* **1990**, 2603. (d) Smith, E. H.; Bhatarah, P. *J. Chem. Soc., Chem. Commun.* **1991**, 277. (e) Smith, E. H.; Bhatarah, P. *J. Chem. Soc., Perkin Trans. 1* **1992**, 2163.

7) (a) Sato, Y.; Nishimata, T.; Mori, M. *J. Org. Chem.* **1994**, *59*, 6133. (b) Daniels, W. E. *J. Chem. Soc., Dalton Trans.* **1964**, 2936.

8) (a) Tsutsui, M.; Zeiss, H. *J. Am. Chem. Soc.* **1959,** *81*, 6090. (b) Sneeden, R. P. A.; Zeiss, H. *J. Organometal. Chem.* **1993**, *452*, 223

9) (a) Collman, J. P.; Kang, J. W.; Little, W. F.; Sullivan, M. F. *Inorg. Chem.* **1968**, *7*, 1298. (b) Grigg, R.; Scott, R.; Stevenson, P. *J. Chem. Soc., Perkin Trans. 1* **1988**, 1357.

(c) Neeson, S. J.; Stevenson, P. J. *Tetrahedron Lett.* **1988**, *29*, 813. (d) Neeson, S. J.; Stevenson, P. J. *Tetrahedron* **1989**, *45*, 6239.

10) Franzus, B.; Canterino, P. J.; Wickliffe, R. A. *J. Am. Chem. Soc.* **1959**, *81*, 1514.

11) (a) Trost, B. M.; Tanoury, G. J. *J. Am. Chem. Soc.* **1987**, *109*, 4753. (b) Maitlis, P. M. *Acc. Chem. Res.* **1976**, *9*, 93. (c) Negishi, E.; Harring, L. S.; Owczarczyk, Z.; Mohamud, M. M.; Ay, M. *Tetrahedron Lett.* **1992**, *33*, 3253

12) (a) Trost, B. M.; Imi, K.; Indolese, A. F. *J. Am. Chem. Soc.* **1993**, *115*, 8831. (b) Chatani, N.; Fukumoto, Y.; Ida, T.; Murai, S. *J. Am. Chem. Soc.* **1993**, *115*, 11614.

13) (a) Strickler, J. R.; Bruck, M. A.; Wigley, D. E. *J. Am. Chem. Soc.* **1990**, *112*, 2814. (b) Takai, K.; Yamada, M.; Utimoto, K. *Chem. Lett.* **1995**, 851.

14) (a) Takahashi, T.; Xi, Z.; Yamazaki, A.; Liu, Y.; Nakajima, K.; Kotora, M. . *J. Am. Chem. Soc.***1998**, *120*, 1672. (b) Takahashi, T.; Tsai, F. Y. Li, Y.; Nakajima, K.; Kotora, M. *J. Am. Chem. Soc.* **1999**, *121*, 11093

15) Cioni, P.; Diversi, P.; Ingrosso, G.; Lucherini, A.; Ronca, P. *J. Mol. Catal.* **1987**, *40*, 337.

16) Sato, Y.; Nishimata, T.; Mori, M. *Heterocycles* **1997**, *44*, 443.

17) Schmit, H. J.; Singer, H. *J. Organomet. Chem.* **1978**, *153*, 165.

18) Grigg, R.; Scott, R.; Stevenson, P. *Tetrahedron Lett.* **1982**, *23*, 2691.

19) Hillard, R. L.; Vollhardt, K. P. C. *J. Am. Chem. Soc.* **1977**, *99*, 4058.

20) Vollhardt, K. P. C. *Angew. Chem. Int. Ed. Engl.* **1984**, *23*, 539.

21) Sternberg, E. D.; Vollhardt, K. P. C. *J. Org. Chem.* **1982**, *47*, 3447.

22) Budzinski, A. *Chem. Ind. (Dűsseldorf)* **1981**, *33*, 529.

23) Yamazaki, H.; Wakatsuki, Y. *Tetrahedron Lett.* **1973**, 3383.

24) Hillard, R. L.; Vollhardt, K. P. C. *Tetrahedron* **1983**, *39*, 905.

25) Vollhardt, K. P. C. *Angew. Chem.* **1984**, *96*, 525.

26) Parnell, C. A.; Vollhardt, K. P. C. *Tetrahedron* **1983**, *41*, 5791.

27) Colman, J. P.; Hegedus, L. S.: *Principles and Application of Organotransition Metal Chemistry*, University Science Books, Menlo Park, 1980

28) Bönnemann, H.; Brijoux, W. *The Cobalt-Catalyzed Synthesis of Pyridine and Its Derivatives*, Ugo, R. Ed.; D. Reidel, 1984; Vol. 5, pp 75.

29) Brien, D. J.; Naiman, A.; Vollhardt, K. P. C. *J. Chem. Soc., Chem. Comm.* **1982**, 133.

30) Karabet, F.; Heller, B.; Kortus, K.; Oehme, G. *App. Organomet. Chem.* **1995**, *9*, 651.

31) Heller, B.; Oehme, G. *J. Chem. Soc., Chem. Comm.* **1995**, 179.

32) Heller, B.; Heller, D.; Oehme, G. *J. Mol. Cat. A.* **1996**, *110*, 211.

33) Naiman, A.; Vollhardt, K. P. C. *Angew. Chem. Int. Ed. Engl.* **1977**, *16*, 708.

34) Chelucci, G.; Cabras, M. A.; Saba, A. *J. Heterocyclic Chem.* **1994**, *31*, 1289.

35) Du Plessis, J. A. K.; Vijoen, J. S. *J. Mol. Cat. A.* **1995**, *99*, 71

36) Bönnemann, H.; Brinkmann, R.; Schenkluhn, H. *Synthesis* **1974,** 575.

37) Bönnemann, H. *Angew. Chem. Int. Ed. Engl.* **1978**, *17*, 505.

38) Paquette, L. A. *Comprehensive Organometallic Synthesis*; Trost, B. M., Ed.; Pergamon Press: New York, 1991; Vol. 5, pp1129.

39) Grotjahn, D. B. *Comprehensive Organometallic Chemistry*; Abel, E. W., Stone, F. G. A., Wlikinson, G. and Hegedus, L. S., Ed.; Pergamon: Tarrytown, 1995.

40) Rerek, M. E.; Basolo, F. *Organometallics* **1983**, *2*, 372.

41) Rerek, M. E.; Basolo, F. *J. Am. Chem. Soc.* **1984**, *106*, 5908.

42) O'Connor, J. M.; Casey, C. P. *Chem. Rev.* **1987**, *87*, 307.

43) Albright, T. A. *Orbital Interactions in Chemistry*; Burdett, J. K., Whangbo, M. H., Ed.; John Willey & Sons: New York, 1985.

44) Bönnemann, H. *Angew. Chem. Int. Ed. Engl.* **1985**, *24*, 248.

45) Diversi, P.; Giusti, A.; Ingrosso, G.; Lucherini, A. *J. Organomet. Chem.* **1985**, *205*, 239.

46) Herberich, G. E.; Greiss, G. *Chem. Ber.* **1972**, *105*, 3413.

47) Ashe, A. J.; Shu, P. *J. Am. Chem. Soc.* **1971**, *93*, 1804.

48) Siebert, W. *Adv. Organomet. Chem.* **1980**, *18*, 301.

49) Binger, P. *Angew. Chem. Int. Ed. Engl.* **1968**, *7*, 286.

50) Bochmann, M.; Siebert, W. *Angew. Chem. Int. Ed. Engl.* **1977**, *16*, 468.

51) Yong, L.; Butenschon, H. *Chem. Comm.* **2002**, 2852

52) Eaton, E. B.; Fatland, A. W. *Organ. Lett.* **2000**, *2(20)*, 3131.

53) Eaton, E. B.; Fatland, A. W.; Sigman, M. S. *J. Am. Chem. Soc.* **1998**, *120*, 5130.

54) Hart, W. P.; Macomber, D. W.; Rausch, M. D. *J. Am. Chem. Soc.* **1980,** *102*, 1196

55) Yamazaki, H.; Wakatsuki, Y. *J. Organomet. Chem.* **1984**, *272*, 251.

56) Yamazaki, H.; Yasufuku, K.; Wakatsuki, Y. *Organometallics* **1983**, *2*, 726

57) Yasufuku, K.; Hamada, A.; Aoki, K.; Yamazaki, H. *J. Am. Chem. Soc.* **1980,** *102*, 4363

58) Bonnemann, H.; Goddard, R. Grub, J.; Mynott, R.; Raabe, E.; Wendel, S. *Organometallics* **1989**, *8*, 1941

59) Unpublished result in Eaton group.

CHAPTER TWO

COBALT (I) CATALYZED ALKYNE AND ISOCYANATE COCYCLOTRIMERIZATION TO FORM SUBSTITUED 2-PYRIDONES; A SYNTHETIC AND MECHANISTIC INVESTIGATION

1. History of Cobalt (I)-mediated Cyclotrimerization to Form 2-Pyridones

Substituted 2-pyridone ring systems and their derivatives are found in a wide variety of natural products, which have considerable potential in the pharmaceutical industry. For example, anti-nicotinism drug Cytisine[1], acetylcholinesterase inhibitor Huperzine A[2], antidepressant Lirequinil (Ro-41-3696) [3], free radical scavenger Pyridoxatin[4], cardiotonic agent Milrinone[5], and antimicrobial agent A-86719.1[6].

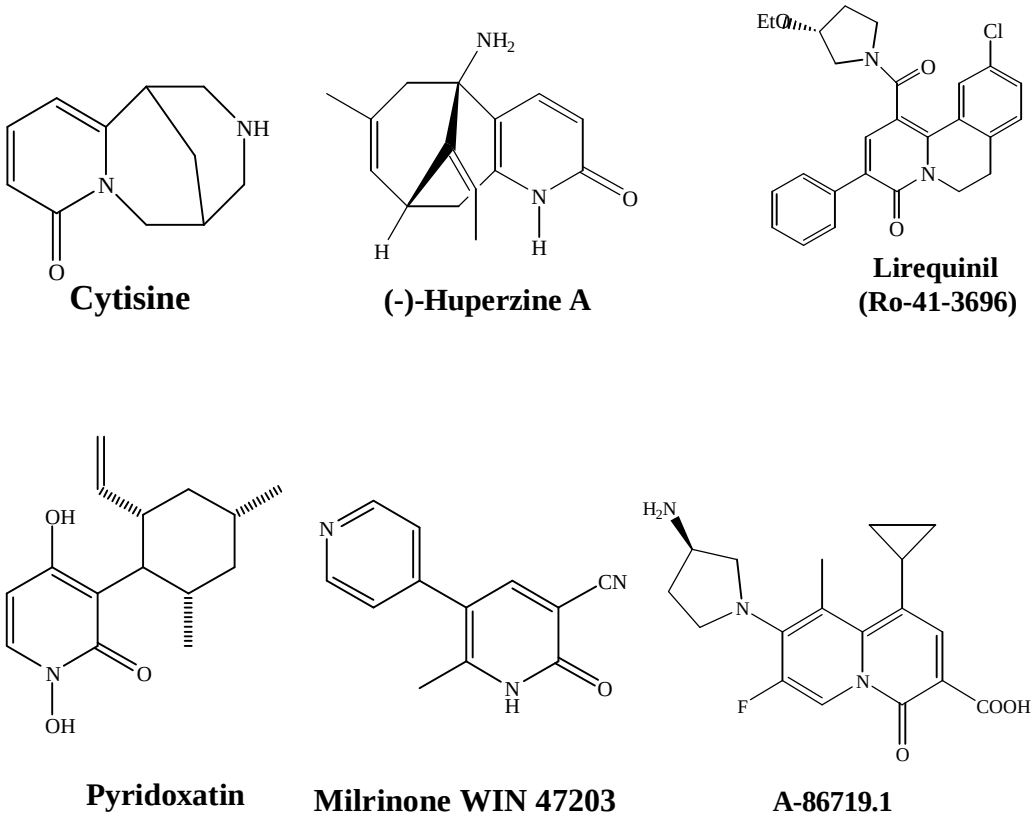

Cytisine **(-)-Huperzine A** **Lirequinil (Ro-41-3696)**

Pyridoxatin **Milrinone WIN 47203** **A-86719.1**

Figure 2-1. Structures for some substituted 2-pyridone rings compounds

Many other compounds with 2-pyridone cores are also reported to have antibacterial[7], antitumor[8, 9], and other biological activities[10-12]. Meanwhile, 2-pyridone compounds are also used widely in the dye industry[13-15], and the tautomerization phenomenon between 2-pyridone and 2-hydroxypyridine also has a lot of interesting research work[16-18].

Cocyclotrimerization of two molecules of alkynes and an isocyanate (Scheme 2-1) would be an efficient method to construct substituted 2-pyridone rings.

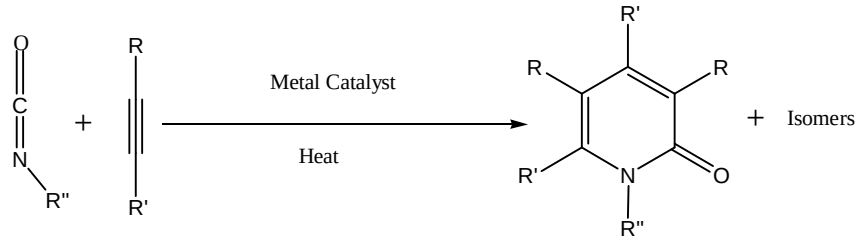

Scheme 2-1. Cyclotrimerization of alkynes and isocyanates

Metal mediated [2 + 2 + 2] heterocyclotrimerization of 2-Pyridone formation has first been accomplished independently by Yamazaki[19] using $CpCo(CO)_2$ catalyst and by Hoberg[20] using $Ni(COD)_2$ catalysts at the beginning of 1980. And several 2-pyridones were synthesized[21]. In 1984, Vollhardt and his coworkers used this methodology to accomplish the synthesis of Camptothecin, an antitumor agent the first time (Scheme 2-2) [22].

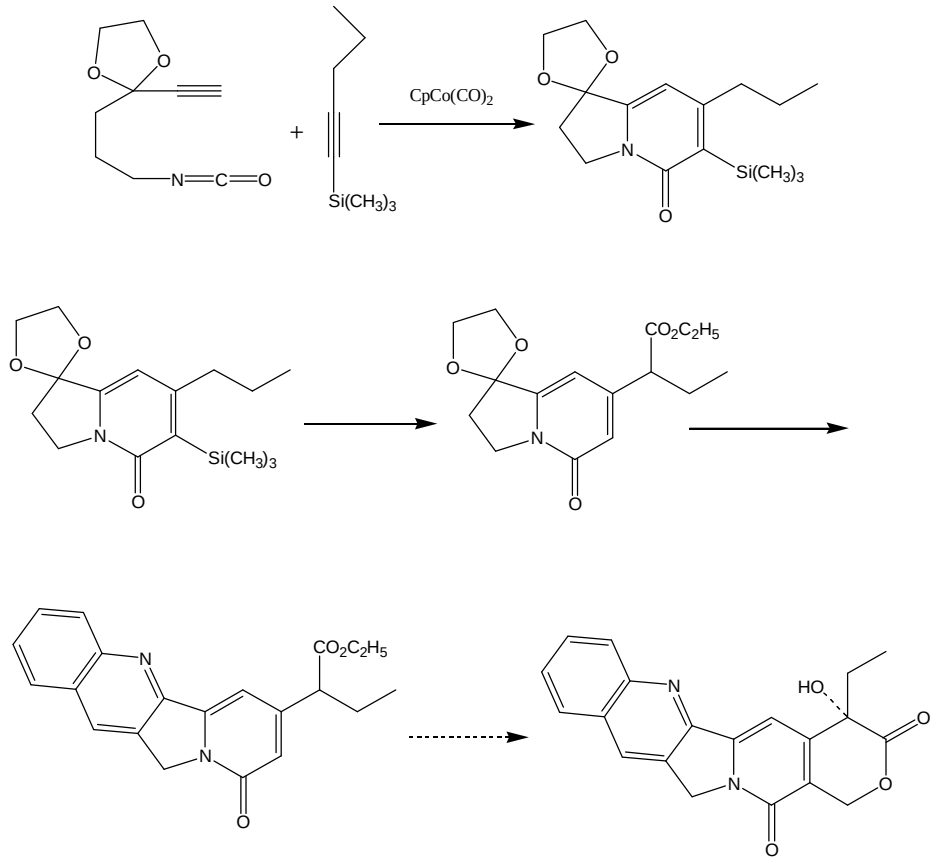

Scheme 2-2. Vollhardt's synthetic scheme of Camptothecin

Unlike the heterocyclotrimerization of alkynes and nitrile molecules, the successful examples of heterocyclotrimerization of alkynes and isocyanate are rare. In most cases, the yields of those transformations were low, and with large amount of benzene derivatives, which comes from cyclotrimerization of alkyne, as side product [23, 24]. There were no reports of new catalysts with improved performance. All of these facts make this transformation not very valuable for synthetic purposes.

Except cyclotrimerization of alkynes to form benzenes, some research shows that the isocyanate molecule could undergo dimerization or trimerization with presence of metal

catalysts [25-29]. And isocynante also could substitute ligands of cobalt catalyst with lone-pair electrons on the oxygen atom binding with cobalt center, which will cause the loss of catalytic activity of catalyst[30].

In this chapter, we will test our new cobalt catalyst, $Cp^{CF3}CoCOD$, under different reaction conditions to determine if 2-pyridones with different functional groups can be prepared.

2. Investigation of the reaction condition for Cyclotrimerization of alkynes and isocyanates

2.1 Reagents Ratio for Cyclotrimerization of alkynes and isocyanate

The initial investigation was to determine if the synthesis of 2-pyridone by $Cp^{CF3}CoCOD$ was a reasonable expectation from this new catalyst system. The first attempt was set up to catalyze the 1,4-dimethoxy-2-butyne and phenyl isocyanate cocyclotrimerization(Scheme 2-3).

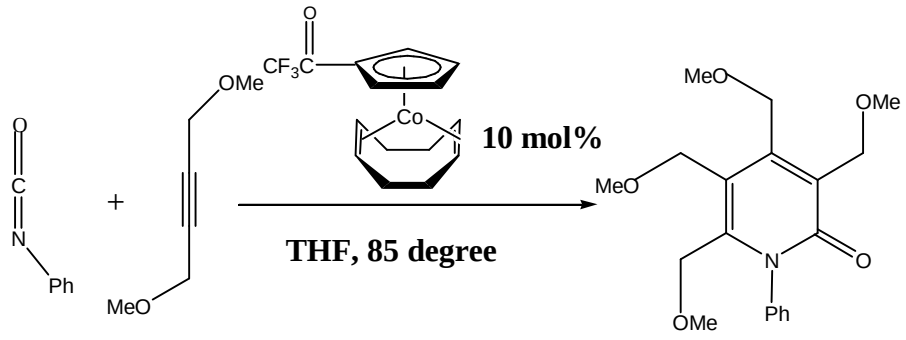

Scheme 2-3. Cocyclotrimerization of 1,4-dimethoxy-2-butyne and phenyl isocyanate by $Cp^{CF3}CoCOD$, **1**.

The first reaction was carried out with two equivalents of 1,4-dimethoxy-2-butyne, **2a**, and one equivalent of phenyl isocyanate with a catalyst loading of 10mol%. The reaction mixture was heated to 85 ˚C and the reaction was monitored by proton NMR. NMR data showed most of 1,4-dimethoxy-2-butyne, **2a**, was consumed. Unfortunately, significant benzene derivative, **7a**, was produce, with about only 7-8% of the heterocyclotrimerization product, **4d**.

Considering this result as competition binding with metal center of 1,4-dimethoxy-2-butyne, **2a**, and phenyl isocyanate, two and half equivalents of phenyl isocyanate and one equivalent 1,4-dimethoxy-2-butyne, **2a** were used to set up the second experiment. The other experimental conditions were identical. After separation by chromatography on the sillca gel, 73% expected 2-pyridone products, **4d,** with 6-7% benezene derivative, **7a,** were obtained.

It seemed the products ratio of this cyclotrimerization depended on the ratio of **2a** and isocyanate. Ten equivalents of phenyl isocyanate and one equivalent **2a** were used for the third attempt to see if better chemoselectivity could be obtained. This time, the yield and the

product ratio were almost the same as second experiment. According to this result, five times excess isocyanate was used for the following experiments.

2.2 Solvent Effect

The initial solvent that was employed for this transformation was anhydrous THF-d_8. In order to examine the solvent effect of this cyclotrimerization, a nonpolar solvent, toluene-d_8, was used. Using identical concentrations of substrates and catalyst for each solvent, the relative rates of cyclotrimeriztion were measured in THF-d_8 and toluene-d_8 (figure 2-2).

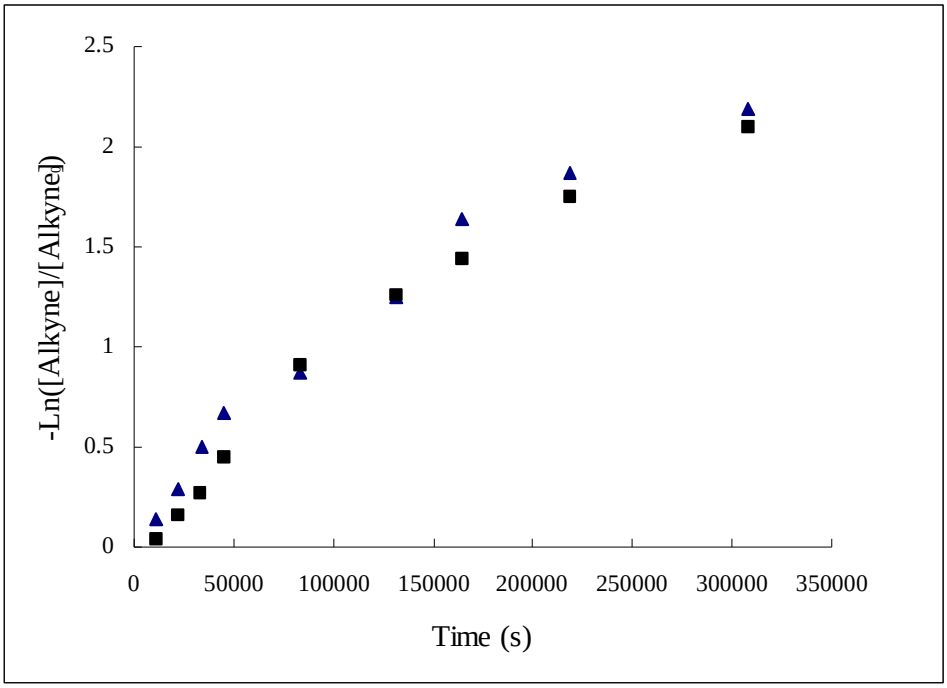

Figure 2-2. The solvent effect of cyclotrimerization of **2a** and phenyl isocyanate to give **4a**. (■) THF, (▲) Toluene.

Within experimental error, the kinetic data of both solvents exhibited very similar rates. Considering toluene has a higher boiling point than THF, it is safer to heat toluene than THF at 85 ˚C. So, toluene was used for the following experiments.

2.3 Reaction Temperature

The last factor we examined was reaction temperature. In order to shorten the reaction time, the reaction temperature was increase to 120 ℃. The reaction time was decrease from about 160 hours to 24 hours. But the 2-pyridone and benzene ratio also dropped to 70:30. If the reaction temperature was lower to 70 ℃, no cyclotrimerization happened. So, the reaction temperature was kept at 85 ℃ for the best 2-pyridone and benzene product ratio.

3.Functional Group Diversity of Cyclotrimerization of Alkynes and Isocyanates

Monitored by NMR, cyclotrimerization of **2a** and phenyl isocyanante revealed a high yield and an unexpected excellent chemoselectivity. The total alkyne conversion percentage is 94.2%, and the yield of 2-pyridone was 86.2% and the yield of benzene was 8%. The ^{1}HNMR spectra of this transformation are shown as figure 2-3.

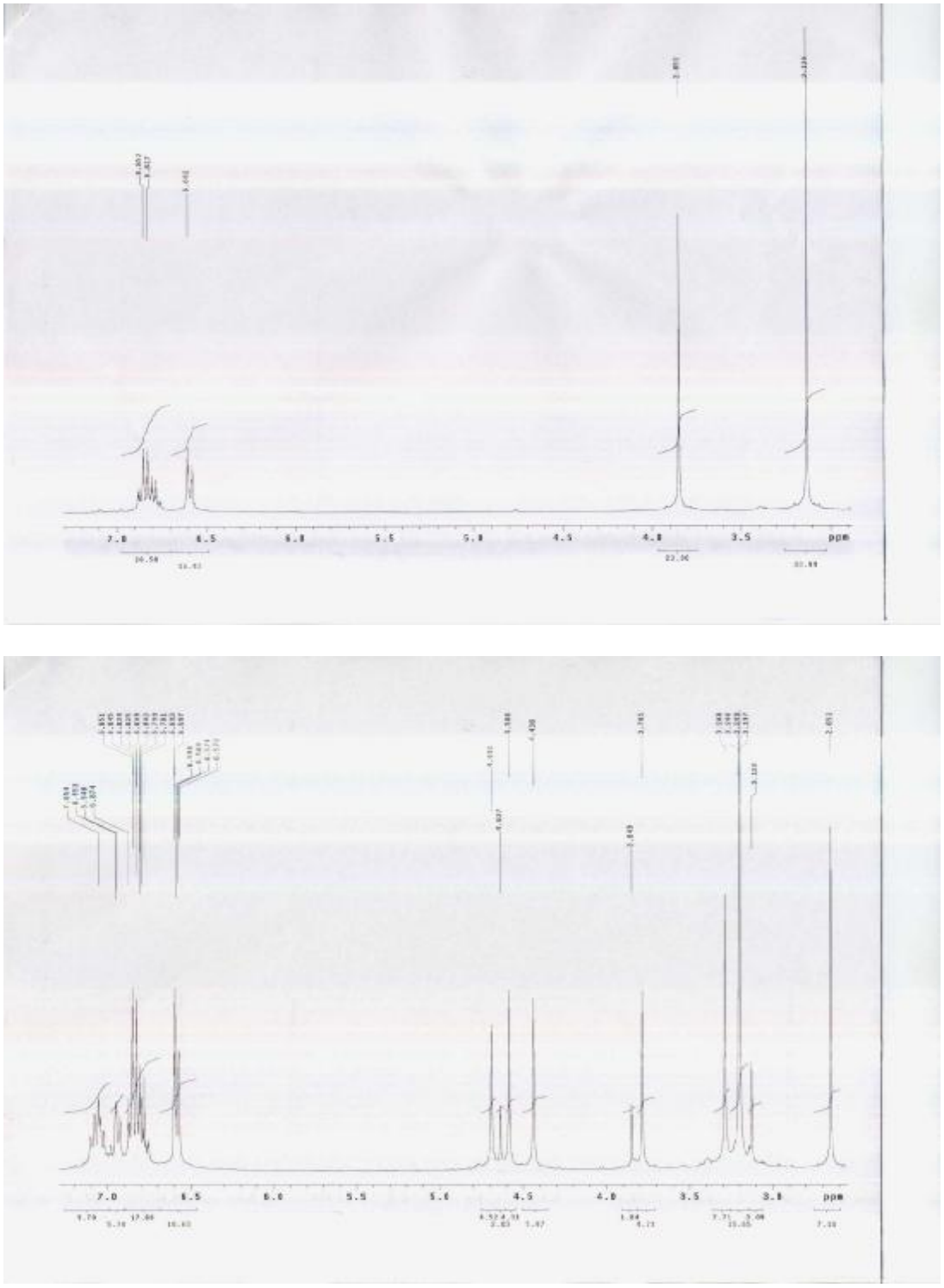

Figure 2-3. [1]HNMR spectra of Cyclotrimerization of **2a** and Phenyl Isocyanate

Spectrum before the cyclotrimerization (above) and Spectrum after the cyclotrimerization (bottom)

On the bottom spectrum, signals at 4.691, 4.586, 4.438 and 3.849 ppm were assigned to methylene hydrogen atoms on carbon **A, B, C** and **D** of 3,4,5,6-Tetrakis-methoxymethyl-1-phenyl-1H-pyridin-2-one **4d,** the 2-pyridone products (figure 2-4, (a)). The signal at 4.637 ppm was for the methylene hydrogen atoms on **E** carbon of 1,2,3,4,5,6-Hexakis-methoxymethyl-benzene, **7a** (figure 2-4, (b))**.**

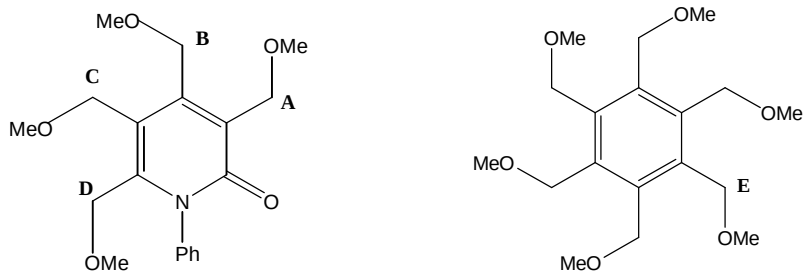

a **b**

Figure 2-4. Structures of 3,4,5,6-Tetrakis-methoxymethyl-1-phenyl-1H-pyridin-2-one, **4d**(a) and 1,2,3,4,5,6-Hexakis-methoxymethyl-benzene, **7a** (b).

From previous work[23, 24] on cyclotrimerization of alkynes and isocyanate, it is known that the yield and regioselectivity of this kind of reactions were very sensitive to the structural variation of the substrates. It was of significant interest to determine if difference of functional groups of substrates were tolerated on this type of cyclotrimerization reaction. Different substituents included ester, ether, aliphatic chains and aromatic rings were tested, and we hoped these experiments would help us to understand the scope and limitation of this cyclotrimerization better.

The reactions were set up with identical experimental conditions and monitored by ^{1}HNMR. Benzene products (scheme 2-5), 2-pyridone products (scheme 2-4) and other aspects of the reactions were investigated.

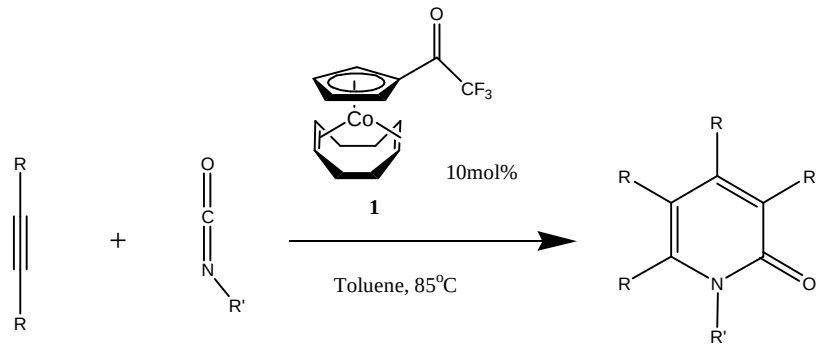

2a: R=CH_2OCH_3
2b: R=COOMe
3c: R=CH_3
3d: R=CH_2CH_3

Scheme 2-4. 2-pyridone products of cyclotrimerization of alkynes and Isocyanates

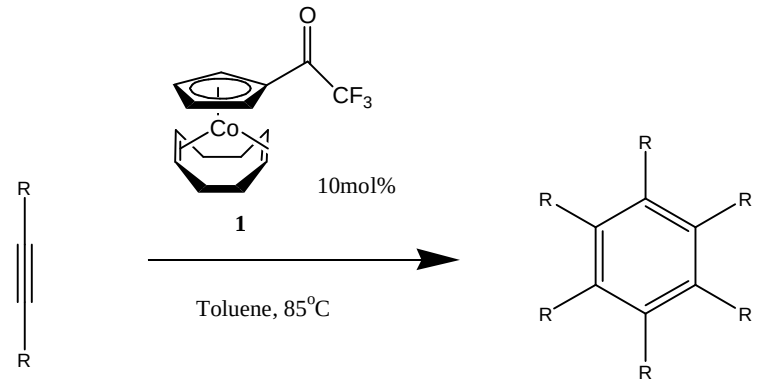

2a: R=CH_2OCH_3
2b: R=COOMe
3c: R=CH_3
3d: R=CH_2CH_3

7a: R=CH_2OCH_3
7b: R=COOMe

Scheme 2-5. Benzene products of cyclotrimerization of alkynes and Isocyanates

Table 2-1. Products from various isocyanates cyclotrimerized with alkynes **2a** under general reaction conditions

Entry	Alkyne	Isocyanate	Time (h)	Yield %* (Conversion)	2-Pyridone Product (%)*	Benzene Product (%)*
1	**2a**		120	91.6%	**4a** (90.7%)	**7a** (0.9%)
2	**2a**		118	94.0%	**4b** (93.3%)	**7a** (0.7%)
3	**2a**	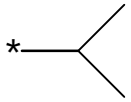	93	95.9%	**4c** (93.2%)	**7a** (2.7%)
4	**2a**	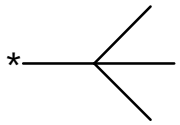	144	74.6%	**4d** (36.8%)	**7a** (37.8%)
5	**2a**	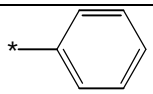	162	94.2%	**4e** (86.2%)	**7a** (8.0%)
6	**2a**	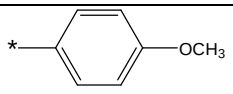	124	91.0%	**4f** (83.3%)	**7a** (7.7%)
7	**2a**		106	90.7%	**4g** (83.7%)	**7a** (7.0%)

* NMR yield

It was not clear if the great chemoselectivity came from an electronic effect, a steric one or a combination of both effects, so two sets of sterically and electronically different isocyanates were chosen for further investigation. One set involved propyl isocyanate, hexyl isocyanate, isopropyl isocyanate and t-butyl isocyanate. The other set included phenyl isocyanate, which had almost the same steric effect as isopropyl isocyanate, 4-methoxy-phenyl isocyanate and 4-fluoro-phenyl isocyanate.

The results of cyclotrimerization of **2a** and isocyanate are shown in the following table (Table 2-1). The reaction time, alkyne conversion yield, the percentage of 2-pyridone products and benzene products are shown.

All the entries except entry 4 showed an excellent alkyne conversion percentage and product ratio, which indicated the high activity and chemoselectivity of catalyst, **1**.

For entry 4, benzene side products were 37.8%, with only 36.8% 2-pyridone products found, according to the NMR spectra. This overall yield and chemospecificity dropping obviously was due to the steric effect.

Comparing entry 5, entry 6 and entry 7, all three aromatic isocyanates had very similar experimental outputs, even though their electronic properties had significant differences. This result suggests that there is little isocyanate electronic effect for cyclotrimerization of alkynes and isocyanate.

It was clear from above data that the product ratio depended on the size of substituent on the isocyanate. The larger group on isocyanate gave more benzene side products. We conclude that steric effect of isocyanate is one of the predominant factors for the process of cyclotrimerization of alkynes and isocyanate.

Another interesting phenomenon was that the cyclotrimerization of **2a** and aliphatic isocyanate was clearly faster than the cyclotrimerization of **2a** and aromatic isocyanate. This phenomenon indicated that the different structures of isocyanates would affect not only the products ratio but also the rate of the transformation.

One the other hand, the substituent effect of alkyne was also an interesting aspect that we investigated in order to understand the cyclotrimerization of lakynes and isocyanate better.

According to the discussion above, it was easy to predict that there must be some level of steric effect for alkynes to cyclotrimerized with isocyanate. The bigger substituents not only prohibit alkyne molecules to come close to metal center and form the cobaltapentadiene intermediate but also hinder the interaction between cobaltapentadiene and isocyanate molecule.

Now, the question was if there was any electronic effect of alkyne for the cyclotrimerization of lakynes and isocyanate. In order to answer this question, 1,4-dimethoxy-2-butyne**, 2a,** dimethyl acetylenedicarboxylate, **2b,** 2-butyne**, 2c** and 3-hexyne, **2d,** were cyclotrimerized with propyl isocyanate under general reaction conditions.

The experimental results were shown in table 2-2. Entry 8 and 9 gave the good yield and products ratios. The slight change of products ratio probably was due to the small steric difference of two alkynes. Surprisingly, Entry 10 and 11 detected no product either of cocyclotrmerization between alkynes and isocyanate or of self-cyclotrimerization on alkyne. Increased the reaction temperature from 85 °C to 100°C gave no reaction.

Table 2-2. Products from propyl isocyanate cyclotrimerized with alkyne 1,4-dimethoxy-2-butyne**, 2a,** dimethyl acetylenedicarboxylate, **2b,** 2-butyne**, 2c** and 3-hexyne, **2d,** under general reaction conditions

Entry	Alkyne	Isocyanate	Time (h)	Yield %* (Conversion)	2-Pyridone Product (%)*	Benzene Product (%)*
8	**2a**		120	91.6%	**4a** (90.7%)	**7a** (0.9%)
9	**2b**		115	90.5%	**4h** (84.9%)	**7b** (5.6%)
10	**2c**		85	00.0%	**4i** (00.0%)	**7b** (0.0%)
11	**2d**		85	00.0%	**4j** (00.0%)	**7b** (0.0%)

* NMR yield

Obviously, the failures of **2c** and **2d** cyclotrimerizing with propyl isocyanate were not caused by a steric effect. We currently have two possible explanations for these failures. First, without the appearance of electron withdrawing group, the electron densities of alkynes' triple bonds are not deficient enough to undergo oxidative coupling reaction, so no

cobaltacyclopentadiene intermediate was produced during the experimental period. The other possibility is that the cobaltacyclopentadiene intermediate is not active enough to react with isocyanate or another alkyne molecules, even though it could be form during the reaction.

From current experimental data, we could conclude that both steric and electronic effects of alkynes could influence the efficiency of cyclotrimerization of alkyne and isocyanate.

Diyne molecules have been used widely in different types of cyclotrimerization reactions. Two triple bonds were connected with carbon or other atom chain (oxygen, nitrogen, sulfur, etc), which could dramatically lower the transition energy of the process that alkyne molecules bind with the metal center. Normally, compared to mono-alkynes, diyne molecules could undergo cyclotrimerization reaction under milder reaction condition and provide higher yields[25]. Moreover, the connection of the triple bonds also restricted the number of regioisomers of cobaltacyclopentadiene intermediates. The cyclotrimerization involving diyne molecule has been used to construct various bicyclic compounds. All these aspects of diynes make them very important molecules for practically synthetic goal.

Unfortunately, under some circumstance, with the presence of a metal catalyst, diyne molecules undergo competing side reactions like dimerization, trimerization and oligomerization[31]. Sometimes, these side reactions will decrease the yield to an unacceptable level.

In order to examine the activity of our new catalyst, **1**, for cyclotrimerizing diyne and isocyanate, propargyl ether, **5a**, 2,2-Di-prop-2-ynyl-malonic acid dimethyl ester, **5b**, 1,6-heptadiyne, **5c**,and 1,7-octadiyne, **5d** were set up to cyclotrimerize with either phenyl

isocyanate or propyl isocyanate (Scheme 2-6) under general experimental conditions discussed previously.

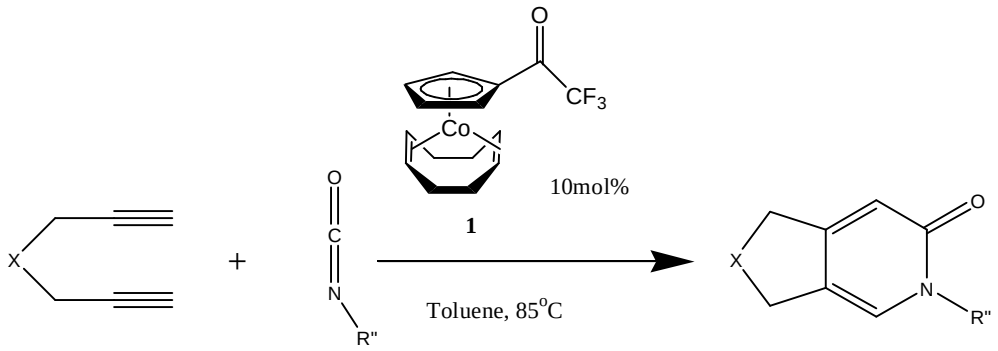

5a: x = O
5b: x = $C(COOMe)_2$
5c: x = C
5d: x = C_2

6a: x = O; R"=$CH_2CH_2CH_3$
6b: x = $C(COOMe)_2$**;**
R"=$CH_2CH_2CH_3$
6c: x = C; R" = Phenyl
6d; x = C_2; R" = Phenyl

Scheme 2-6. Cyclotrimerization of various diynes and propyl or phenyl isocyanates

The NMR spectra of the crude reaction mixture for these entries were very complicated. So, it was not suitable to determine the yield with NMR spectra. The only thing we saw from the NMR spectra was all the diynes were consumed after the reaction. The abundance of signals in the aliphatic and olefinic regions also indicated the dimmer, trimer or oligmer of diynes.

After complete reaction, chromatography was used to separate the reaction mixture. Only the 2-pyridone products were collected and characterized. There were several benzene isomers to be possibly produced. All the benzene isomers and oligomer mixtures were not

separated completely by using regular column chromatography techniques. It is still not clear what kind of structures the rest of the diyne was converted to.

Table 2-3. 2-pyridone products from cyclotrimerization of propargyl ether, **5a**, 2,2-Di-prop-2-ynyl-malonic acid dimethyl ester, **5b**, 1,6-heptadiyne, **5c**,and 1,7-octadiyne, **5d** with either phenyl isocyanate or propyl isocyanate

Entry	Alkyne	Isocyanate	Time (h)	Yield %* (Conversion)	2-Pyridone Product (%)**	Benzene Product (%)
12	**5a**		66	100%	**6a** (77.5%)	N/A
13	**5b**		60	100%	**6b** (89.2%)	N/A
14	**5c**	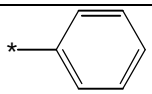	78	100%	**6c** (65.0%)	N/A
15	**5d**	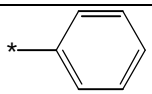	60	100%	**6d** (34.0%)	N/A

** Isolated yield

The isolated yields of cyclotrimerizations of various diynes with either phenyl isocyanate or propyl isocyanate were reported in Table 2-3.

The reaction times of all the entries were much shorter than the time needed to complete the cyclotrimerization of alkyne and isocyanate. This phenomenon was consistent with the

above statement made for the diyne cyclotrimerization. The tether made the binding between two triple bonds and the cobalt metal facile.

The 2-pyridone products were produced in moderate to excellent yields. With only one more carbon on the tether, the yield of **6d** dropped dramatically. This result was consistent with Vollhardt's previous report about cyclotrimerizing diyne with isocyanate with $CpCo(CO_2)_2$ catalyst. The yield distribution of all four entries probably was due to the Thorpe - Ingold effect[32-34]. **5b** with the tertiary carbon in the tether giving the highest yield.

In our above discussion, 2-butyne, **2c** and 3-hexyne**, 2d** failed to cyclotrimerize with propyl isocyanate. We have two possible explanations for these failures. The experimental data of diyne cyclotrimeriztion give us a chance to judge these two possibilities. If the cobaltacyclopentadiene intermediates of **2c** and **2d** could be generate, the steric and electronic properties should be very similar as the cobaltacyclopentadiene intermediates of **5c** and **5d.** Unlikely, these intermediates would undergo no reaction. So, the only reasonable explanation right now is no cobaltacyclopentadiene intermediate was produced during the experimental period.

4. Mechanistic Investigation of Cocyclotrimerization of Alkynes and Isocyanates to Form 2-Pyridones

Previous mechanistic investigations[36-38] involving cobalt catalyzed benzene and pyridine formation provide a suitable background within which to view the analogous reaction to prepare 2- pyridones. Since this cocyclotrimerization transformation requires excess phenyl isocyanate, the first investigation is to examine whether the phenyl isocyanate molecule is involved in any rate determine steps among the catalytic cycle.

The experiments were carried out with 5 times exceeding phenyl isocyanate and 20 times exceeding phenyl isocyanate(Figure 2-5) under the same reaction volume and concentrations of catalyst and alkyne in toluene-d_8. The reactions were monitored by ^{1}HNMR and ^{19}FNMR, and the kinetic data were collected over three half-life periods.

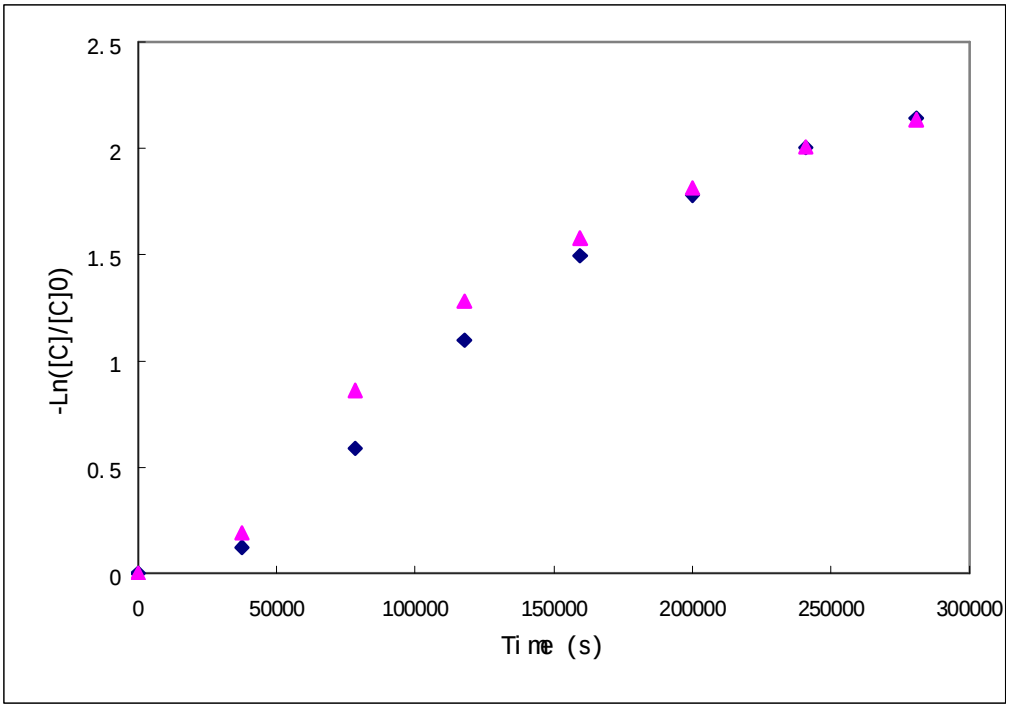

Figure 2-5. Plot of cocyclotrimerization of 1,4-dimethoxy-2-butyne with phenyl isocyanate by Cp^{CF3}CoCOD with excess isocyanate. (Triangles represent the data for 20 times excess isocyanate; diamonds represent the data for 5 times excess isocyanate)

Within experimental error, both experiments showed very similar rates, which proved that the reaction rate of cocyclotrimerization of 1,4-dimethoxy-2-butyne and phenyl isocyanate was not dependent on the concentration of phenyl isocyanate.

A possible associative mechanism of cyclotrimerization for the alkynes and isocyanate is proposed in scheme 2-7.

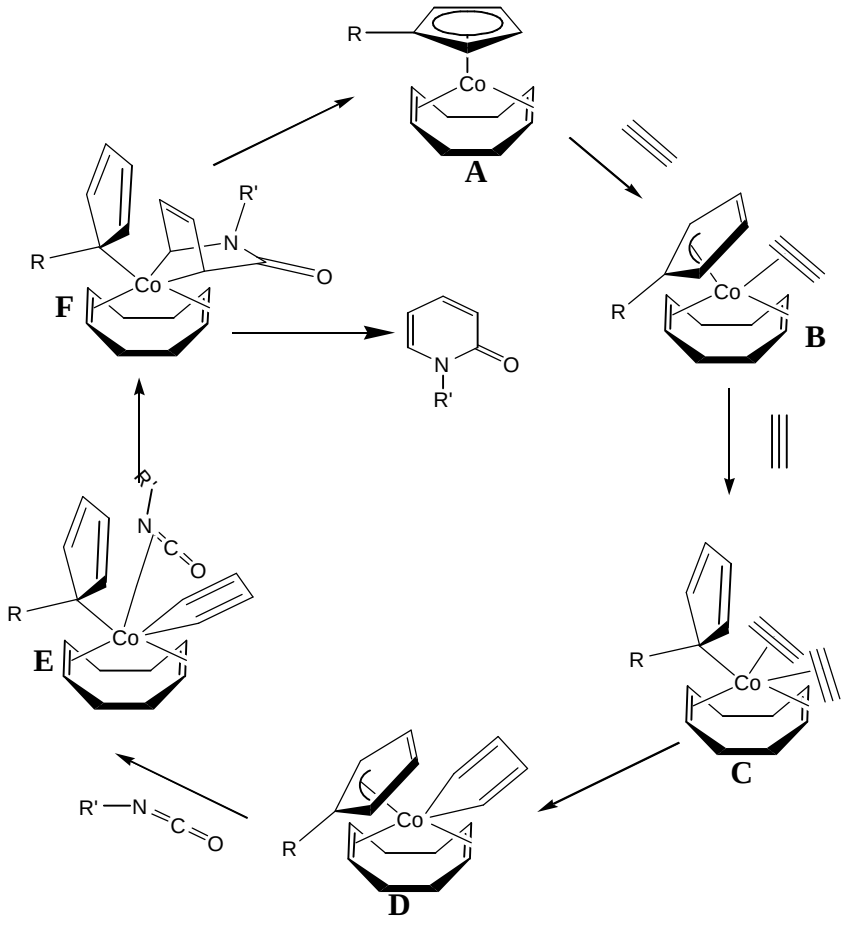

Scheme 2-7. Proposed mechanism of two alkynes and one isocyanate to form 2-pyridone (**R=COCF$_3$**)

The reaction was initiated by the substituted Cp ring of Cp^{CF3}CoCOD slipping from η^5 to η^3 coordination pattern, which opens a vacant coordination site for the first alkyne (intermediate **A**). A second alkyne could then coordinate by further Cp slippage from η^3 to η^1 coordination pattern (intermediate **B**). Oxidative coupling of two alkyne ligands to form the

cobaltapentadiene with Cp ring slips back from η^1 to η^3 gives the cobaltacyclopentadiene intermediate **D**. Subsequently, the Cp ring slips from η^3 to η^1 again and is followed by the isocyanate molecule binds with cobalt center, which is shown as intermediate **E**. The isocyanate undergoes some sort of Diels-Alder addition to form the intermediate complex **F**. Reductive elimination of **F** would give the product, and the slippage of the Cp ring from η^1 to η^5 would regenerate the resting state of the catalyst.

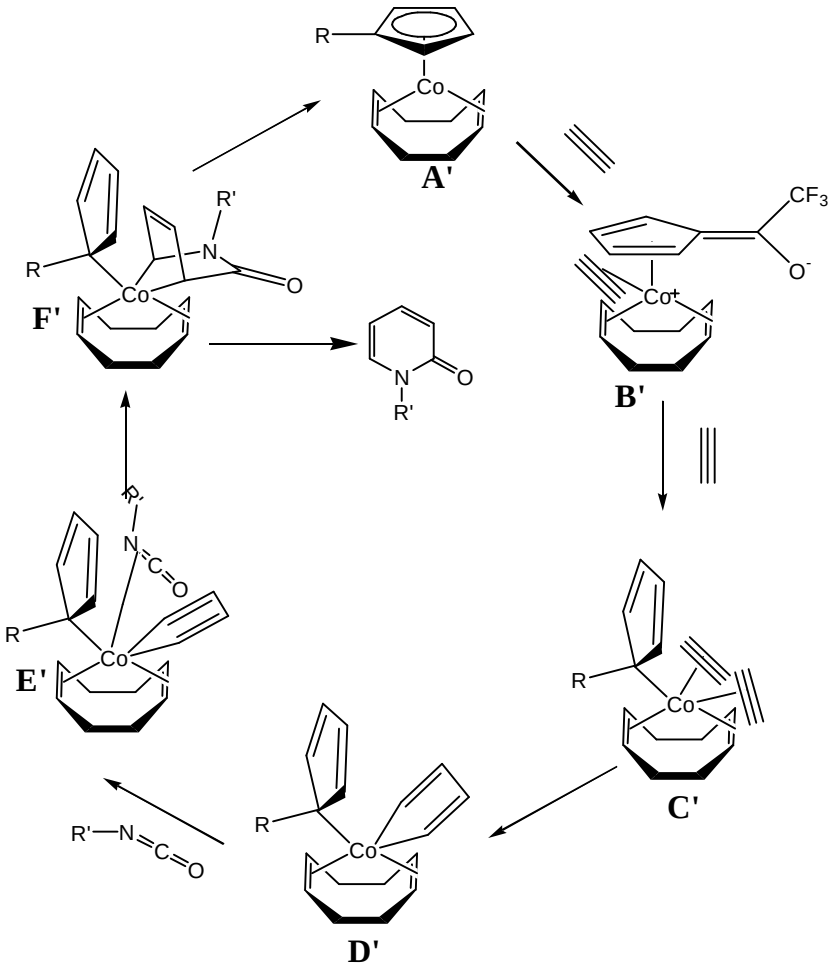

Scheme 2-8. Alternative mechanism of two alkynes and one isocyanate to form 2-pyridone (**R=COCF$_3$**)

Depends on our x-ray structural investigation for $Cp^{CF3}CoCOD$, an alternative mechanism is also proposed here.

Catalyst **A'** is converted to a coordinatively unsaturated 16e complex through a conjugated effect. Then, an alkyne molecule binds with cobalt center to give intermediate **B'**. The Cp ring could slip from η^4 to η^1 to give the vacant coordination site for the second alkyne with the enolate group becoming neutral carbonyl group (intermediate **C'**). Oxidative coupling of two alkyne ligands to form the cobaltapentadiene gives the cobaltacyclopentadiene intermediate **D'**. Subsequently, the isocyanate molecule binds with cobalt center (intermediate **E')**. The isocyanate undergoes Diels-Alder addition to form the intermediate complex **F'**. Reductive elimination of **F'** would give the product, and the slippage of the Cp ring from η^1 to η^5 would regenerate the resting state of the catalyst.

Since reaction rate was not dependent on the concentration of phenyl isocyanate, the binding of isocyanate with cobalt center and the following addition or insertion steps would not be the rate-limiting step. And the consuming rate of alkyne is definitely not constant. That excludes the ring slippage step as the rate-limiting step. So, probably, the rate depends on the formation of cobaltacyclopentadiene intermediate. But it is still not clear which on is the rate-limiting step, the binding of first and second alkyne or the oxidative coupling step.

5. Conclusions

In summary, the applicability of cyclotrimerization between alkyne and isocyanate with new cobalt catalyst, $Cp^{CF3}CoCOD$, has been investigated. It turns out highly functionalized 2-pyridones could be formed under very mild experimental conditions with excellent yields and incredible chemospecificity. The yield and product distribution depends greatly on the steric

and electronic effects of alkyne. Meanwhile, it seems there are also steric effect of isocyanate on the rate of the cyclotrimerization reaction.

The possibility of cyclotrimerizing diyne and isocynante has also been examined. Overall, moderate to good yields were obtained for various diyne compounds. And the yield of 2-pyridones seems to be controlled by the Thorpe - Ingold effect. The kinetic experiments showed there is no solvent effect for cyclotrimerization between alkyne and isocyante, and the reaction rate is independent of the concentration of isocyanate. An associative Cp ring slippage mechanism has been proposed for cyclotrimerization of alkyne and isocyante.

With the effective performance, it is anticipated that catalyst, Cp^{CF3}CoCOD, will find significant utility in the synthesis of various bioactive and pharmaceutical-useful 2-pyridone structures.

6. References

1) Slater, Y. E.; Houlihan, L. M.; Maskell, P. D.; Exley, R.; Bermudez, I.; Lukas, R. J.; Valdivia, A. C.; Cassels, B. K. *Neuropharmacology* **2003**, *44(4)*, 503.

2) Darvesh, Sultan; Walsh, Ryan; Martin, Earl. *Cellular and Molecular Neurobiology* **2003**, *23(1)*, 93.

3) Dingemanse, Jasper; Pedrazzetti, Elisabetta; van Giersbergen, Paul L. M. *Clinical Neuropharmacology* **2001**, *24(2)*, 82.

4) (a) Teshima, Y.; Shin-ya, K.; Shimazu, A.; Furihate, K.; Chul, H.S.; Furihata, K.; Hayakawa, Y.; Nagai, K.; Seto, H. *J. Antibiot.* **1991**, *44*, 685; (b) Cai, P.; Smith, D.; Cunningham, B.; Brown-Shimer, S.; Katz, B.; Pearce, C.; Venables, D.; Houck, D. *J. Nat. Prod.* **1999**, *62*, 397.

5) (a) Pastelin, G.; Mendez, R.; Kabela, E.; Farah, A. *Life Sci.* **1983**, *33*, 1787; (b) Altomare, C.; Cellamare, s.; Summo, L.; Fossa, P.; Mosti, L.; Carotti, A. *Bioorg. Med. Chem.* **2000,** *8*, 909

6) Eliopoulos, G. M., Wennersten, C. B.; Cole, G., Chu, D.; Pizzuti, D.; Moellering, Jr. R. C. *Antimicrobial Agents And Chemotherapy* **1995**, *35(4)*. 850

7) Li, Q.; Mitscher, L.A.; Shen, L.L. *Med. Res. Rev.* **2000**, *20*, 231

8) Anderson, W. K.; Dean, D. C.; Eado, T. *J. Med. Chem.* **1990,** *33*, 1667

9) Margolin, S. B. US Patent 5,962, 478, 1999.

10) Drgovich, P. S.; Prins, T. J.; Zhou, R.; Brown, E. L.; Maldonado, F. C.; Fuhrman, S. A.; Zalman, L. S.; Tuntland, T.; Lee, C. A.; Patick, a. K.; Mattews, D. A.; Hendrickson, T. F.; Kosa, M. B.; Liu, B.; Batugo, M. R.; Gleeson, J. P. R.; Sakata, S. K.; Chen, L.; Guzman, M. C.; Meador, J. W., III; Ferre, R. A.; Worland, S. T. *J. Med. Chem.* **2002,** *45*, 1607.

11) Drgovich, P. S.; Prins, T. J.; Zhou, R.; Johnson, T. O.; Brown, E. L.; Maldonado, F. C.; Fuhrman, S. A.; Zalman, L. S.; Patich, A. K.; Mattews, D. A.; Hou, X.; Meador, J. W.; Ferre, R. A.; Worland, S. T. *Bioorg. Med. Chem. Lett.* **2002,** *12*, 733.

12) Patankar, S. J.; Jurs, P. C. *J. Chem. Inf. Comput. Sci.* **2002,** *42*, 1053.

13) 13Mijin, Dusan Z.; Uscumlic, Gordana S.; Perisic-Janjic, Nada U.; Valentic, Natasa V. *Chem. Phys. Lett.* **2006**, *418(1-3)*, 223

14) Karcl, Fikret. *Color. Tech*. **2005**, *121(5*), 275

15) Uscumlic, Gordana S.; Mijin, Dusan Z.; Valentic, Natasa V.; Vajs, Vlatka V.; Susic, Biljana M. *Chem. Phys. Lett.* **2004**, 397(1-3), 148.

16) Hazra, Montu K.; Chakraborty, Tapas *J. Phys. Chem*. A **2006**, *110(29),* 9130

17) de Candia, Modesto; Fossa, Paola; Cellamare, Saverio; Mosti, Luisa; Carotti, Angelo; Altomare, Cosimo. *Eur. J. Pharm. Sci.* **2005**, *26(1),* 78

18) Esboui, M.; Nsangou, M.; Jaidane, N.; Ben Lakhdar, Z. *Chem.Phys.* **2005**, *311(3),* 277

19) Hong, P.; Yamazaki, H. *Tetrahedron Lett.* **1977**, 1333.

20) Hoberg, H.; Oster, B. W. *J. Organomet. Chem.* **1982**, *234*, C35.

21) (a)H. Bonnemann, *Angrew. Chem. Int. Ed. Engl*. **1978**, *17*, 505; (b) Diversi, P.; Ingrosso, G.; Lucherini, A.; Malquori, S. *J. Mol. Catal.* **1987**, *40*, 267

22) Earl, R. A.; Vollhardt, K. P. C. *J. Org. Chem.*, **1984**, *49*, 4786.

23) Diversi, P.; Ingrosso, G.; Lucherini, A. Malquori, S. *J. Mol. Cat.***1987**, *40*, 267

24) Montilla, F. Clara, E. Aviles, T. Casimiro, T. Ricardo, A. daPonte, M. N. *J. Organomet. Chem.* **2001**, *62*, 227.

25) Hoberg, H.; Oster, B. W. *J. Organomet. Chem.* **1983**, *252*, 359.

26) Braunstein, P.; Nobel, D.; *Chem. Rev.* **1989**, *89*, 1927.

27) Ozaki, S. *Chem. Rev.* **1972**, *72*, 457.

28) Ulrich, H. " Cycloaddition Reaction of Heterocumulenes"; Academic Press; New York, 1967

29) " The Chemistry of Cyanates and Their Thio Derivatives"; Patai, S., Ed.; Wiley-Interscience: New York, 1977; Parts 1 and 2

30) Kakoschke, A.; Yong, L. Wartchow, R. Butenschon, H. *J. Organomet. Chem.* **2003,** *674(1-2)*, 86.

31) Hoberg, H.; Oster, B. W. *Synthesis* **1982**, 324.

32) Searles, S., Jr.; Lutz, E. F.; Tamres, M. *J. Am. Chem. Soc.* **1960**, *82*, 2932

33) Jager, J.; Graafland, T.; Schenk, H.; Kirby, A. J.; Engberts, J. B. F. N. *J. Am. Chem. Soc.* **1984**, *106(1)*, 139

34) Kaneti, J.; Kirby, A. J.; Koedjikov, A. H.; Pojarlieff, I. G. *Organ. & Biomol. Chem.* **2004**, *2(7)*, 1098

35) Taylor, Edward C.; Macor, John E. *Tetrahedron Lett.* **1986,** *27(19)*, 2107.

36) Eaton, E. B.; Fatland, A. W. *Organic Letters* **2000**, *2(20)*, 3131.

37) Eaton, E. B.; Fatland, A. W.; Sigman, M. S. *J. Am. Chem. Soc.* **1998**, *120*, 5130.

38) Unpublished result in Eaton group.

CHAPTER THREE

NEW LINKAGE CHEMISTRY FOR RNA MEDIATED NANOPARTICLE GROWTH ON GOLD SURFACE

1.Background of RNA Mediated Nanoparticle Growth On Gold Surfaces

1.1 RNA in vitro selection

It is well known that Ribonucleic acid (RNA) molecules, as a type of highly functioned biopolymer, have been shown high binding affinities and catalytic activities to various proteins, organic molecules or other biomolecules[1-15]. Different RNA molecules have demonstrated the ability of substrate binding specificity[16, 17] and stereospecific product formation[18]. These features make RNA a useful platform for discovering new catalysts and carrying out new transformations.

RNA's binding or catalytic properties are determined greatly by three-dimensional structure. Different sequence RNA molecules fold up to three-dimensional structure with intricate binding pockets and active sites. We do not have enough knowledge to understand the relationship between sequence and three-dimensional structure. So, it is impossible to design a sequence with a desirable property directly. If a random pool of RNA sequences is applied to certain target, normally, only very small fraction of sequences in a random population will bind with the target molecule or catalyze a chemical transformation. Most sequences will have no special activity to the target molecule. With conventional methods, it is hard to separate this extremely small numbers of active RNA sequences from a very large candidate pool. RNA in vitro selection[18-25] methodology has been used to study this problem.

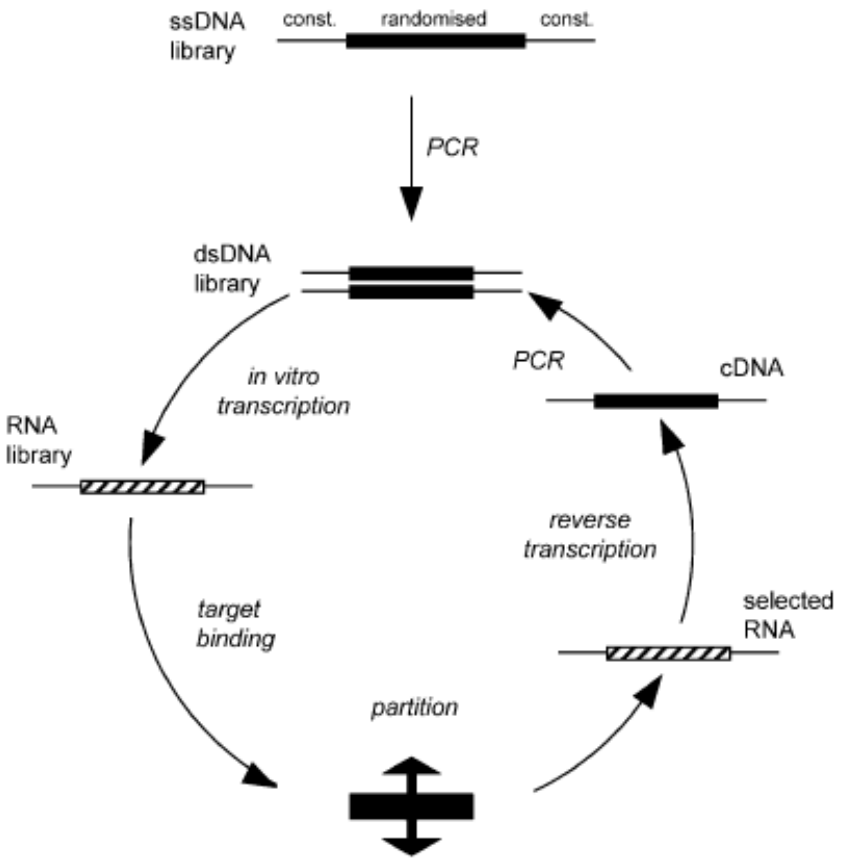

Figure 3-1. Steps of general RNA in vitro selection cycle[26]

The general process of RNA in vitro selection is shown in Figure 3-1. It starts from an ssDNA library sequence, which is made chemically on an automated DNA synthesizer. There is a fixed region at each end of the sequences and completely random sequences in the middle region. The fixed regions are required for the enzymes used in the following amplification steps, and the random region provides enough sequences for the candidate pool (40 random nucleotides bases will give about 10^{24} different sequences). The starting ssDNA library is converted to a dsDNA library by 2-cycle PCR. dsDNA template is transcribed to generate a new ssRNA library by using RNA polymerase. In the next step, this ssRNA

library is applied to the target, like proteins or small organic molecules. The active sequences will bind to the target molecules or bind with the product coming from target molecules. The active sequences and inactive sequences will be partitioned in the following step through a suitable separation method (membrane size exclusion, electrophoresis gel-mobility shift, HPLC, dialysis, etc). After isolation the active sequences are reverse transcribed by reverse transciptase to produce the cDNA sequences. This cDNA is amplified to give a new dsDNA library by a standard PCR procedure. And this new library is ready to enter the next cycle of selection at in vitro transcription step.

If the partition step is 100% effective, the new dsDNA library will contain only the active sequences. Practically, there always is some inactive ssRNA sequences will be carried along to the next step and be amplified with the active ones. So, typically, this selection cycle will be repeated to decrease the population of inactive sequences. It normally takes 8 to 16 cycles to obtain a convergence on the functional sequences, which will consist of only about 10 to 100 functional sequences.

The functional dsDNA sequences could be used in a standard plasmid cloning procedure and the *E. Coli* colonies containing individual sequences are isolated. Sequencing the isolated DNA from colonies could provide the data for further comparison, grouping and characterization of the active sequences, which could help us to understand the behavior of RNA better. Then, each RNA sequence could be synthesized chemically or enzymatically for more investigation.

After the RNA in vitro selection methodology was established, the narrow range of RNA-catalyzed reactions was subsequently expanded. Specific RNA sequences were selected for all types of reactions including acyl transfers[27-30], peptidy transfers[31], ester and

amide bond formation[32, 33], cofactor synthesis[34], Michael additions[35], nucleophilic substitutions[36], prophyrin metallations[37, 38] and Diels-Alder cycloaddition[39-42], etc.

1.2 Shape-controlled and Size-controlled Nanoparticle

Due to their special properties and unique advantages, nanoparticles become more and more important in today's material science field. Different types of nanoparticles have been applied as catalyst[43], and photocatalyst[44]. They have applications in optical[45], magnetic[46], and electronic[47] devices and are also used for drug delivery[48]. It is not surprising that the properties of nanoparticles depend critically on the composition, the size, and the shape of nanoparticles themselves[49]. Therefore, establishing a methodology to synthesize nanoparticle with well-controlled shape and size is important. There are a lot of studies focusing on the size control[50] and growth kinetics[51]. Meanwhile, the report for shape-controlled nanoparticle is rare[52].

Current methods for nanoparticle formation, typically, include combination of a handful of inorganic salts. The salts, as precurors, are reduced and the reaction mixture is heated to high temperature. At the same time, some capping materials are added to stabilize the fresh-formed nanoparticles.

It is normal that the desired property is not found after a lot of time and money are spent to optimize the nanoparticle formation conditions. The possibility of all nanoparticles with different composition, size and shape is countless. These facts make construction and examination every possible nanoparticle impossible. A new methodology has to be established in order to screen nanoparticles with desired property in a more efficient manner.

1.3 RNA Mediated Nanoparticle Growth

Although RNA has been used successfully in organic transformations, protein binding and other biochemical processes, there are little reported concerning the RNA evolution approach to inorganic materials synthesis. Recently, Eaton and Feldheim groups reported a discovery of RNA sequences that could catalyze the formation of Pd or Pt nanoparticles by using a RNA in vitro selection method[53-55].

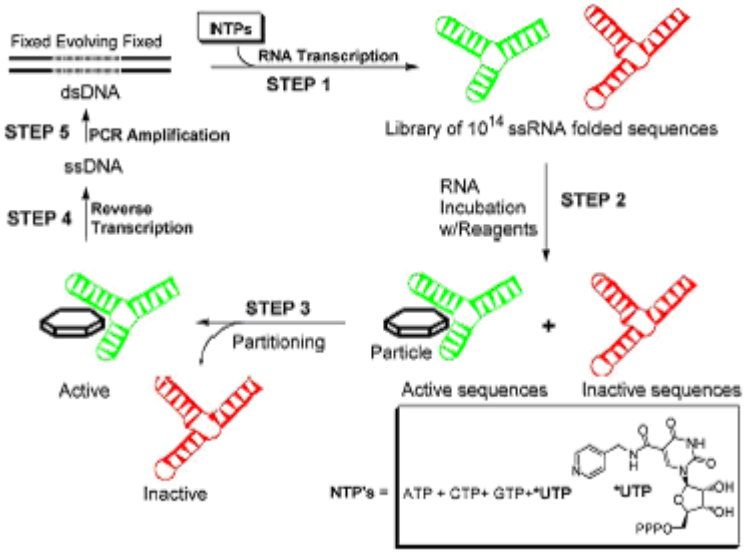

Figure 3-2. Steps of the RNA in vitro selection cycles for nanoparticle formation[53]

The RNA in vitro selection began with a library of 10^{14} unique ssDNA (87 bp in length with 40 bp as random region). 2-cycle PCR was used to convert ssDNA pool to dsDNA pool. T7 RNA polymerase was used to transcribe dsDNA pool into ssRNA pool. In order to provide extra metal coordination sites, 5-(4-pyridylmethyl)-UTP was used instead of native UTP during the T7 RNA polymerase transcription step. The RNA library was incubated with

$Pd_2(DBA)_3$. Membrane size exclusion, and electrophoresis gel-mobility shift were used for partition. The winning RNA sequences were reverse-transcribed to cDNA by AWV-reverse transcriptase.

The selection cycle was repeated 8 times and hexagonal Pd nanoparticles were synthesized with the presence of RNA molecules with special sequence Figure 3-3.

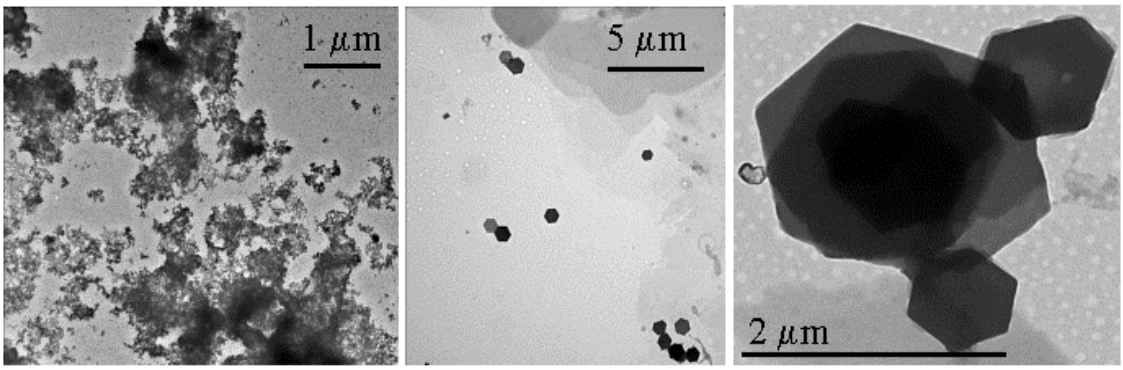

Figure 3-3. Transmission electron micrograph images of palladium particles formed in the presence of cycle 0 RNA (left), and the evolved cycle 8 RNA pool (middle and right)[53]

The evolved dsDNA library from the last cycle was cloned and sequenced. The active sequences were divided into families according to the conserved regions (figure 3-4).

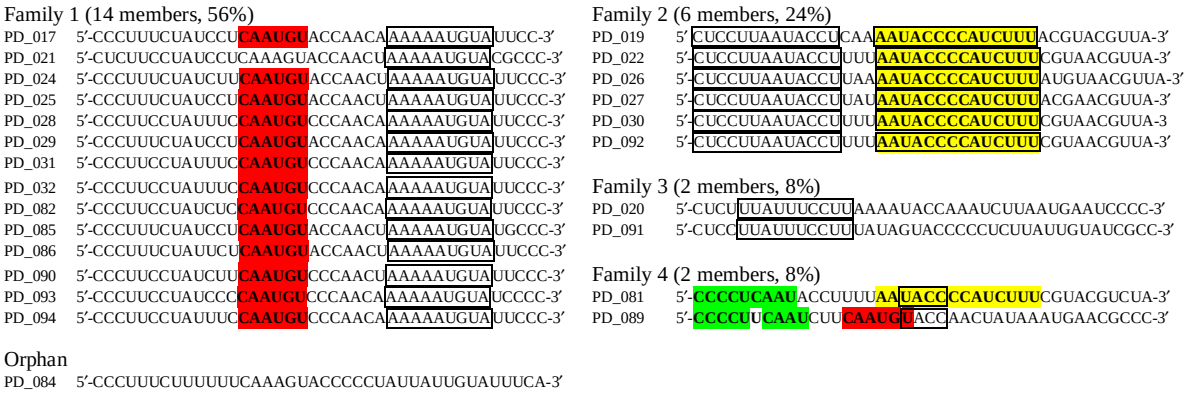

Figure 3-4. RNA sequences capable of catalyzing the formation of hexagonal palladium platelets. Highly conserved regions are outlined in boxes[53].

Two isolate sequences, isolate 17 and isolate 34 (Figure 3-5)[55], were selected to grow Pd nanoparticles individually. After incubated with $Pd_2(DBA)_3$, isolate 17 sequence gave hexagonal platelets, while isolated 34 sequence provided cubic nanoparticles. This result demonstrated that RNA in vitro selection could be used to find special sequences not only for size-controlled nanoparticle formation but also for shape-controlled nanoparticle formation.

Isolate 17: 5'-CCCUUUCUAUCCUCAAUGUACCAACAAAAAAUGUAUUCC-3'

Isolate 34: 5'-UCCAACAUCUUUUAAUUUUGUGGCGUCCACAUAUCAUCCA-3'

Figure 3-5. Isolated RNA Sequence for Hexagonal (Isolate 17) and cubic (Isolate 34) Pd nanoparticles

RNA in vitro selection turns out to be a very remarkable and efficient methodology, if only one RNA sequence in about 10^{12} works to form the nanoparticle, it could be selected out and amplified during a reasonable time scale.

1.4 RNA Mediated Nanoparticle Growth on Gold surface

Introducing catalytic RNA onto the surface would make possible a solution to building well-ordered nanoscale chips and devices. To construct nanoscale devices, different functional nanomaterials are required to be combined together with precise positioning[56-58]. Currently, this requirement is satisfied by coating the nanomaterials with organic molecules or biomolecules, like ssDNA[59, 60]. With the interaction among coating molecules, nanomaterials could be linked with each other in the pattern needed.

With catalytic the RNA strategy, the relevant catalytic RNA molecule could be printed on the surface at the spot where certain nanomaterial needs to be for functional devices. Then, the nanoscale materials are synthesized under the help of catalytic RNA. If all the RNA sequences could work appropriately, nanoparticle arrays or other nanomaterials devices will be constructed. Combined with the powerful RNA in vitro selection methodology, this strategy should be an attractive approach for material science.

In order to maintain the catalytic activity to make excepted nanoparticles, keeping appropriate folding structure of RNA is necessary. Previous reports[61, 62] showed that RNA could interact with many metal surfaces. This interaction could disturb the three dimensional structure of RNA. RNA that is denatured will lose its catalytic activity if it is bound to a metal surface directly. Our control experiment also verified that if RNA molecules bind with gold surface directly, no shape-controlled nanoparticles were observed.

Blockers are needed to prevent RNA molecules from losing their activities on the metal surface. Blockers are used to bind onto metal surface with appropriate density. Large molecules, like RNA or DNA should not penetrate blocker layer, so the interaction of RNA and metal surface is minimized. In order to attach the RNA covalently, linker molecules, which could connect RNA and the metal surface, are necessary.

2. Improved Synthesis of 12-thioacetic 3,6,9-trioxadodecane-1-maleimide

The normal attachment strategy is showed in figure 3-6. A linker with free thiol group at one terminal and maleimide group at the other terminal is used. Linker molecules were first assembled onto gold surfaces with the thiol terminal. And 5'-phosphorothioate-modified RNA covalently coupled with maleimide double bond through a Michael addition reaction. In this strategy, the linker molecules are also used as blocker at the same time.

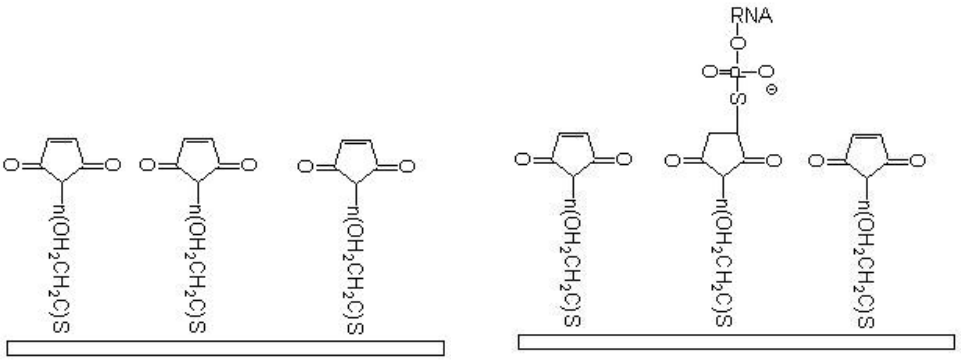

Figure 3-6. General attachment strategy of maleimide linker and 5'-phosphorothioate-modified RNA on gold surfaces

A synthetic scheme (scheme 3-1) was used in Feldheim group to make the linker molecule, 12-thioacetic 3,6,9-trioxadodecane-1-maleimide **11**.

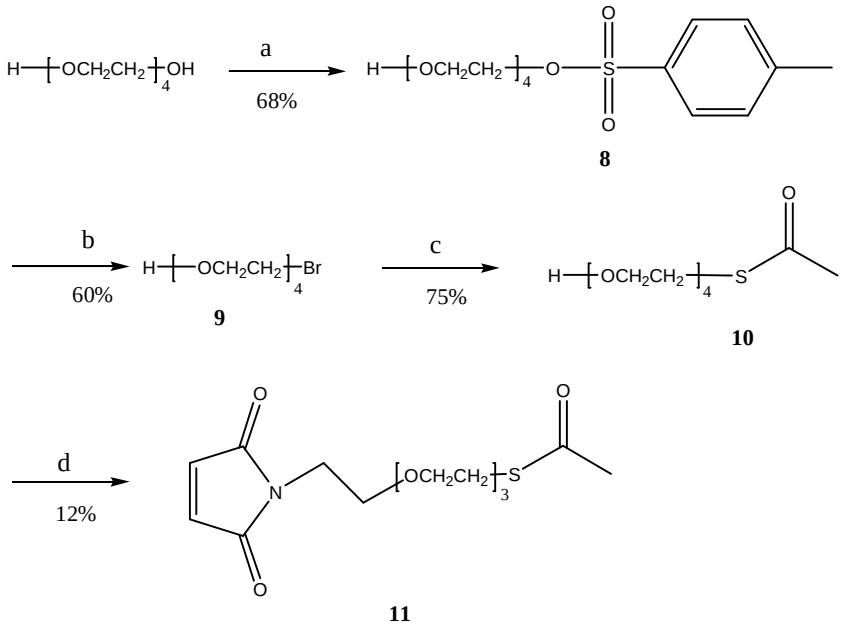

(a) p-toluenesulfonyl chloride, triethylamine, acetonitrile; (b) LiBr, acetone, 80˚C;

(c) Potassium thioacetate, ethanol, 85˚C; (d) 1. neopentyl alcohol, 2. triphenyl phosphine, 3. maleimide, 4. DIAD, 0˚C.

Scheme 3-1. Synthetic procedure for 12-thioacetic 3,6,9-trioxadodecane-1-maleimide **11**

This procedure was repeated, and the target molecule was synthesized successfully. The overall yield was very low (3-4%) with large amount side products.

In order to improve the yield, the procedure was checked again. Normally, tosyl group is an excellent leaving group for S_N2 substitution. It is not necessary to convert tosyl group to bromo substituents compound **9** before thioacetate anion undergoing a nucleophilic attack to form 12-thioacetic 3,6,9-trioxadodecane-1-ol, **10**. Step 2 could be skipped and compound **8**

could be used for the S_N2 reaction with thioactate anion directly. In 2001, Zhang's group also presented the same synthetic scheme for compound **10**[63].

The lowest yield step for the whole procedure is the last step. When the alcohol is converted to maleimide group compound **11** through Mitsunobu reaction, the yield was only about 12%. The current procedure was to mix compound 9, neopentyl alcohol and triphenyl phosphine at 0 ˚C. The maleimide and DIAD was added in turn. Walker[64] pointed out in his paper that if maleimide was added before DIAD, it was very possible that triphenyl phosphine would attack the maleimide double bond with a Micheal addition reaction, which will decrease the yield dramatically. In the same paper, Walker also mentioned that lower reaction temperature would also help to improve the yield. Considering all the facts discussed above, a new alternative synthesis pathway for compound **11** was proposed.

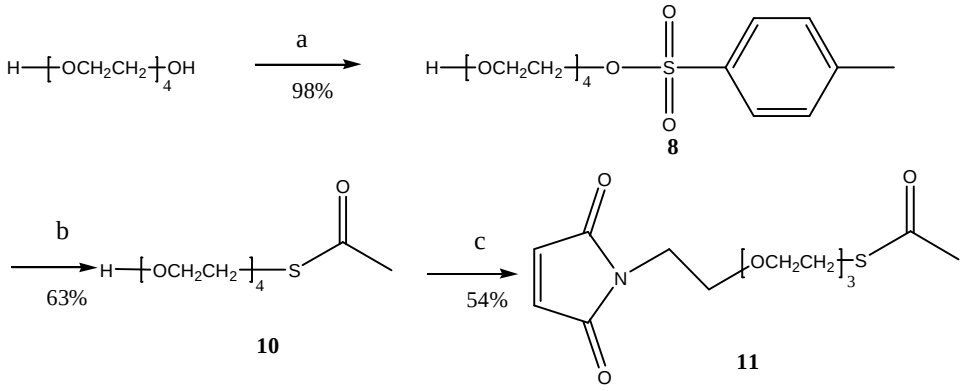

(a) p-toluenesulfonyl chloride, Pyridine, CH_2Cl_2; (b) Potassium thioacetate, DMF, 85˚C; (c) 1. triphenyl phosphine, 2. DIAD, 3. neopentyl alcohol, 4. maleimide, -78 ˚C.

Scheme 3-2. Improved synthesis pathway for compound **11**

p-Toluenesulfonyl chloride solution was added dropwise into large exceeding amount of tetraethylene glycol to minimize the possibility of di-substituted products. After extraction and the solvent was took off. The ^{1}HNMR for crude products showed exclusive compound **8** with trace amount of pyridine. Both procedures mentioned the crude products could be purified with column chromatography. But the endeavor of purification was not successful. Compound **8** partially decomposed on the column, which probably was caused by moisture adsorbed on the silica gel. So, the crude products were used for the next step directly.

In order to improve the solubility of potassium thioacetate, anhydrous DMF were used instead of acetone in Zhang's paper. The reaction could be carried out with small volume organic solvent and the final yield was good (62.8%).

Triphenyl phosphine was dissolved in anhydrous THF and the solution was cooled to -78˚C. Then, DIAD, compound **9**, and neopentyl alcohol were added in turn. With this starting material adding sequence, the final yield was improved to 54.1%.

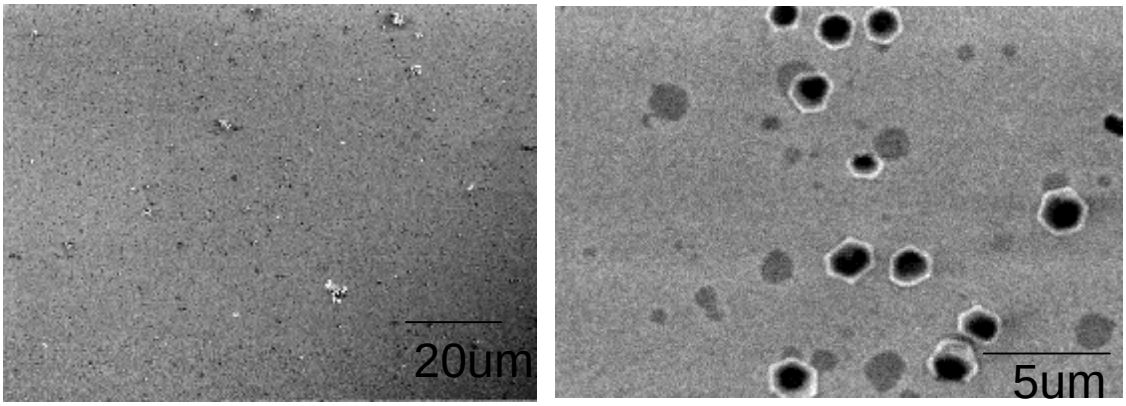

Figure 3-7. SEM images of Pd particles formed in the presence of 5'-phosphorothioate-modified PdRNA017 with compound **11** as linker on a gold surface

The new synthetic linker **11** was assembled on gold slides and treated with 5'-phosphorothioate-modified PdRNA017. After incubated with $Pd_2(DBA)_3$, the slides were examined with SEM. The resulting images are presented in figure 3-7.

The SEM images exhibited the hexagonal nanoparticles clearly. They demonstrated that the linker and linker attachment strategy both worked well.

A control experiment without the 5'-phosphorothioate-modified PdRNA017 was also carried out. After attached with the linker molecules, the gold slides were incubated with $Pd_2(DBA)_3$ directly. The SEM images of this control experiment are showed in figure 3-8.

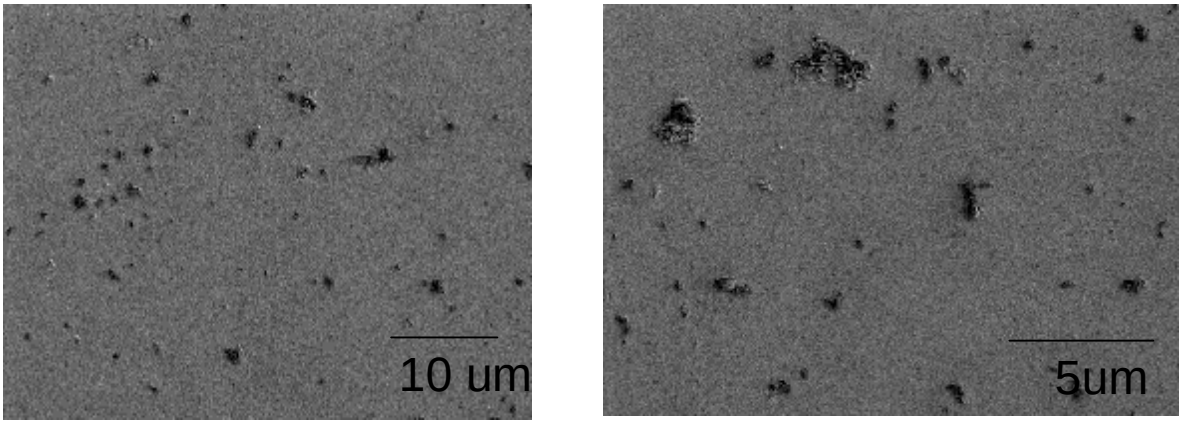

Figure 3-8. SEM images of control experiment (without 5'-phosphorothioate-modified PdRNA017) with compound **11** as linker on a gold surface

These images obviously showed that there were amorphous nanoparticles generated by the linker **11**. Maybe, the free double bond of maleimide could compete with DBA ligands to cause the decomposition of $Pd_2(DBA)_3$.

3. Establishment of New Linkage Chemistry for RNA Mediated Nanoparticle Growth On Gold Surface

As the SEM above showed the maleimide and phosphorothioate-modified RNA approach could work well to generate desired shape-controlled nanoparticles. But there are amorphous nanoparticles presented as background at the same time. When we try to examine the property of shaped nanoparticles, background nanoparticles will produce unwanted effect to the results.

On the other hand, phosphorothioate-modified RNA has a high affinity to gold surface. Due to the sulfur atom, the binding of phosphorothioate-modified RNA with the gold surface is probably irreversible. As long as the RNA molecules penetrate the blockers, they will stay on the surface and not go back in solution. This maybe another reason that maleimide and phosphorothioate-modified RNA approach generates heavy background.

5'-phosphorothioate-modified RNA will be covalently coupled with maleimide double bond through Michael addition reaction. Although this is a general approach for many biomolecule-involving processes, it is not very efficient or fast. This reaction requires long reaction times and high concentrations of RNA. Long reaction could cause RNA molecules to penetrate and decompose. Meanwhile, using high concentration of RNA not only wastes the expensive RNA materials, but also may cause RNA aggregation, which will make RNA molecules lose their activity.

Due to all the facts we discussed above, new linkage chemistry for RNA mediated nanoparticle growth on gold surfaces was established in our group, providing an alternative strategy to connect RNA molecules and gold surface.

Another approach is to attach the linker to the RNA molecule chemically or enzymatically firstly, while the other end has the thiol group, which could be assembled on gold surface in the following step.

In 2001, Zhang's group presented a synthetic scheme for *O*- [ω-mercapto-tetra (ethylene glycol)]-*O*- (5'-Guanosine) monophosphate[63]. And this monophosphate was attached to RNA successfully through in vitro transcription. This molecule seems to be the appropriate structure we are looking for; except that the free thiol group could be oxidized to a disulfide compound. In order to avoid this unwanted oxidation, a large amount of mercaptoethanol is need. Since compound **11** could bind to gold surfaces, we think that we could use a thioacetyl group on the surface-binding end, so that no unpleasant oxidation will happen.

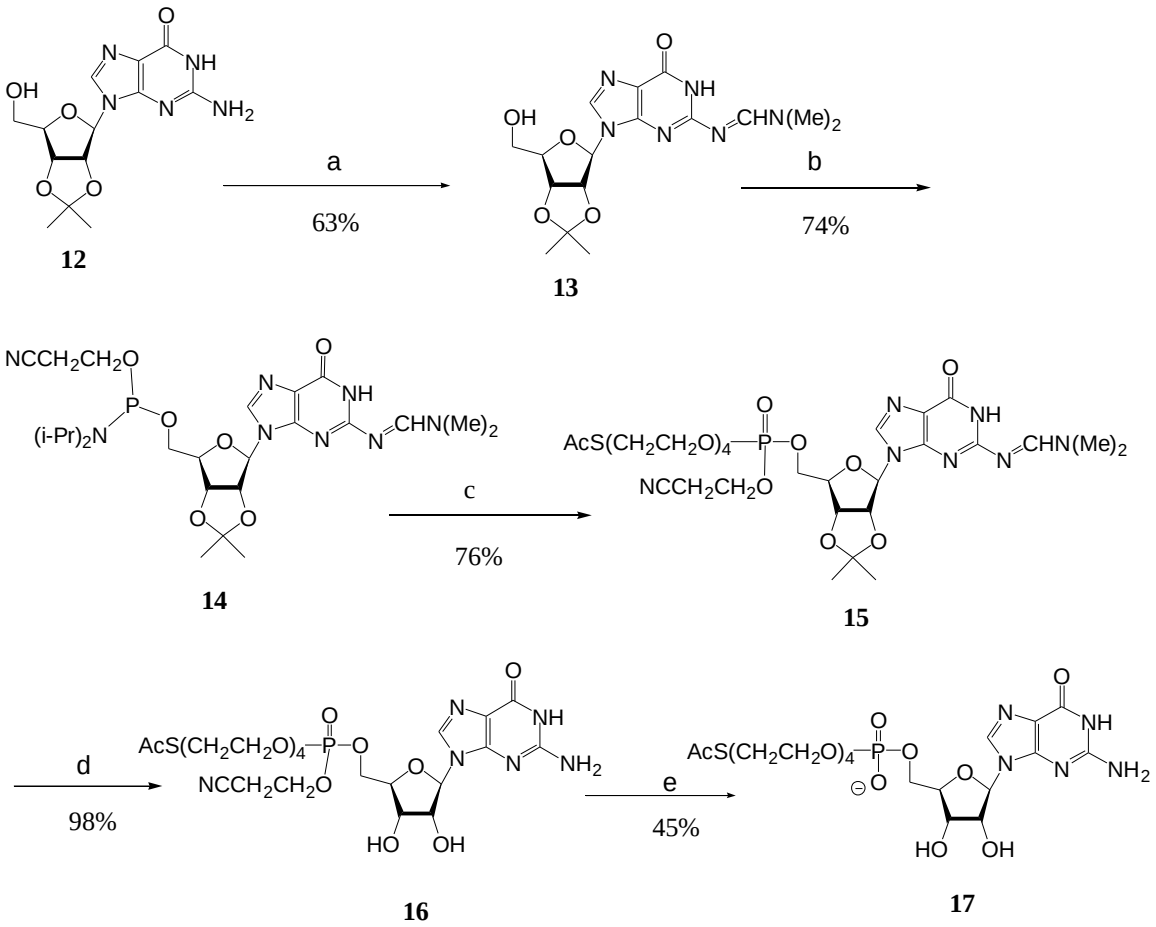

(a) $Me_2NCH(OMe)_2$, DMF, 55 ˚C; (b) $ClP(NPr^i_2)(OCH_2CH_2CN)$, NPr^i_2Et, CH_2Cl_2, 0 ˚C; (c) (1) $H(OCH_2CH_2)_4SCOCH_3$, 1*H*-tetrazole, MeCN, (2) *t*-BuOOH; (d) 60%$HCOOH/H_2O$; (e) 1.0M DBU

Scheme 3-3. Synthesis pathway for compound **17**

A new compound, *O*- [ω-Thioacetyl tetra (ethylene glycol)]-*O*- (5'-Guanosine) Monophosphate (TA-PEG_4-GMP) **17,** was designed. The synthesis route was presented in scheme 3-3. The Zhang's procedures of step a to step d was repeated first. Then, the experimental conditions and workup process for each step was modified to obtain a good yield.

Compound **12** was reacted with N, N-dimethylformamide dimethyl acetal to protect the active amino group on guanosine. Without concentrating the mother liquor, product **13** was obtained smoothly in 63% with Zhang's procedure.

Compound **13** was treated with (2-cyanoethyl-N, N-diisopropyl) chlorophoramidite with the presence of diisopropylethyl amine in anhydrous CH_2Cl_2 at 0 °C. The solvent was removed from the system after the reaction was completed. According to Zhang's procedure, the residue was diluted with ethyl acetate and then submitted to the extraction step. It turned out that residue has very low solubility to ethyl acetate, and recovered no product. So, CH_2Cl_2 was used instead of ethyl acetate. Also, CH_2Cl_2/triethylamine/MeOH was used for column chromatography. Compound **14** was synthesized successfully with 73.9% overall yield.

Tetra(ethylene glycol) monothioacetate **10** was produced with the above synthetic route (Scheme 3-2). Compound **10** and Compound **14** react with each other by using 1*H*-tetrazole as catalyst. The workup procedure met the same problem as the previous step. Product **15** could not dissolved in ethyl acetate. So, CH_2Cl_2 was used to substitute ethyl acetate at the step where ethyl acetate was needed in Zhang's paper. Compound **15** was obtained with 76% yield.

Deprotecting the amino group of Compound **15** with 60% aqueous formaic acid using Zhang's procedure provided Compound **16** with almost quantitative yield.

In Zhang's paper, ammonia/methanol solution was used to the deprotect thiol group and decyanoethylate at the same time. In order to remain the thioacetyl group, a neutral 1.0 M DBU/acetonitrile solution was used to do the decyanoethylation. After the solvent was

removed, the residue was applied to a reverse-phase HPLC column. The target compound **17** was separated as a foam solid with 44.8% yield.

To examine if the desired linked RNA (TA-PEG_4-GMP-PdRNA017) could be prepared or not, Compound **17** was used for the in vitro transcription. Since the molecule weigh of Compound **17** is not big enough, it is hard to tell the difference between TA-PEG_4-GMP-PdRNA017 and regular PdRNA017 by electrophoresis gel-mobility shift. So, the RNA products after the transcription were assembled on gold slides with mercaptoethanol as blocker molecules. The slides were incubated with $Pd_2(DBA)_3$, SEM images for these slides are shown in figure 3-9.

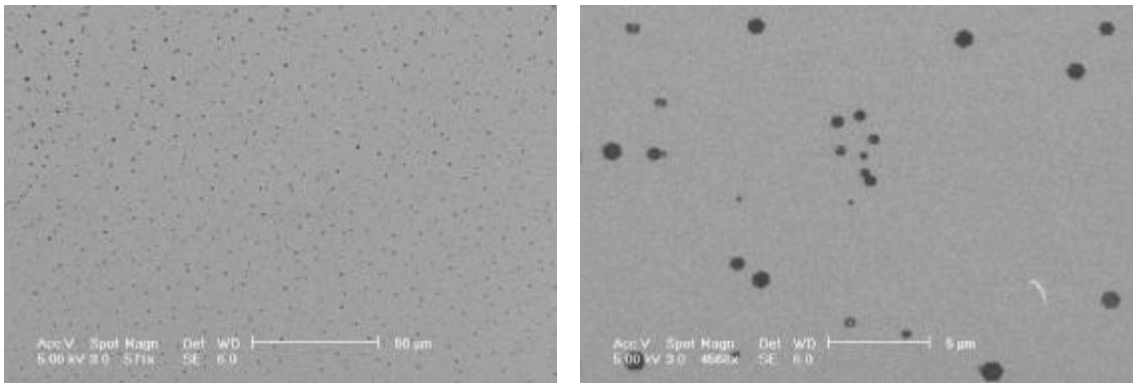

Figure 3-9. SEM images of Pd particles formed in the presence of TA-PEG_4-GMP-PdRNA017 with mercaptoethanol as blockers on a gold surface

The SEM images showed obviously the formation of hexagonal Pd nanoparticles with good coverage on the gold surface. No amorphous nanoparticles were observed on the gold slides, the background looked very clear. But we do observed small amount of cubic Pd

nanoparticles, which probably came from tiny cross contamination with another isolate RNA sequence, PdRNA034.

The preliminary results demonstrated that our alternative strategy to attach RNA molecules on gold surface is successful. A synthetic route with reasonable overall yield was established.

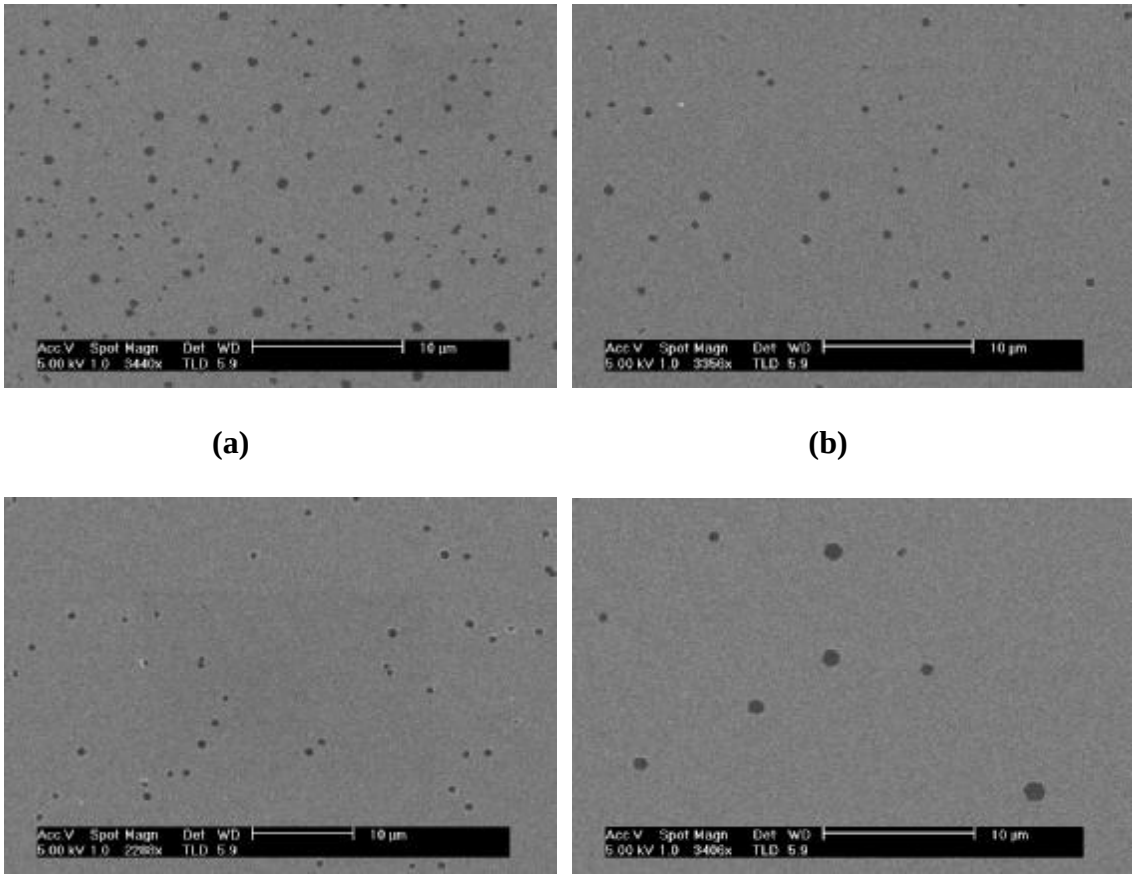

(a) **(b)**

(c) **(d)**

Figure 3-10. SEM images of Pd particles formed in the presence of various TA-PEG$_4$-GMP-PdRNA017 concentrations with mercaptoethanol as blockers on a gold surface. (a) 0.55 μM; (b) 0.14 μM; (c) 35 nM; (d) 8.75 nM.

In order to understand the relationship between RNA and nanoparticle growth, a set of gold slides were prepared with various RNA concentrations. The bare gold slides was treated with 0.1 μM mercaptoethanol and various concentrations of TA-PEG_4-GMP-PdRNA017 (0.55 μM, 0.14 μM, 35 nM and 8.75 nM). All the slides were incubated under the general method with identical time and $Pd_2(DBA)_3$ concentration.

All the slides were checked by SEM, and the images were shown in figure 3-10.

The SEM images showed some interesting results. The hexagonal Pd nanoparticles were prepared successfully with very clean background at all the concentration levels, but the particle densities on the gold surface clearly depended on the concentration of RNA. The average nanoparticle size in image d was obviously bigger then the averge nanoparticle size in the other images. Is that because of extremely low concentration of RNA? This question still remained and need further investigation.

To understand the behavior of RNA on surface, the first and important question is how many RNA molecules stay on the surface? This question could be answer with a scintillation counting experiment. α-[^{32}P]-ATP radiolabeled TA-PEG_4-GMP-PdRNA017 was prepared through in vitro transcription. The gold slides were treated with 0.1 μM mercaptoethanol and various concentrations of radiolabeled TA-PEG_4-GMP-PdRNA017 (0.55 μM, 0.14 μM, 35 nM and 8.75 nM).

The counting results showed a surface density of $3.2*10^{10}$ RNAs/cm^2 for 0.55 μM RNA solution, $1.2*10^{10}$ RNAs/cm^2 for 0.14 μM RNA solution, $5.8*10^9$ RNAs/cm^2 for 35 nM RNA solution, and $2.0*10^9$ RNAs/cm^2 for 8.75 nM RNA solution. It is interesting to mention that the surface density almost dropped 2 times with concentration dropping 4 times.

If the RNA molecules were loaded on the gold surface in a closest-packed and uniform array and the surface density of RNA is $2.0*10^9$ RNAs/cm^2, the distance between two RNA molecules should be about 300 nm. An estimated diameter for TA-PEG_4-GMP-PdRNA017 (87 bases) is about 10-20 nm. So, it is reasonable to hypothesize that a single RNA could possibly catalyze the nanoparticle formation and control the particle shape at least when particle size is smaller than 300 nm. The normal size of hexagonal Pd nanoparticle is about 1μm, so the number of RNA molecules needed for particle growth is still nuclear.

4. Conclusions

In this chapter, two strategies were examined to assemble RNA molecules on gold surfaces. Strategy one assembles Compound **11** onto gold surface first, and then 5'-phosphorothioate-modified RNA is introduced to covalently couple with maleimide double bond on Compound **11** through Michael addition reaction.

An alternative synthetic route for Compound **11** was established with improved yield and less steps. The gold slides prepared according to strategy one were examined by SEM. SEM images showed well shaped hexagonal Pd nanoparticles and demonstrated that this strategy could work well.

The other strategy, strategy two, uses chemical or enzymatic method to bind the linker with RNA molecules first. Following that step, Linker and RNA molecule were introduced onto gold surface.

A synthetic pathway was build up for new Compound **17**, according to Zhang's method. The final products were obtained with reasonable yield. Compound **17** was

transcribed and combined to RNA by T7 RNA polymerase. Expected RNA, TA-PEG_4-GMP-PdRNA017, was obtained.

The slides prepared due to the second strategy were also checked with SEM. well shaped hexagonal Pd nanoparticles were observed with satisfied particle density and neat background.

Strategy two was also showed to be an attractive methodology with more potential in material, surface chemistry and biochemistry.

Finally, series of scintillation counting experiments and SEM examinations were performed to help us understand the behavior of RNA on gold surface. SEM images showed that particle density had a dependence on RNA concentration. Higher concentration gave more particles, but it seems that larger particles were obtained at lower concentration end.

With the counting data, a hypothesis was presented that a single RNA could possibly catalyze the nanoparticle formation and control the particle shape.

5. References

1) Malonga, H.; Neault, J.; Tajmir-Riahi, H. *DNA and Cell Bio*, **2006**, *25(7)*, 393

2) Law, M. J.; Rice, A. J.; Lin, P.; Laird-Offringa, I.*RNA*, **2006**, *12(7)*, 1168

3) Guo, X.; Campbell, F. E.; Sun, L.; Christian, E. L.; Anderson, V. E.; Harris, M. E. *J. Mol. Bio.* **2006**, *360(1)*, 190

4) Kijas, A. W.; Harris, J. L.; Harris, J. M.; Lavin, M. F. *J. Mol. Bio.* **2006**, *281(20)*, 13939

5)Davidovic, L.; Bechara, E.; Gravel, M.; Jaglin, X. H.; Tremblay, S.; Sik, A.; Bardoni, B.; Khandjian, E. W. *Hum. Mol. Gene.* **2006**,*15(9)*, 1525

6) Tarasow, T. M.; Eaton, B. E., *Biopoly.* **1998**, *48*, 29

7) Dewey, T. M. *J. Am. Chem. Soc.*, **1995**, 117, 8474

8) Eaton, B. E. *Curr. Opinion in Chem. Bio.* **1997**, *1*, 10

9) Vaish, N. K. *Nucleic Acids Research* **2000**, *28*, 3316

10) Lutz, S.; Burgstaller, P.; Benner, S. A. *Nucleic Acids Research*, **1999**, *82*, 1005

11) Eaton, B. E.; Pieken, W. A. *Ann. Rev. Biochem.* **1995**, *64*, 837

12) Gourlain, T. *Nucleic Acids Research*, **2001**, *29*, 1898

13) Aurup, H.; Williams, D. M.; Eckstein, F. *Biochem.* **1992**, *31*, 9636

14) Perrin, D. M.; Garestier, T.; Helene, C. *Nucleosides & Nusleotides*, **1999**, *18*, 377

15) Thum. O.; Jager, S.; Famulok, M. *Angew. Chemie. Intl. Ed.*, **2001**, *40*, 3990

16) Seelig, B., *Angew. Chemie. Intl. Ed.* **2000**, *39*, 4576

17) Sengle, G. *Bioorg. Med. Chem.* **2000**, *8*, 1317

18) Stuhlmann, F.; Jaschke, A. *J. Am. Chem. Soc.* **2002**, *124*, 3238

19) Gopinath, S. C. B.; Sakamaki, Y.; Kawasaki, K.; Kumar, P. K. R. *J. Biochem.* **2006**, *139(5)*, 837

20) Nganvongpanit, K.; Mueller, H.; Rings, F.; Hoelker, M.; Jennen, D.; Tholen, E.; Havlicek, V.; Besenfelder, U.; Schellander, K.; Tesfaye, D., *Reproduction* **2006**, *131(5),* 861

21) Takahashi, T.; Tada, K.; Mihara, H., *Peptide Sci.* **2006**, *42*, 483

22) Vergne, J.; Cognet, J. A. H.; Szathmary, E.; Maurel, M., *Gene* **2006**, *371(2),* 182

23) Ryu, Y.; Kim, K.; Roessner, C. A.; Scott, A. I., *Chem. Comm.* **2006**, *13*, 1439

24) Nehdi, A.; Perreault, J., *Nucleic Acids Research* **2006**, *34(2),* 584

25) Anderson, P. C.; Mecozzi, S., *Nucleic Acids Research*, **2005,** *33(22),* 6992

26) Goringer, U. H.; Homann, M.; Lorger, M. *Intl. J. Parasito.* **2003**, *33*, 1309

27) Lohse, P. A.; Szostak, J. W., *Nature* **1996**, *381*, 442

28) Suga, H.; Lohse, P. A.; Szostak, J. *J. Am. Chem. Soc.* **1998**, *120*, 1151

29) Illangasekare, M.; Yakus, M., *Science* **1995**, *267*, 643

30) Lee, S. E. *Nucleic Acids Research*, **2001,** *29,* 1565

31) Zhang, B. L.; Cech, T. R. *Chem. Bio.* **1998**, *5*, 539

32) Zhang, B. L.; Cech, T. R. *Nature* **1997**, *390*, 96

33) Wiegand, T. W.; Janssen, R. C.; Eaton, B. E. *Chem. Bio.* **1997**, *4,* 675

34) Huang, F. Q.; Bugg, C. W.; Yarus, M. *biochem.* **2000**, *39*, 15548

35) Sengle, G. *Chem. Bio.* **2001**, *8,* 459

36) Wechwe, M.; Smith, D.; Gold, L. *Rna-A Pub. Of Rna Soc.* **1996,** *2*, 982

37) Li, Y. F.; Sen, D. *Nature structural Bio.* **1996**, *3*, 743

38) Li, Y. F.; Sen, D. *biochem.* **1997**, *36*, 5589

39) Tarasow, T. M.; Eaton, B.E. *Nature* **1997**, *389*, 54

40) Tarasow, T. M.; Eaton, B.E. *J. Am. Chem. Soc.* **2000**, *122*, 1015

41) Tarasow, T. M.; Eaton, B.E. *J. Am. Chem. Soc.* **1999**, *121*, 3614

42) Seelig, B.; Jaschke, A. *Chem. Bio.* **1999**, *6,* 167

43) Palaniyandi, V.; Shamsuzzoha, M.; Ada, E. T.; Zangari, G.; Reddy, R. G. *J Electron. Mater.* **2006**, *35(5),* 814

44) Zou, J.; Chen, C.; Liu, C.; Zhang, Y.; Han, Y.; Cui, L. *Mater. Lett.* **2005**, *59(27),* 437

45) Tseng, R. J.; Ouyang, J.; Chu, C.; Huang, J.; Yang, Y. *Appl. Phys. Lett.* **2006,** *8(12),* 123506/1-123506/3.

46) Teng, X.; Yang, H *J. Am. Chem. Soc.* **2003**, *125*, 14559

47) McConnell, W.; Brousseau, L. C., III; House, A. B.; Lowe, L. B.; Tenent, R. C.; Feldheim, D. L. *Metal Nanoparticles* **2002,** 319

48) Pandey, R.; Khuller, G. K., *J. of Antimicrobial Chemotherapy* **2006,** *57(6),* 1146

49) Ahmadi, T. S.; Wang. Z. L.; Green, T. C.; henglein, A.; El-sayed, M. A.; *Sicence* **1996**, *272*, 1924.

50) Saito, T.; Ohshima, S.; Xu, W.; Ago, H.; Yumura, M.; Iijima, S.; *J. Phys. Chem. B* **2005**, *109(21),* 10647

51) Liu, X.; Worden, J. G.; Huo, Q.; Brennan, J. P. *J. of Nanoscience and Nanotechnology* **2006**, *6(4),* 1054

52) Zhou, Q. F.; Bao, J. C.; Xu, Z.; *J Mater. Chem*. **2002,** *12(2),* 384

53) Gugliotti, L. A., Feldheim, D. L.; Eaton, B. E.; *Science* **2004**, *304*, 850

54) Gugliotti, L. A., Feldheim, D. L.; Eaton, B. E.; *J. Am. Chem. Soc.* **2005**, *127*, 17814

55) Liu, D.; Gugliotti, L. A., Wu, T.; Dolska, M. Tkachenko, A. G.; Shipton, M. K.; Eaton, B. E.; Feldheim, D. L.; *Langmuir* **2006**, *22,* 5862

56) Gatdner, T. J.; Frisbie, C. D.; Wrighton, M. S. *J. Am. Chem. Soc.* **1995**, *117*, 6927

57) Gates, B. D.; Xu, Q.; Stewart, M.; Ryan, D.; Willson, C. G.; Whitesides, G. M. *Chem. Rev.* **2005**, *105*, 1171

58) Love, J. C.; Estroff, L. A.; Kriebel, J. K.; Nuzzo, R. G.; Whitesides, G. M. *Chem. Rev.* **2005**, *105*, 1103

59) Li., H.; Park, S. H.; Reif, J. H.; Labean T. H.; Yan, H. *J. Am. Chem. Soc.* **2004**, *126*, 418

60) Yan, H.; Park, S. H.; Finkelstein, G.; Reif, J. H.; Labean T. H.; *Science* **2003**, *301*, 1882

61) Zhang, R. Y.; Pang, D.; Zhang, Z.; Yan, J.; Tian, Z.; Yao, J.; Mao, B.; Sun, S.; *J. Phys. Chem. B* **2002**, *106*, 11233

62) Pang, D. W.; Abruna, H. D. *Anal. Chem.* **2000,** *72*, 4700

63) Zhang, L.; Sun, L.; Cui, Z.; Gottieb, R.; Zhang, B. *Bioconjugate Chem.,* **2001**, 12, 939

64) Walker, M. A. *J. Org. Chem.* **1995,** *60*, 5352

CHAPTER FOUR

GENERAL EXPERIMENTAL PROCEDURE AND ANALYTICAL DATA

1. General Experimental for Chapter One

All reactions and manipulation were conducted under a dry argon atmosphere either using an inert atmosphere drybox or standard Schlenk techniques. All chemicals were purchased from Aldrich Chemical Company and alkynes and hexanes were purified by stirring with CaH and bulb-to-bulb transfer under high vacuum level. THF and toluene were distilled from Na/benzophenone, diethyl ether and pentane came from the Mraun dry-solvent system. Toluene-d8 and THF-d8 were distilled from Na/benzophenone. Fisher isotemp 3016H heating circulator was used as precise temperature-controlled heating bath. ^{1}H and ^{13}CNMR data were recorded on either a Varian Mercury 300 or 400 MHz spectrometer. Chemical shifts were reported in parts per million (ppm) referenced to the ^{1}H resonance of the residual solvent proton signal or ^{13}C resonance of the deuterated solvent. ^{19}FNMR spectra were recorded on a Varian Mercury 300 or 400 MHz spectrometer with hexafluorobenzene (-162.9 ppm) as external standard. The analytic X-ray structure data were obtained from Enraf-Nonius CAD4-MACH diffractometer and the structure solution and refinement were processed by NRCVAX program.

1.1 Synthesis of new substituted Cp ring compound

$Cp^{CF3}Na$: In a flame dried 100 mL round bottom flask, a solution of ethyl trifluoroacetate (10mmol, 1.42g) in THF (15mL) was transferred dropwise via cannula into a solution of sodium cyclopentadienylide in THF (10 mL). The mixture solution was stirred for seven hours. After the color of the solution became pale yellow, the solution was filtered though a medium glass fritted funnel and the solvent of the filtrate was took off under

vacuum. The pale yellow powder was collected, and dried completely on the vacuum line to give the yield 1.76g (95.6%). The power was used without further purification. ^{1}HNMR (400M, THF-d_8) δ5.853 (m, 1H), 5.952 (m, 1H), 6.385 (m, 1H), 6.499 (m, 1H); ^{13}CNMR (400M, THF-d_8) δ115.858, 118.866(m), 119.292, 120.556; ^{19}FNMR(400M, THF-d_8) δ-66.508.

Cp$^{\%}$Na In a flame dried 100 mL round bottom flask, a solution of dimethyl oxolate (10mmol, 1.18g) in THF (15mL) was transferred dropwise via cannula into a solution of sodium cyclopentadienylide in THF (10 mL). The mixture solution was stirred for six hours. After the color of the solution became brown, the solution was filtered though a medium glass fritted funnel and the filtrate was concerntrated to 10mL. Drop the concentrated filtrate to 70ml rapidly stirring diethyl ether (distilled with Sodium and benzophenone). The solution was kept in refrigerator overnight to separate an orange power. The powder was collected, washed with diethyl ether and dried on the vacuum line to yield 0.73g 42.4%). ^{1}HNMR(300MHz: D_2O) δ 3.75 (s, 3H), 6.18 (m, 2H), 6.51 (m, 2H).

1.2 Synthesis of new cobalt (I) catalyst

Synthesis of Cp^{CF3}CoCOD, 1: In a flame dried 50 mL round bottom flask, toluene (anhydrous, 5mL) and cyclooctadiene(3.6mL, 28.7 mmol) were freeze-pumped-thawed three cycles. The flask was then charged with chlorotris(triphenylphosphine)cobalt(1.9g, 2.15 mmol) and stirred vigorously. A solution of substituted Cp^{CF3}Na power (0.528g, 2.87mmol) in THF (5mL) was added. After stirring at room temperature for 14 hours, the reaction mixture was applied to alumina column (2 cmX20cm, neutral, Brockmann I, deactivated with 4% water) and eluted with THF. The eluent was concentrated on the vacuum line to *ca.*

3mL, which was applied to a column of alumina(2cmX30cm, neutral, Brockmann I, deactivated with 4% water). The column was washed with pentane (50mL) firstly, then 5%THF/pentane to elute an orange band which was collected. The eluent was concentrated to almost half volume, then stored in the refrigerator (-30˚C) overnight. The precipitate was filtrated under low temperature. Separated the dark red catalyst crystal and the PPh_3 crystal firstly, and then recrystallized the catalyst twice with pentane. The whole procedure gave 213mg (30.1%) dark red crystal as the final product. ^{1}HNMR (400M, THF-d_8) δ1.712 (AA', 4H), δ2.396 (BB', 4H), δ3.694 (XX', 4H), δ4.289(s, 2H), δ5.552(s, 2H); ^{13}CNMR (400M, THF-d_8) δ32.552, 72.802, 72.802, 83.684, 92.586; ^{19}FNMR(400M, Toluene-d_8) δ-118.376.

Synthesis of $Cp^{\%}$CoCOD: In a flame dried 50 mL round bottom flask, toluene (anhydrous, 5mL) and cyclooctadiene(3.6mL, 28.7 mmol) were freeze-pumped-thawed three cycles. The flask was then charged with chlorotris(triphenylphosphine)cobalt(3.8g, 4.31 mmol) and stirred vigorously. A solution of $Cp^{\%}$Na (0.5g, 2.87mmol) in THF (5mL) was added. After stirring at room temperature for 14 hours, the reaction mixture was applied to Florisil column (2 cmX20cm, 30-60 mesh) and eluted with THF. The eluent was concentrated on the vacuum line to *ca.* 3mL, which was applied to a column of alumina(2cmX30cm, 30-60 mesh). The column was washed with hexanes (50mL). 20%THF/hexanes(50mL), 50%THF/hexanes(50mL),and finally THF(50mL) to elute an orange band which was collected. THF was removed in vacuo. This new catalyst decomposed on the alumina column.

Synthesis of $Cp^{\$}$CoCOD: As previously reported[1].

1.3 Kinetics

Experiments were conducted in silanized 5 mm NMR tubes that were sealed under vacuum using a propane torch. In a typical experiment, 0.10mmol 1,4-dimethoxyl-2-butyne (**2a**), and 50μL 100mM Cp^{CF3}CoCOD or $Cp^{\$}$CoCOD solution (in THF-d8) were combined in a NMR tube and added THF-d8 to make total volume to 500μL. Freeze-pump-thawed the tube three cycles, and sealed the tube using propane torch. Took initial NMR. Heated the tube in 85^{o}C heating bath. Used the NMR technique to monitor the reaction for at least 7 data points over three half lives. The disappearance of starting material was measured and record with corresponding time.

1.4 X-ray Crystal Structure Analysis of $Cp^{CF3}CoCOD$, 1

Structure Determination Summary

Completed by the Departmental Facility at NCSU

Crystal data

Empirical Formula	$C_{15}H_{16}CoF_3O$
Formula Mass	328.22
Crystal Size, mm	0.44 X 0.16 X 0.16
Crystal Color, habit	Dark Red
Crystal System	Monoclinic
Space Group	P21/n
a, Å	8.1329(8)
b, Å	13.9614(9)
c, Å	12.0847(11)
α, °	90
β, °	102.465(7)
γ, °	90
Volume, $Å^3$	1339.83(20)
Z, Formula units/cell	4
Density (calculated), mg/m^3	1.627
F(000)	673.91
Absorption Coefficient, mm^{-1}	1.31

Data Collection Parameters

Diffractometer	Enraf-Nonius CAD4-MACH
Temperature, K	193
Radiation(λ), Å	0.70930
Scan Mode	ω mode
2 θ (Max), $^\circ$	49.7
Index Ranges	
	$-9 < h < 9$
	$0 < k < 16$
	$0 < l < 14$
Reflection Collected	2329
Unique reflections	2329
Reflections with Inet. > 1.0 δ	1947
Standard Reflections	3 measured every 4800 Sec.
Range Transmission Coefficient	0.94725 to 0.99680
Merging R-value	0.000
Absorption corrections	Empirical absorption correction was applied using data from psi scans of several reflection

Solution and Refinement

Data Reduction Program	NRCVAX
Structure Solution Program	SIR92
Number of Parameters Refined	209
Reflections Observed	2329
The Weight Modifier (K)	0.000100
R Indices (all data)	R = 0.043
	R_w = 0.035
R Indices (significant reflection)	R = 0.029
	R_w = 0.035
	Go = 1.92
The Highest Peak	0.390 e $Å^{-3}$
The Deepest Hole	-0.340 e $Å^{-3}$
Secondary Ext. Coeff.	0.0232 microns
Sigma	0.0064

* The CF3 group exhibited an orientational disorder with the fluorine atoms occupying two distinct sets of sites.

Table 4-1. Atomic Parameters x, y, z (Å) for $C_{15}H_{16}CoF_3O$

	x		y		z	
Co1	0.99324	(3)	0.31255	(2)	0.88169	(2)
C1	0.75477	(29)	0.26060	(17)	0.88592	(19)
C2	0.74278	(31)	0.34226	(18)	0.81243	(21)
C3	0.80906	(32)	0.42319	(18)	0.81635	(23)
C4	0.86844	(32)	0.39356	(18)	0.98917	(22)
C5	0.83986	(31)	0.29372	(17)	0.99642	(20)
C6	0.70886	(31)	0.16527	(18)	0.84560	(21)
C7	0.74783	(37)	0.08041	(21)	0.92782	(26)
C8	1.18491	(34)	0.22501	(24)	0.95736	(24)
C9	1.22821	(32)	0.32049	(24)	0.98336	(22)
C10	1.34748	(36)	0.37832	(24)	0.92959	(27)
C11	1.30226	(37)	0.37333	(24)	0.80093	(27)
C12	1.11510	(35)	0.35530	(23)	0.75730	(22)
C13	1.04684	(35)	0.26412	(23)	0.73455	(22)
C14	1.14126	(45)	0.17084	(25)	0.75469	(31)
C15	1.25388	(42)	0.16602	(22)	0.87181	(31)
O1	0.63689	(24)	0.14581	(14)	0.74786	(15)
F1	0.88991	(97)	0.08330	(64)	1.00196	(71)
F2	0.72547	(127)	-0.00231	(29)	0.88772	(37)
F3	0.64032	(80)	0.08852	(42)	1.00372	(47)

Table 4-1. Atomic Parameters x, y, z (Å) for $C_{15}H_{16}CoF_3O$ (continued)

F1'	0.86222	(98)	0.02564	(48)	0.88239	(52)
F2'	0.61763	(78)	0.02508	(50)	0.91505	(80)
F3'	0.82059	(140)	0.09400	(66)	1.02503	(55)
H2	0.69818	(0)	0.34157	(0)	0.73212	(0)
H3	0.81259	(0)	0.48757	(0)	0.84903	(0)
H4	0.91983	(0)	0.43428	(0)	1.05101	(0)
H5	0.87253	(0)	0.25487	(0)	1.06310	(0)
H8	1.10721	(0)	0.19466	(0)	0.99581	(0)
H9	1.17801	(0)	0.35193	(0)	1.03854	(0)
H10a	1.34334	(0)	0.44413	(0)	0.95186	(0)
H10b	1.45935	(0)	0.35392	(0)	0.95639	(0)
H11a	1.36316	(0)	0.32128	(0)	0.77670	(0)
H11b	1.33292	(0)	0.43223	(0)	0.76969	(0)
H12	1.04110	(0)	0.40968	(0)	0.74668	(0)
H13	0.92798	(0)	0.26064	(0)	0.70327	(0)
H14a	1.06213	(0)	0.11897	(0)	0.74711	(0)
H14b	1.20839	(0)	0.16432	(0)	0.69881	(0)
H15a	1.26594	(0)	0.10054	(0)	0.89648	(0)
H15b	1.36213	(0)	0.19134	(0)	0.86766	(0)

Table 4-2. Bond lengths (Å) for $C_{15}H_{16}CoF_3O$

Co1-C1	2.082	(2)	C9-C10	1.512	(4)
Co1-C2	2.070	(3)	C9-H9	0.960	(3)
Co1-C3	2.143	(3)	C10-C11	1.520	(5)
Co1-C4	2.137	(3)	C10-H10a	0.960	(3)
Co1-C5	2.072	(2)	C10-H10b	0.960	(3)
Co1-C8	2.036	(3)	C11-C12	1.520	(4)
Co1-C9	2.040	(3)	C11-H11a	0.960	(3)
Co1-C12	2.059	(3)	C11-H11b	0.960	(3)
Co1-C13	2.036	(3)	C12-C13	1.392	(5)
C1-C2	1.435	(4)	C12-H12	0.960	(3)
C1-C5	1.441	(3)	C13-C14	1.505	(5)
C1-C6	1.439	(4)	C13-H13	0.960	(3)
C2-C3	1.409	(4)	C14-C15	1.512	(5)
C2-H2	0.960	(3)	C14-H14a	0.960	(3)
C3-C4	1.407	(4)	C14-H14b	0.960	(3)
C3-H3	0.960	(3)	C15-H15a	0.960	(3)
C4-C5	1.419	(4)	C15-H15b	0.960	(3)
C4-H4	0.960	(3)	F1-F2	2.080	(10)
C5-H5	0.960	(2)	F1-F3	2.036	(10)
C6-C7	1.535	(4)	F1-F1'	1.627	(11)
C6-O1	1.230	(3)	F1-F3’	0.697	(14)
C7-F1	1.301	(8)	F2-F3	2.115	(9)

Table 4-2. Bond lengths (Å) for $C_{15}H_{16}CoF_3O$ (continued)

C7-F2	1.250	(5)	F2-F1’	1.193	(13)
C7-F3	1.402	(5)	F2-F2’	1.072	(14)
C7-F1’	1.404	(6)	F2-F3'	2.146	(8)
C7-F2’	1.293	(6)	F3-F2'	1.372	(13)
C7-F3'	1.211	(7)	F3-F3'	1.435	(13)
C8-C9	1.397	(5)	F1' -F2'	2.110	(11)
C8-C15	1.521	(5)	F1'-F3'	2.061	(10)
C8-H8	0.960	(3)	F2' -F3'	2.114	(11)

Table 4-3. Bond angles (°) for $C_{15}H_{16}CoF_3O$

C1-Co1-C2	40.45	(10)	C9-C10-H10b	108.3	(3)
C1-Co1-C3	66.61	(10)	C11-C10-H10a	108.4	(3)
Cl-Co1-C4	66.55	(10)	C11-C10-H10b	109.3	(3)
C1--Co1-C5	40.60	(9)	H10a-C10-H10b	109.5	(3)
C1-Co1-C8	114.02	(11)	C10-C11-C12	111.4	(2)
C1-Co1-C9	139.55	(11)	C10-C11-H11a	108.6	(3)
C1-Co1-C12	135.78	(10)	C10-C11-H11b	109.7	(3)
C 1-Co1-C13	106.39	(11)	C12-C11-H11a	108.2	(3)
C2-Co1-C3	39.01	(10)	C12-C11-H11b	109.3	(3)
C2-Co1-C4	65.46	(10)	H11a-C11-H11b	109.5	(3)
C2-Col-C5	67.30	(10)	Co1-C12-C11	113.47	(19)
C2-Col-C8	153.26	(12)	Co1-C12-C13	69.20	(16)
C2-Co1-C9	160.87	(11)	Co1-C12-H12	86.57	(17)
C2-Co1-C12	103.49	(11)	C11-C12-C13	123.1	(3)
C2-Co1-C13	95.22	(11)	C11-C12 –H12	117.9	(3)
C3-Co1--C4	38.38	(10)	C13-C12-H12	119.0	(3)
C3-Co1-C5	66.03	(10)	Co1-C13-C12	71.05	(16)
C3-Co1-C8	155.33	(12)	Co1-C13-C14	110.1	(2)
C3-Co1-C9	122.47	(11)	Co1-C13-H13	88.48	(18)
C3-Co1-Cl2	102.27	(11)	C12-C13-C14	126.3	(3)
C3-Co1-C13	119.55	(12)	C12-C13-H13	116.7	(3)
C4-Co1-C5	39.37	(10)	C14-C13-H13	117.1	(3)

Table 4-3. Bond angles (°) for $C_{15}H_{16}CoF_3O$ (continued)

C4-Co1-C8	117.57	(11)	C13-C14-C15	112.0	(3)
C4-Co1-C9	96.39	(11)	C13-C14-H14a	109.2	(3)
C4-Co1-C12	131.06	(12)	C13-C14-H14b	108.4	(3)
C4-Co1-C13	157.85	(11)	C15-C14-H14a	108.3	(3)
C5-Co1-C8	97.84	(11)	C15-C14-H14b	109.4	(3)
C5-Co1-C9	102.99	(11)	H14a-C14-H14b	109.4	(3)
C5-Co1-C12	168.28	(11)	C8-C15-C14	112.0	(3)
C5-Co1-Cl3	144.65	(11)	C8-C15-H15a	109.4	(3)
C8-Co1-C9	40.10	(14)	C8-C15-H15b	108.3	(3)
C8-Co1-C12	93.41	(11)	C14-C15-H15a	109.5	(3)
C8-Co1-C13	84.57	(12)	C14-C15-H15b	108.2	(3)
C9-Co1-C12	83.57	(11)	H15a-C15-H15b	109.5	(3)
C9-Co1-C13	101.24	(11)	C7-F1-F2	34.6	(3)
C12-Co1-C13	39.75	(13)	C7-F1-F3	43.0	(3)
Co1-C1-C2	69.35	(14)	C7-F1-F1’	56.0	(4)
Co1-C1-C5	69.35	(14)	C7-F1-F3'	66.9	(8)
Co1 -C1 –C6	119.27	(17)	F2-F1-F3	61.8	(4)
C2-C1-C5	105.9	(2)	F2-F1-F1'	34.9	(4)
C2-C1-C6	123.2	(2)	F2-F1-F3'	85.9	(9)
C5-C1-C6	130.4	(2)	F3-F1-F1'	94.6	(5)
Co1-C2-C1	70.20	(14)	F3-F1-F3'	25.0	(7)
Co1-C2-C3	73.29	(15)	F1'-F1-F3'	119.5	(10)

Table 4-3. Bond angles (°) for $C_{15}H_{16}CoF_3O$ (continued)

Co1-C2-H2	122.1	(2)	C2-F2-F1	36.2	(3)
C1-C2 -C3	109.3	(2)	C7 -F2 -F3	39.7	(3)
C1-C2-H2	125.3	(3)	C7 -F2-F1'	70.1	(5)
C3-C2-H2	125.4	(3)	C7-F2-F2'	67.1	(5)
Co1-C3-C2	67.70	(14)	C7 -F2-F3'	28.8	(3)
Co1-C3-C4	70.57	(15)	F1-F2-F3	58.1	(3)
Co1-C3-H3	127.8	(2)	F1-F2-F1'	51.3	(5)
C2-C3-C4	107.8	(2)	F1-F2 -F2'	92.4	(5)
C2-C3-H3	126.8	(3)	F1-F2-F3'	18.9	(4)
C4-C3-H3	125.4	(3)	F3-F2-F1'	106.4	(5)
Co1-C4-C3	71.06	(15)	F3-F2-F2'	34.4	(5)
Co1-C4-C5	67.87	(14)	F3-F2-F3'	39.3	(4)
Co1-C4-H4	127.1	(2)	F1'-F2-F2'	137.2	(6)
C3-C4-C5	108.8	(2)	F1'-F2-F3'	69.7	(5)
C3-C4-H4	125.5	(3)	F2'-F2-F3'	73.8	(6)
C5-C4-H4	125.7	(3)	C7-F3-F1	39.3	(3)
Co1-C5-C1	70.05	(13)	C7 -F3-F2	34.7	(3)
Co1-C5-C4	72.77	(14)	C7-F3 -F2'	55.6	(4)
Co1-C5-H5	122.40	(19)	C7-F3-F3'	50.5	(3)
C1-C5-C4	108.1	(2)	F1-F3-F2	60.1	(4)
C1-C5-H5	126.0	(2)	F1-F3-F2'	86.3	(4)
C4-C5-H5	126.0	(2)	F1-F3-F3'	11.8	(4)

Table 4-3. Bond angles (°) for $C_{15}H_{16}CoF_3O$ (continued)

C1-C6-C7	119.5	(2)	F2-F3-F2'	26.2	(4)
C1--C5-O1	124.4	(2)	F2-F3-F3'	71.5	(4)
C7-C5-O1	116.1	(2)	F2'-F3-F3'	97.7	(5)
C6-C7-F1	116.8	(5)	C7-F1'-F1	50.2	(4)
C6-C7-F2	118.0	(3)	C7-F1'-F2	56.9	(4)
C5-C7-F3	106.9	(3)	C7-F1'-F2'	36.7	(3)
C6-C'7-F1'	103.2	(3)	C7-F1'-F3'	34.8	(3)
C6-C7 -F2'	109.6	(3)	F1-F1'-F2	93.8	(5)
C5-C7-F3'	119.8	(5)	F1-F1'-F2'	77.9	(4)
F1-C7-F2	109.2	(6)	F1-F1'-F3'	17.1	(4)
F1-C7-F3	97.7	(5)	F2-F1'-F2'	20.2	(4)
F1-C7-F1'	73.8	(5)	F2-F1'-F3'	77.5	(5)
F1-C7-F2'	133.1	(5)	F2'-F1'-F3'	60.9	(4)
F1-C7-F3'	32.0	(7)	C7-F2'-F2	63.0	(5)
F2-C7 -F3	105.6	(6)	C7-F2'-F3	63.4	(4)
F2-C7-F1'	53.0	(6)	C7-F2'-F1'	40.5	(4)
F2-C7-F2'	49.8	(7)	C7-F2'-F3'	31.2	(4)
F2-C7-F3'	121.4	(6)	F2-F2'-F3	119.3	(6)
F3-C7-F1'	149.2	(4)	F2-F2'-F1'	22.6	(4)
F3-C7-F2'	61.0	(6)	F2-F2'-F3'	77.1	(5)
F3-C7-F3'	66.2	(6)	F3-F2'-F1'	99.8	(4)
F1'-C7-F2'	102.9	(6)	F3-F2'-F3'	42.3	(4)

Table 4-3. Bond angles (°) for $C_{15}H_{16}CoF_3O$ (continued)

F1'-C7-F3'	103.8	(6)	F1'-F2'-F3'	58.4	(4)
F2'-C7-F3'	115.2	(7)	C7-F3'-F1	81.2	(9)
Co1-C8-C9	70.10	(16)	C7-F3'-F2	29.8	(3)
Co1-C8-C15	112.3	(2)	C7-F3'-F3	63.3	(5)
Co1-C8-H8	87.84	(17)	C7-F3'-F1'	41.4	(4)
C9-C8 -C15	123.9	(3)	C7-F3'-F2'	33.6	(4)
C9-C8-H8	118.2	(3)	F1-F3'-F2	75.2	(9)
C15-C1-H8	117.9	(3)	F1-F3'-F3	143.2	(10)
Co1-C9-C8	69.80	(16)	F1-F3'-F1'	43.4	(8)
Co1-C9-C10	112.00	(19)	F1-F3'-F2'	103.9	(9)
Co1-C9-H9	87.69	(16)	F2-F3'-F3	69.1	(5)
C8-C9-C10	124.5	(3)	F2-F3'-F1'	32.9	(4)
C8-C9-H9	117.9	(3)	F2-F3'-F2'	29.1	(4)
C10-C9-H9	117.6	(3)	F3-F3'-F1'	99.9	(5)
C9-C10-C11	112.3	(2)	F3-F3'-F2'	40.0	(4)
C9-C10-H10a	109.0	(3)	F1'-F3'-F2’	60.7	(4)

Table 4-4. Atomic Parameters x, y, z (Å) And Biso for $C_{15}H_{16}CoF_3O$

	x	y	z	Biso
Co1	0.99324 (4)	0.31255 (2)	0.88169 (3)	1.670 (14)
C1	0.7548 (3)	0.2606 (18)	0.88592 (20)	1.75 (10)
C2	0.7428 (3)	0.34226 (19)	0.8124 (2)	2.08 (10)
C3	0.8091 (3)	0.42319 (19)	0.8164 (2)	2.30 (11)
C4	0.8684 (3)	0.39356 (19)	0.9892 (2)	2.23 (11)
C5	0.8399 (3)	0.29372 (18)	0.9964 (2)	1.88 (10)
C6	0.7089 (3)	0.16527 (18)	0.8456 (2)	1.98 (10)
C7	0.7478 (4)	0.0804 (2)	0.9278 (3)	2.98 (13)
C8	1.1849 (3)	0.225 (2)	0.9574 (2)	2.99 (13)
C9	1.2282 (3)	0.3205 (2)	0.9834 (2)	2.85 (12)
C10	1.3475 (4)	0.3783 (2)	0.9296 (3)	3.47 (13)
C11	1.3023 (4)	0.3733 (2)	0.8009 (3)	3.61 (14)
C12	1.1151 (4)	0.3553 (2)	0.7573 (2)	2.78 (12)
C13	1.0468 (4)	0.2641 (2)	0.7345 (2)	2.97 (13)
C14	1. 1413 (5)	0.1708 (3)	0.'7547 (3)	4.27 (16)
C15	1.2539 (4)	0.166 (2)	0.8718 (3)	3.88 (15)
O1	0.6369 (2)	0.14581 (15)	0.74786 (16)	2.90 (8)
F1	0.8899 (10)	0.0833 (6)	1.002 (7)	7.5 (4)
F2	0.'7255 (13)	-0.0023 (3)	0.8877 (4)	7.5 (4)
F3	0.6403 (8)	0.0885 (4)	1.0037 (5)	6.9 (3)
F1'	0.8622 (10)	0.0256 (5)	0.8824 (5)	5.8 (3)

Table 4-4. Atomic Parameters x, y, z (Å) And Biso for $C_{15}H_{16}CoF_3O$ (continued)

F2'	0.6176 (8)	0.0251 (5)	0.9151 (8)	6.1 (3)
F3'	0.8206 (14)	0.094 (7)	1.025 (6)	5.9 (6)
H2	0.698	0.342	0.732	2.8
H3	0.813	0.488	0.849	3.1
H4	0.92	0.434	1.051	3.0
H5	0.873	0.255	1.063	2.7
H8	1.107	0.195	0.996	3.8
H9	1.178	0.352	1.039	3.6
H10a	1.343	0.444	0.952	4.2
H10b	1.459	0.354	0.956	4.2
H11a	1.363	0.321	0.777	4.5
H11b	1.333	0.432	0.770	4.5
H12	1.041	0.410	0.747	3.6
H13	0.928	0.261	0.703	3.8
H14a	1.062	0.119	0.747	5.3
H14b	1.208	0.164	0.699	5.3
H15a	1.266	0.101	0.896	4.8
H15b	1.362	0.191	0.868	4.8

* Biso is the Mean of the Principal Axes of the Thermal Ellipsoid

Table 4-5. Anisotropic Displacement Parameters (Å^2) for $C_{15}H_{16}CoF_3O$

	u11 (U)		u22		u33		u12		u13		u23	
Co1	1.81	(19)	2.64	(2)	1.856	(19)	0.05	(15)	0.308	(12)	0.11	(15)
C1	1.79	(12)	2.77	(14)	2.21	(13)	0	(11)	0.68	(10)	-0.08	(11)
C2	1.86	(13)	3.04	(14)	2.86	(14)	0.2	(11)	0.22	(11)	0.29	(11)
C3	2.4	(14)	2.34	(14)	4.01	(15)	0.2	(11)	0.68	(12)	0.14	(12)
C4	2.47	(14)	2.7	(14)	3.38	(15)	0.06	(11)	0.83	(12)	-0.96	(12)
C5	2.12	(13)	2.74	(15)	2.44	(13)	0.03	(10)	0.87	(10)	-0.06	(10)
C6	2.1	(13)	3.02	(15)	2.54	(13)	-0.22	(10)	0.81	(11)	-0.35	(11)
C7	3.47	(17)	3.11	(16)	4.58	(19)	-0.5	(13)	0.52	(14)	0.06	(14)
C8	2.37	(15)	5.36	(19)	3.8	(16)	1.46	(13)	1.09	(13)	1.78	(14)
C9	1.76	(13)	6.2	(2)	2.62	(14)	0.82	(13)	-0.02	(11)	-0.54	(14)
C10	2.27	(15)	5.6	(2)	5.27	(19)	-0.66	(14)	0.64	(14)	-1.83	(16)
C11	3.3	(17)	5.5	(2)	5.26	(19)	-0.96	(15)	1.56	(15)	0.9	(16)
C12	2.82	(15)	5.2	(19)	2.76	(14)	0.01	(14)	1.08	(12)	1.09	(13)
C13	2.94	(15)	6.03	(20)	2.57	(14)	-0.56	(15)	1.16	(12)	-0.62	(14)
C14	5.6	(2)	5.5	(2)	6.2	(2)	-0.39	(17)	3.57	(18)	-1.9	(17)
C15	4.55	(19)	4.06	(19)	6.8	(2)	1.45	(15)	2.74	(17)	0.88	(16)
O1	4.25	(12)	3.85	(11)	2.81	(10)	-0.89	(9)	0.55	(9)	-0.74	(9)
F1	6.3	(4)	5.7	(4)	13.7	(8)	-1.3	(30)	-4.1	(4)	5.3	(5)
F2	19.9	(8)	2.2	(2)	4.7	(3)	-1.2	(4)	-0.7	(4)	-0.57	(17)
F3	9.8	(4)	10.3	(4)	7.9	(3)	4.1	(30	5.7	(3)	5.9	(3)
F1'	9.8	(5)	5.7	(4)	7	(4)	5	(3)	3.2	(4)	2.2	(3)

Table 4-5. Anisotropic Displacement Parameters ($Å^2$) for $C_{15}H_{16}CoF_3O$ (continued)

F2'	5.2	(4)	4.5	(4)	12	(7)	-2.5	(3)	-1.4	(4)	4.1	(4)
F3'	17.3	(13)	2.7	(3)	0.8	(2)	-1.4	(6)	-1.5	(4)	-0.1	(18)
H2	3.6											
H3	3.9											
H4	3.8											
H5	3.4											
H8	4.8											
H9	4.5											
H10a	5.4											
H10b	5.4											
H11a	5.7											
H11b	5.7											
H12	4.6											
H13	4.8											
H14a	6.8											
H14b	6.8											
H15a	6.1											
H15b	6.1											

Table 4-6. Torsion angles (˚) for $C_{15}H_{16}CoF_3O$

C2	Co1	C1	C2	0.0	(2)	C2	Co1	C1	C5	-117.0	(3)
C2	Co1	C1	C6	117.3	(3)	C3	Co1	C1	C2	37.1	(2)
C3	Co1	C1	C5	-79.9	(3)	C3	Co1	C1	C6	154.4	(3)
C4	Co1	C1	C2	79.1	(3)	C4	Co1	C1	C5	-37.9	(2)
C4	Co1	C1	C6	-163.6	(3)	C5	Co1	C1	C2	117.0	(3)
C5	Co1	C1	C5	0.0	(2)	C5	Co1	C1	C6	-125.7	(3)
C8	Co1	C1	C2	-169.9	(3)	C8	Co1	C1	C5	73.1	(3)
C8	Co1	C1	C6	-52.5	(2)	C9	Co1	C1	C2	150.3	(3)
C9	Co1	C1	C5	33.3	(2)	C9	Co1	C1	C6	-92.3	(3)
C12	Co1	C1	C2	-46.4	(2)	C12	Co1	C1	C5	-163.4	(3)
C12	Co1	C1	C6	70.9	(3)	C13	Co1	C1	C2	-78.5	(3)
C13	Co1	C1	C5	164.4	(3)	C13	Co1	C1	C6	38.8	(2)
C1	Co1	C2	C1	0.00	(20)	C1	Co1	C2	C3	118.4	(3)
C3	Co1	C2	C1	-118.4	(3)	C3	Co1	C2	C3	0.0	(2)
C4	Co1	C2	C1	-82.0	(3)	C4	Co1	C2	C3	36.4	(2)
C5	Co1	C2	C1	-38.9	(2)	C5	Co1	C2	C3	79.5	(3)
C8	Co1	C2	C1	20.9	(2)	C8	Co1	C2	C3	139.3	(4)
C9	Co1	C2	C1	-101.4	(3)	C9	Co1	C2	C3	17.0	(2)
C12	Co1	C2	C1	148.7	(3)	C12	Co1	C2	C3	-92.9	(3)
C13	Co1	C2	C1	109.2	(3)	C13	Co1	C2	C3	-132.4	(3)
C1	Co1	C3	C2	-38.5	(2)	C1	Co1	C3	C4	81.3	(3)

Table 4-6. Torsion angles (˚) for $C_{15}H_{16}CoF_3O$ (continued)

C2	Co1	C3	C2	0.0	(2)	C2	Co1	C3	C4	119.7	(3)
C4	Co1	C3	C2	-119.7	(3)	C4	Co1	C3	C4	0.0	(2)
C5	Co1	C3	C2	-83.0	(3)	C5	Co1	C3	C4	36.7	(2)
C8	Co1	C3	C2	-135.4	(4)	C8	Co1	C3	C4	-15.7	(2)
C9	Co1	C3	C2	-173.5	(4)	C9	Co1	C3	C4	-53.8	(3)
C12	Co1	C3	C2	96.4	(3)	C12	Co1	C3	C4	-143.9	(4)
C13	Co1	C3	C2	57.7	(3)	C13	Co1	C3	C4	177.5	(4)
C1	Co1	C4	C3	-81.4	(3)	C1	Co1	C4	C5	39.1	(2)
C2	Co1	C4	C3	-36.9	(2)	C2	Co1	C4	C5	83.5	(3)
C3	Co1	C4	C3	0.0	(2)	C3	Co1	C4	C5	120.5	(3)
C5	Co1	C4	C3	-120.5	(3)	C5	Co1	C4	C5	0.0	(2)
C8	Co1	C4	C3	172.7	(4)	C8	Co1	C4	C5	-66.8	(3)
C9	Co1	C4	C3	136.8	(4)	C9	Co1	C4	C5	-102.7	(3)
C12	Co1	C4	C3	49.8	(3)	C12	Co1	C4	C5	170.2	(4)
C13	Co1	C4	C3	-5.9	(2)	C13	Co1	C4	C5	114.6	(3)
C1	Co1	C5	C1	0.00	(19)	C1	Co1	C5	C4	-117.3	(3)
C2	Co1	C5	C1	38.8	(2)	C2	Co1	C5	C4	-78.5	(3)
C3	Co1	C5	C1	81.4	(3)	C3	Co1	C5	C4	-35.8	(2)
C4	Co1	C5	C1	117.3	(3)	C4	Co1	C5	C4	0.0	(2)
C8	Co1	C5	C1	-118.1	(3)	C8	Co1	C5	C4	124.7	(3)
C9	Co1	C5	C1	-158.5	(3)	C9	Co1	C5	C4	84.2	(3)

Table 4-6. Torsion angles (˚) for $C_{15}H_{16}CoF_3O$ (continued)

C12	Co1	C5	C1	78.3	(3)	C12	Co1	C5	C4	-39.0	(2)
C13	Co1	C5	C1	-26.4	(2)	C13	Co1	C5	C4	-143.7	(3)
C1	Co1	C8	C9	-139.8	(4)	C1	Co1	C8	C15	100.7	(3)
C2	Co1	C8	C9	-154.5	(4)	C2	Co1	C8	C15	85.9	(3)
C3	Co1	C8	C9	-53.9	(3)	C3	Co1	C8	C15	-173.4	(4)
C4	Co1	C8	C9	-64.8	(3)	C4	Co1	C8	C15	175.7	(4)
C5	Co1	C8	C9	-100.9	(3)	C5	Co1	C8	C15	139.6	(4)
C9	Co1	C8	C9	0.0	(2)	C9	Co1	C8	C15	-119.5	(4)
C12	Co1	C8	C9	75.8	(3)	C12	Co1	C8	C15	-43.7	(3)
C13	Co1	C8	C9	114.6	(4)	C13	Co1	C8	C15	-4.9	(3)
C1	Co1	C9	C8	65.2	(3)	C1	Co1	C9	C10	-174.6	(4)
C2	Co1	C9	C8	143.8	(4)	C2	Co1	C9	C10	-96.0	(3)
C3	Co1	C9	C8	156.4	(4)	C3	Co1	C9	C10	-83.4	(3)
C4	Co1	C9	C8	126.2	(4)	C4	Co1	C9	C10	-113.7	(3)
C5	Co1	C9	C8	86.7	(3)	C5	Co1	C9	C10	-153.1	(4)
C8	Co1	C9	C8	0.0	(3)	C8	Co1	C9	C10	120.2	(4)
C12	Co1	C9	C8	-103.1	(4)	C12	Co1	C9	C10	17.1	(2)
C13	Co1	C9	C8	-67.3	(3)	C13	Co1	C9	C10	52.9	(3)
C1	Co1	C12	C11	-171.1	(4)	C1	Co1	C12	C13	-52.9	(3)
C2	Co1	C12	C11	160.0	(4)	C2	Co1	C12	C13	-81.8	(3)
C3	Co1	C12	C11	119.9	(4)	C3	Co1	C12	C13	-121.9	(4)

Table 4-6. Torsion angles (˚) for $C_{15}H_{16}CoF_3O$ (continued)

C4	Co1	C12	C11	90.9	(3)	C4	Co1	C12	C13	-150.9	(4)
C5	Co1	C12	C11	122.9	(4)	C5	Co1	C12	C13	-118.9	(4)
C8	Co1	C12	C11	-40.9	(3)	C8	Co1	C12	C13	77.3	(3)
C9	Co1	C12	C11	-1.9	(2	C9	Co1	C12	C13	116.2	(4)
C13	Co1	C12	C11	-118.2	(4)	C13	Co1	C12	C13	0.0	(3)
C1	Co1	C13	C12	144.6	(4)	C1	Co1	C13	C14	-92.7	(3)
C2	Co1	C13	C12	104.9	(4)	C2	Co1	C13	C14	-132.4	(4)
C3	Co1	C13	C12	72.6	(3)	C3	Co1	C13	C14	-164.7	(4)
C4	Co1	C13	C12	76.7	(3)	C4	Co1	C13	C14	-160.6	(4)
C5	Co1	C13	C12	162.1	(4)	C5	Co1	C13	C14	-75.2	(3)
C8	Co1	C13	C12	-102.0	(4)	C8	Co1	C13	C14	20.7	(3)
C9	Co1	C13	C12	-65.3	(3)	C9	Co1	C13	C14	57.4	(3)
C12	Co1	C13	C12	0.0	(2)	C12	Co1	C13	C14	122.7	(4)
Co1	C1	C2	Co1	0.00	(2)	Co1	C1	C2	C3	-63.2	(3)
C5	C1	C2	Co1	60.1	(3)	C5	C1	C2	C3	-3.2	(2)
C6	C1	C2	Co1	-112.2	(4)	C6	C1	C2	C3	-175.4	(5)
Co1	C1	C5	Co1	0.00	(2)	Co1	C1	C5	C4	63.3	(3)
C2	C1	C5	Co1	-60.1	(3)	C2	C1	C5	C4	3.2	(2)
C6	C1	C5	Co1	111.4	(4)	C6	C1	C5	C4	174.7	(5)
Co1	C1	C6	C7	88.5	(3)	Co1	C1	C6	O1	-92.4	(3)
C2	C1	C6	C7	171.8	(5)	C2	C1	C6	O1	-9.1	(2)

Table 4-6. Torsion angles (˚) for $C_{15}H_{16}CoF_3O$ (continued)

C5	C1	C6	C7	1.6	(2)	C5	C1	C6	O1	-179.3	(5)
Co1	C2	C3	Co1	0.00	(2)	Co1	C2	C3	C4	-59.4	(3)
C1	C2	C3	Co1	61.3	(3)	C1	C2	C3	C4	1.9	(2)
Co1	C3	C4	Co1	0.000	(20)	Co1	C3	C4	C5	-57.5	(3)
C2	C3	C4	Co1	57.6	(3)	C2	C3	C4	C5	0.1	(2)
Co1	C4	C5	Co1	0.0	(2)	Co1	C4	C5	C1	-61.5	(3)
C3	C4	C5	Co1	59.4	(3)	C3	C4	C5	C1	-2.1	(2)
C1	C6	C7	F1	-38.2	(6)	C1	C6	C7	F2	-171.4	(8)
C1	C6	C7	F3	69.9	(5)	C1	C6	C7	F1’	-116.5	(7)
C1	C6	C7	F2’	134.5	(8)	C1	C6	C7	F3’	-1.9	(7)
O1	C6	C7	F1	142.7	(8)	O1	C6	C7	F2	9.4	(5)
O1	C6	C7	F3	-109.3	(6)	O1	C6	C7	F1’	64.4	(6)
O1	C6	C7	F2’	-44.7	(6)	O1	C6	C7	F3’	179.0	(9)
C6	C7	F1	F2	-137.1	(9)	C6	C7	F1	F3	113.3	(9)
C6	C7	F1	F1’	-96.9	(9)	C6	C7	F1	F3’	104.0	(19)
F2	C7	F1	F2	0.0	(7)	F2	C7	F1	F3	-109.5	(11)
F2	C7	F1	F1’	40.2	(8)	F2	C7	F1	F3’	-119.0	(2)
F3	C7	F1	F2	109.5	(10)	F3	C7	F1	F3	0.0	(5)
F3	C7	F1	F1’	149.7	(12)	F3	C7	F1	F3’	-9.3	(14)
F1’	C7	F1	F2	-40.2	(7)	F1’	C7	F1	F3	-149.7	(11)
F1’	C7	F1	F1’	0.0	(6)	F1’	C7	F1	F3’	-159.0	(2)

Table 4-6. Torsion angles (°) for $C_{15}H_{16}CoF_3O$ (continued)

F2’	C7	F1	F2	52.4	(8)	F2’	C7	F1	F3	-57.1	(8)
F2’	C7	F1	F1’	92.6	(11)	F2’	C7	F1	F3’	-66.5	(18)
F3’	C7	F1	F2	118.9	(12)	F3’	C7	F1	F3	9.3	(8)
F3’	C7	F1	F1’	159.1	(14)	F3’	C7	F1	F3’	0.0	(15)
C6	C7	F2	F1	136.5	(8)	C6	C7	F2	F3	-119.4	(7)
C6	C7	F2	F1’	85.7	(9)	C6	C7	F2	F2’	-92.7	(11)
C6	C7	F2	F3’	169.4	(9)	C6	C7	F2	F1	0.0	(7)
F1	C7	F2	F3	104.1	(10)	F1	C7	F2	F1’	-50.9	(9)
F1	C7	F2	F2’	130.8	(14)	F1	C7	F2	F3’	32.9	(8)
F3	C7	F2	F1	-104.1	(9)	F3	C7	F2	F3	0.0	(5)
F3	C7	F2	F1’	-155.0	(13)	F3	C7	F2	F2’	26.7	(8)
F3	C7	F2	F3’	-71.3	(8)	F3	C7	F2	F1	50.9	(7)
F1’	C7	F2	F3	155.0	(10)	F1’	C7	F2	F1’	0.0	(7)
F1’	C7	F2	F2’	-178.4	(14)	F1’	C7	F2	F3’	83.7	(8)
F2’	C7	F2	F1	-130.8	(10)	F2’	C7	F2	F3	-26.7	(7)
F2’	C7	F2	F1’	178.4	(14)	F2’	C7	F2	F2’	0.0	(9)
F2’	C7	F2	F3’	-97.9	(10)	F2’	C7	F2	F1	-32.9	(9)
F3’	C7	F2	F3	71.3	(9)	F3’	C7	F2	F1’	-83.7	(12)
F3’	C7	F2	F2’	97.9	(14)	F3’	C7	F2	F3’	0.0	(9)
C6	C7	F3	F1	-121.1	(7)	C6	C7	F3	F2	126.5	(7)
C6	C7	F3	F2’	103.4	(9)	C6	C7	F3	F3’	-115.7	(9)

Table 4-6. Torsion angles (˚) for $C_{15}H_{16}CoF_3O$ (continued)

F1	C7	F3	F1	0.0	(7)	F1	C7	F3	F2	-112.5	(9)
F1	C7	F3	F2’	-135.5	(12)	F1	C7	F3	F3’	5.4	(9)
F2	C7	F3	F1	112.5	(9)	F2	C7	F3	F2	0.0	(6)
F2	C7	F3	F2’	-23.1	(8)	F2	C7	F3	F3’	117.9	(11)
F1’	C7	F3	F1	71.1	(8)	F1’	C7	F3	F2	-41.3	(6)
F1’	C7	F3	F2’	-64.4	(8)	F1’	C7	F3	F3’	76.5	(9)
F2’	C7	F3	F1	135.5	(10)	F2’	C7	F3	F2	23.1	(7)
F2’	C7	F3	F2’	0.0	(8)	F2’	C7	F3	F3’	140.9	(12)
F3’	C7	F3	F1	-5.4	(8)	F3’	C7	F3	F2	-117.9	(10)
F3’	C7	F3	F2’	-140.9	(13)	F3’	C7	F3	F3’	0.0	(9)
C6	C7	F1’	F1	114.4	(9)	C6	C7	F1’	F2	-115.3	(11)
C6	C7	F1’	F2’	-114.0	(8)	C6	C7	F1’	F3’	125.6	(8)
F1	C7	F1’	F1	0.0	(8)	F1	C7	F1’	F2	130.3	(13)
F1	C7	F1’	F2’	131.6	(11)	F1	C7	F1’	F3’	11.2	(8)
F2	C7	F1’	F1	-130.3	(11)	F2	C7	F1’	F2	0.0	(70
F2	C7	F1’	F2’	1.3	(7)	F2	C7	F1’	F3’	-119.1	(10)
F3	C7	F1’	F1	-77.5	(9)	F3	C7	F1’	F2	52.8	(8)
F3	C7	F1’	F2’	54.0	(7)	F3	C7	F1’	F3’	-66.3	(8)
F2’	C7	F1’	F1	-131.6	(12)	F2’	C7	F1’	F2	-1.3	(8)
F2’	C7	F1’	F2’	0.0	(7)	F2’	C7	F1’	F3’	-120.4	(10)
F3’	C7	F1’	F1	-11.2	(9)	F3’	C7	F1’	F2	119.1	(14)

Table 4-6. Torsion angles (°) for $C_{15}H_{16}CoF_3O$ (continued)

F3’	C7	F1’	F2’	120.4	(11)	F3’	C7	F1’	F3’	0.0	(9)
C6	C7	F2’	F2	110.6	(12)	C6	C7	F2’	F3	-99.0	(9)
C6	C7	F2’	F1’	109.3	(8)	C6	C7	F2’	F3’	-138.5	(9)
F1	C7	F2’	F2	-78.4	(12)	F1	C7	F2’	F3	72.0	(10)
F1	C7	F2’	F1’	-79.8	(9)	F1	C7	F2’	F3’	32.4	(8)
F2	C7	F2’	F2	0.0	(8)	F2	C7	F2’	F3	150.4	(13)
F2	C7	F2’	F1’	-1.3	(6)	F2	C7	F2’	F3’	110.8	(11)
F3	C7	F2’	F2	-150.4	(14)	F3	C7	F2’	F3	0.0	(6)
F3	C7	F2’	F1’	-151.8	(10)	F3	C7	F2’	F3’	-39.6	(7)
F1’	C7	F2’	F2	1.3	(8)	F1’	C7	F2’	F3	151.8	(12)
F1’	C7	F2’	F1’	0.0	(6)	F1’	C7	F2’	F3’	112.2	(10)
F3’	C7	F2’	F2	-110.8	(15)	F3’	C7	F2’	F3	39.6	(9)
F3’	C7	F2’	F1’	-112.2	(12)	F3’	C7	F2’	F3’	0.0	(9)
C6	C7	F3’	F1	-93.6	(19)	C6	C7	F3’	F2	-169.2	(11)
C6	C7	F3’	F3	96.5	(10)	C6	C7	F3’	F1’	-114.3	(9)
C6	C7	F3’	F2’	134.0	(10)	C6	C7	F3’	F1	0.0	(14)
F1	C7	F3’	F2	-75.5	(10)	F1	C7	F3’	F3	-169.9	(15)
F1	C7	F3’	F1’	-20.7	(8)	F1	C7	F3’	F2’	-132.3	(12)
F2	C7	F3’	F1	75.5	(18)	F2	C7	F3’	F2	0.0	(7)
F2	C7	F3’	F3	-94.3	(12)	F2	C7	F3’	F1’	54.9	(8)
F2	C7	F3’	F2’	-56.8	(9)	F2	C7	F3’	F1	170.0	(2)

Table 4-6. Torsion angles (˚) for $C_{15}H_{16}CoF_3O$ (continued)

F3	C7	F3’	F2	94.3	(9)	F3	C7	F3’	F3	0.0	(6)
F3	C7	F3’	F1’	149.2	(12)	F3	C7	F3’	F2’	37.5	(7)
F1’	C7	F3’	F1	20.7	(14)	F1’	C7	F3’	F2	-54.9	(8)
F1’	C7	F3’	F3	-149.2	(14)	F1’	C7	F3’	F1’	0.0	(6)
F1’	C7	F3’	F2’	-111.6	(11)	F1’	C7	F3’	F1	132.0	(2)
F2’	C7	F3’	F2	56.8	(9)	F2’	C7	F3’	F3	-37.5	(8)
F2’	C7	F3’	F1’	111.6	(12)	F2’	C7	F3’	F2’	0.0	(7)
Co1	C8	C9	Co1	0.00	(2)	Co1	C8	C9	C10	-103.4	(4)
F3	C7	F2’	F2	-150.4	(14)	F3	C7	F2’	F3	0.0	(6)
F3	C7	F2’	F1’	-151.8	(10)	F3	C7	F2’	F3’	-39.6	(7)
F1’	C7	F2’	F2	1.3	(8)	F1’	C7	F2’	F3	151.8	(12)
F1’	C7	F2’	F1’	0.0	(6)	F1’	C7	F2’	F3’	112.2	(10)
F3’	C7	F2’	F2	-110.8	(15)	F3’	C7	F2’	F3	39.6	(9)
F3’	C7	F2’	F1’	-112.2	(12)	F3’	C7	F2’	F3’	0.0	(9)
C6	C7	F3’	F1	-93.6	(19)	C6	C7	F3’	F2	-169.2	(11)
C6	C7	F3’	F3	96.5	(10)	C6	C7	F3’	F1’	-114.3	(9)
C6	C7	F3’	F2’	134.0	(10)	C6	C7	F3’	F1	0.0	(14)
F1	C7	F3’	F2	-75.5	(10)	F1	C7	F3’	F3	-169.9	(15)
F1	C7	F3’	F1’	-20.7	(8)	F1	C7	F3’	F2’	-132.3	(12)
F2	C7	F3’	F1	75.5	(18)	F2	C7	F3’	F2	0.0	(7)
F2	C7	F3’	F3	-94.3	(12)	F2	C7	F3’	F1’	54.9	(8)

Table 4-6. Torsion angles (˚) for $C_{15}H_{16}CoF_3O$ (continued)

F2	C7	F3’	F2’	-56.8	(9)	F2	C7	F3’	F1	170.0	(2)
F3	C7	F3’	F2	94.3	(9)	F3	C7	F3’	F3	0.0	(6)
F3	C7	F3’	F1’	149.2	(12)	F3	C7	F3’	F2’	37.5	(7)
F1’	C7	F3’	F1	20.7	(14)	F1’	C7	F3’	F2	-54.9	(8)
F1’	C7	F3’	F3	-149.2	(14)	F1’	C7	F3’	F1’	0.0	(6)
F1’	C7	F3’	F2’	-111.6	(11)	F1’	C7	F3’	F1	132.0	(2)
F2’	C7	F3’	F2	56.8	(9)	F2’	C7	F3’	F3	-37.5	(8)
F2’	C7	F3’	F1’	111.6	(12)	F2’	C7	F3’	F2’	0.0	(7)
Co1	C8	C9	Co1	0.00	(2)	Co1	C8	C9	C10	-103.4	(4)
C15	C8	C9	Co1	104.0	(4)	C15	C8	C9	C10	0.6	(3)
Co1	C8	C15	C14	-12.0	(2)	C9	C8	C15	C14	-92.4	(5)
Co1	C9	C10	C11	-29.2	(2)	C8	C9	C10	C11	50.8	(4)
C9	C10	C11	C12	27.4	(3)	C10	C11	C12	Co1	-13.4	(2)
C10	C11	C12	C13	-93.1	(5)	Co1	C12	C13	Co1	0.00	(2)
Co1	C12	C13	C14	-101.5	(4)	C11	C12	C13	Co1	105.1	(4)
C11	C12	C13	C14	3.6	(3)	Co1	C13	C14	C15	-32.9	(3)
C12	C13	C14	C15	47.9	(4)	C13	C14	C15	C8	29.3	(3)
C7	F1	F2	C7	0.0	(3)	C7	F1	F2	F3	-46.8	(7)
C7	F1	F2	F1’	110.9	(15)	C7	F1	F2	F2’	-44.3	(10)
C7	F1	F2	F3’	-53.8	(8)	F3	F1	F2	C7	46.8	(7)
F3	F1	F2	F3	0.0	(4)	F3	F1	F2	F1’	157.7	(15)
F3	F1	F2	F2’	2.6	(9)	F3	F1	F2	F3’	-7.0	(5)

Table 4-6. Torsion angles (˚) for $C_{15}H_{16}CoF_3O$ (continued)

F1’	F1	F2	C7	-110.9	(13)	F1’	F1	F2	F3	-157.7	(12)
F1’	F1	F2	F1’	0.0	(7)	F1’	F1	F2	F2’	-155.1	(17)
F1’	F1	F2	F3’	-164.7	(12)	F3’	F1	F2	C7	53.8	(17)
F3’	F1	F2	F3	7.0	(16)	F3’	F1	F2	F1’	165.0	(3)
F3’	F1	F2	F2’	9.5	(15)	F3’	F1	F2	F3’	0.0	(16)
C7	F1	F3	C7	0.0	(3)	C7	F1	F3	F2	37.4	(6)
C7	F1	F3	F2’	35.4	(7)	C7	F1	F3	F3’	-159.3	(15)
F2	F1	F3	C7	-37.4	(6)	F2	F1	F3	F2	0.0	(4)
F2	F1	F3	F2’	-2.0	(7)	F2	F1	F3	F3’	163.3	(13)
F1’	F1	F3	C7	-24.8	(5)	F1’	F1	F3	F2	12.6	(5)
F1’	F1	F3	F2’	10.6	(7)	F1’	F1	F3	F3’	175.9	(15)
F3’	F1	F3	C7	159.0	(2)	F3’	F1	F3	F2	-163.0	(2)
F3’	F1	F3	F2’	-165.0	(2)	F3’	F1	F3	F3’	0.0	(16)
C7	F1	F1’	C7	0.0	(3)	C7	F1	F1’	F2	-39.8	(8)
C7	F1	F1’	F2’	-27.2	(6)	C7	F1	F1’	F3’	-22.2	(6)
F2	F1	F1’	C7	39.8	(6)	F2	F1	F1’	F2	0.0	(7)
F2	F1	F1’	F2’	12.6	(5)	F2	F1	F1’	F3’	17.6	(5)
F3	F1	F1’	C7	20.2	(5)	F3	F1	F1’	F2	-19.6	(7)
F3	F1	F1’	F2’	-7.0	(4)	F3	F1	F1’	F3’	-2.0	(5)
F3’	F1	F1’	C7	22.2	(15)	F3’	F1	F1’	F2	-17.6	(15)
F3’	F1	F1’	F2’	-5.0	(16)	F3’	F1	F1’	F3’	0.0	(16)
C7	F1	F3’	C7	0.0	(3)	C7	F1	F3’	F2	29.9	(6)

Table 4-6. Torsion angles (˚) for $C_{15}H_{16}CoF_3O$ (continued)

C7	F1	F3’	F3	15.2	(5)	C7	F1	F3’	F1’	19.9	(6)
C7	F1	F3’	F2’	24.9	(6)	F2	F1	F3’	C7	-29.9	(7)
F2	F1	F3’	F2	0.0	(4)	F2	F1	F3’	F3	-14.7	(6)
F2	F1	F3’	F1’	-10.0	(5)	F2	F1	F3’	F2’	-5.0	(5)
F3	F1	F3’	C7	-15.2	(6)	F3	F1	F3’	F2	14.7	(4)
F3	F1	F3’	F3	0.0	(5)	F3	F1	F3’	F1’	4.7	(4)
F3	F1	F3’	F2’	9.7	(4)	F1’	F1	F3’	C7	-19.9	(6)
F1’	F1	F3’	F2	10.0	(5)	F1’	F1	F3’	F3	-4.7	(6)
F1’	F1	F3’	F1’	0.0	(5)	F1’	F1	F3’	F2’	5.0	(6)
C7	F2	F3	C7	0.0	(3)	C7	F2	F3	F1	-42.5	(6)
C7	F2	F3	F2’	133.0	(13)	C7	F2	F3	F3’	-46.0	(8)
F1	F2	F3	C7	42.5	(6)	F1	F2	F3	F1	0.0	(5)
F1	F2	F3	F2’	175.5	(12)	F1	F2	F3	F3’	-3.6	(7)
F1’	F2	F3	C7	24.5	(7)	F1’	F2	F3	F1	-18.0	(7)
F1’	F2	F3	F2’	157.5	(15)	F1’	F2	F3	F3’	-21.5	(9)
F2’	F2	F3	C7	-133.0	(15)	F2’	F2	F3	F1	-175.5	(14)
F2’	F2	F3	F2’	0.0	(9)	F2’	F2	F3	F3’	-179.0	(17)
F3’	F2	F3	C7	46.0	(6)	F3’	F2	F3	F1	3.6	(6)
F3’	F2	F3	F2’	179.0	(12)	F3’	F2	F3	F3’	0.0	(8)
C7	F2	F1’	C7	0.0	(3)	C7	F2	F1’	F1	35.9	(7)
C7	F2	F1’	F2’	-2.2	(5)	C7	F2	F1’	F3’	30.7	(6)
F1	F2	F1’	C7	-35.9	(6)	F1	F2	F1’	F1	0.0	(6)

Table 4-6. Torsion angles (˚) for $C_{15}H_{16}CoF_3O$ (continued)

F1	F2	F1’	F2’	-38.2	(6)	F1	F2	F1’	F3’	-5.2	(6)
F3	F2	F1’	C7	-16.3	(4)	F3	F2	F1’	F1	19.6	(6)
F3	F2	F1’	F2’	-18.6	(5)	F3	F2	F1’	F3’	14.4	(5)
F2’	F2	F1’	C7	2.2	(7)	F2’	F2	F1’	F1	38.2	(10)
F2’	F2	F1’	F2’	0.0	(9)	F2’	F2	F1’	F3’	32.9	(10)
F3’	F2	F1’	C7	-30.7	(6)	F3’	F2	F1’	F1	5.2	(6)
F3’	F2	F1’	F2’	-32.9	(6)	F3’	F2	F1’	F3’	0.0	(6)
C7	F2	F2’	C7	0.0	(3)	C7	F2	F2’	F3	-30.4	(6)
C7	F2	F2’	F1’	2.3	(5)	C7	F2	F2’	F3’	-29.8	(6)
F1	F2	F2’	C7	26.6	(6)	F1	F2	F2’	F3	-3.8	(6)
F1	F2	F2’	F1’	28.9	(5)	F1	F2	F2’	F3’	-3.2	(6)
F3	F2	F2’	C7	30.4	(5)	F3	F2	F2’	F3	0.0	(5)
F3	F2	F2’	F1’	32.7	(5)	F3	F2	F2’	F3’	0.6	(5)
F1’	F2	F2’	C7	-2.3	(6)	F1’	F2	F2’	F3	-32.7	(8)
F1’	F2	F2’	F1’	0.0	(7)	F1’	F2	F2’	F3’	-32.1	(8)
F3’	F2	F2’	C7	29.8	(6)	F3’	F2	F2’	F3	-0.6	(6)
F3’	F2	F2’	F1’	32.1	(6)	F3’	F2	F2’	F3’	0.0	(6)
C7	F2	F3’	C7	0.0	(3)	C7	F2	F3’	F1	-98.0	(2)
C7	F2	F3’	F3	72.5	(11)	C7	F2	F3’	F1’	-85.5	(10)
C7	F2	F3’	F2’	71.9	(9)	F1	F2	F3’	C7	98.2	(12)
F1	F2	F3’	F1	0.0	(16)	F1	F2	F3’	F3	170.6	(14)
F1	F2	F3’	F1’	12.7	(5)	F1	F2	F3’	F2’	170.1	(11)

Table 4-6. Torsion angles (˚) for $C_{15}H_{16}CoF_3O$ (continued)

F3	F2	F3’	C7	-72.5	(9)	F3	F2	F3’	F1	-171.0	(2)
F3	F2	F3’	F3	0.0	(5)	F3	F2	F3’	F1’	-157.9	(11)
F3	F2	F3’	F2’	-0.6	(4)	F1’	F2	F3’	C7	85.5	(14)
F1’	F2	F3’	F1	-12.7	(14)	F1’	F2	F3’	F3	157.9	(18)
F1’	F2	F3’	F1’	0.0	(7)	F1’	F2	F3’	F2’	157.4	(15)
F2’	F2	F3’	C7	-71.9	(13)	F2’	F2	F3’	F1	-170.0	(3)
F2’	F2	F3’	F3	0.6	(8)	F2’	F2	F3’	F1’	-157.4	(17)
F2’	F2	F3’	F2’	0.0	(9)	C7	F3	F2’	C7	0.0	(3)
C7	F3	F2’	F2	30.3	(8)	C7	F3	F2’	F1’	18.2	(5)
C7	F3	F2’	F3’	29.4	(6)	F1	F3	F2’	C7	-26.4	(6)
F1	F3	F2’	F2	3.9	(8)	F1	F3	F2’	F1’	-8.2	(5)
F1	F3	F2’	F3’	3.0	(6)	F2	F3	F2’	C7	-30.3	(5)
F2	F3	F2’	F2	0.0	(8)	F2	F3	F2’	F1’	-12.2	(4)
F2	F3	F2’	F3’	-0.9	(5)	F3’	F3	F2’	C7	-29.4	(7)
F3’	F3	F2’	F2	0.9	(9)	F3’	F3	F2’	F1’	-11.2	(7)
F3’	F3	F2’	F3’	0.0	(8)	C7	F3	F3’	C7	0.0	(3)
C7	F3	F3’	F1	-16.9	(14)	C7	F3	F3’	F2	-32.1	(5)
C7	F3	F3’	F1’	-20.1	(5)	C7	F3	F3’	F2’	-31.6	(6)
F1	F3	F3’	C7	16.9	(6)	F1	F3	F3’	F1	0.0	(15)
F1	F3	F3’	F2	-15.2	(5)	F1	F3	F3’	F1’	-3.3	(5)
F1	F3	F3’	F2’	-14.8	(5)	F2	F3	F3’	C7	32.1	(6)
F2	F3	F3’	F1	15.2	(15)	F2	F3	F3’	F2	0.0	(4)

Table 4-6. Torsion angles (˚) for $C_{15}H_{16}CoF_3O$ (continued)

F2	F3	F3’	F1’	11.9	(4)	F2	F3	F3’	F2’	0.4	(5)
F2’	F3	F3’	C7	31.6	(7)	F2’	F3	F3’	F1	14.8	(15)
F2’	F3	F3’	F2	-0.4	(7)	F2’	F3	F3’	F1’	11.5	(7)
F2’	F3	F3’	F2’	0.0	(7)	C7	F1’	F2’	C7	0.0	(3)
C7	F1’	F2’	F2	-176.9	(17)	C7	F1’	F2’	F3	-25.4	(5)
C7	F1’	F2’	F3’	-34.3	(6)	F1	F1’	F2’	C7	36.0	(7)
F1	F1’	F2’	F2	-140.9	(16)	F1	F1’	F2’	F3	10.5	(7)
F1	F1’	F2’	F3’	1.7	(6)	F2	F1’	F2’	C7	176.9	(17)
F2	F1’	F2’	F2	0.0	(8)	F2	F1’	F2’	F3	151.4	(16)
F2	F1’	F2’	F3’	142.6	(14)	F3’	F1’	F2’	C7	34.3	(7)
F3’	F1’	F2’	F2	-142.6	(15)	F3’	F1’	F2’	F3	8.9	(6)
F3’	F1’	F2’	F3’	0.0	(6)	C7	F1’	F3’	C7	0.0	(3)
C7	F1’	F3’	F1	-149.0	(3)	C7	F1’	F3’	F2	48.5	(7)
C7	F1’	F3’	F3	27.7	(6)	C7	F1’	F3’	F2’	36.1	(6)
F1	F1’	F3’	C7	149.5	(16)	F1	F1’	F3’	F1	0.0	(15)
F1	F1’	F3’	F2	-162.0	(13)	F1	F1’	F3’	F3	177.1	(15)
F1	F1’	F3’	F2’	-174.4	(13)	F2	F1’	F3’	C7	-48.5	(9)
F2	F1’	F3’	F1	162.0	(3)	F2	F1’	F3’	F2	0.0	(7)
F2	F1’	F3’	F3	-20.9	(7)	F2	F1’	F3’	F2’	-12.4	(8)
F2’	F1’	F3’	C7	-36.1	(7)	F2’	F1’	F3’	F1	174.0	(2)
F2’	F1’	F3’	F2	12.4	(5)	F2’	F1’	F3’	F3	-8.5	(6)

Table 4-6. Torsion angles (˚) for $C_{15}H_{16}CoF_3O$ (continued)

F2’	F1’	F3’	F2’	0.0	(5)	C7	F2’	F3’	C7	0.0	(3)
C7	F2’	F3’	F1	-48.8	(17)	C7	F2’	F3’	F2	-58.7	(8)
C7	F2’	F3’	F3	122.1	(15)	C7	F2’	F3’	F1’	-44.9	(7)
F2	F2’	F3’	C7	58.7	(12)	F2	F2’	F3’	F1	9.9	(14)
F2	F2’	F3’	F2	0.0	(9)	F2	F2’	F3’	F3	-179.2	(20)
F2	F2’	F3’	F1’	13.9	(9)	F3	F2’	F3’	C7	-122.1	(16)
F3	F2’	F3’	F1	-171.0	(3)	F3	F2’	F3’	F2	179.2	(14)
F3	F2’	F3’	F3	0.0	(6)	F3	F2’	F3’	F1’	-167.0	(15)
F1’	F2’	F3’	C7	44.9	(8)	F1’	F2’	F3’	F1	-4.0	(16)
F1’	F2’	F3’	F2	-13.9	(4)	F1’	F2’	F3’	F3	167.0	(14)
F1’	F2’	F3’	F1’	0.0	(4)						

2. General Experimental for Chapter Two

All reactions and manipulation were conducted under a dry argon atmosphere either using an inert atmosphere dry box or standard Schlenk techniques. All isocyanates and alkynes were purchased from Aldrich Chemical Company and purified by stirring with CaH and bulb to bulb transfer under high vacuum level. Alkyne **5b** was prepared according to the literature methods.[2] THF and toluene were distilled from Na/benzophenone, pentane came from the Mraun dry-solvent system. Toluene-d8 and THF-d8 were distilled form Na/benzophenone. Fisher isotemp 3016H heating circulator was used as precise temperature-controlled heating bath. ^{1}H and ^{13}CNMR data were recorded on either a Varian Mercury 300 or 400 MHz spectrometer. Chemical shifts were reported in parts per million (ppm) referenced to the ^{1}H resonance of the residual solvent proton signal or ^{13}C resonance of the deuterated solvent. ^{19}FNMR spectra were recorded on a Varian Mercury 300 or 400 MHz spectrometer with hexafluorobenzene (-162.9 ppm) as external standard. IR data were recorded on a MIDAC Corporation M Series FTIR spectrometer. UV spectra were acquired by JASCO V-550 UV-VIS spectrometer. High Resolution Mass Spectral Data were recorded on JEOL (Tokyo, Japan) HX110HF mass spectrometer.

2.1 General cocyclotrimerization procedure for 4a to 4g.

0.25mmol isocyanate, 0.10mmol alkyne, and 50μL 100mM Cp^{CF3}CoCOD solution (in toluene-d8) were combined in a NMR tube and added toluene-d8 to make total volume to 500μL. Freeze-pump-thawed the tube three cycles, and sealed the tube by using propane torch. Took initial NMR. Heated the tube in 85^{o}C heating bath. Used the NMR technique to

monitor the reaction and recorded the reaction time. After the reaction finished, the tube was cooled to ambient temperature and volatiles were removed under vacuum. The remaining residue was subjects to alumina column chromatography with 50% CH_2Cl_2/hexanes, followed by 100% CH_2Cl_2.

4a: light yellow oil. Yield: 90.7%. ^{1}HNMR (400M, $CDCl_3$) δ0.977 (t, J = 7.6Hz, 3H), 1.706 (m, 2H), 3.378 (s, 3H), 3.398 (s, 3H), 3.402 (s, 3H), 3.416(s, 3H), 1.044 (t, J = 8.0Hz, 2H), 4.366 (s, 2H), 4.436 (s, 2H), 4.469 (s, 2H), 4.558 (s, 2H); ^{13}CNMR (400M, $CDCl_3$) δ11.720, 22.412, 47.322, 58.462, 58.585, 58.606, 58.833, 65.871, 66.674, 67.334, 67.918, 116.571, 128.044, 144.196, 147.298, 162.300; HRMS (Fab, M^+): $C_{16}H_{27}NO_5$ calcd 314.1967, found 314.1985; IR (neat) 2928, 1646, 1595, 1095cm^{-1}; UV (CH_2Cl_2) λ_{max} = 327 nm (ε_{max} = 2503), 246 nm (ε_{max} = 2226).

4b: light yellow oil. Yield: 93.3%. ^{1}HNMR (300M, $CDCl_3$) δ0.886 (t, J = 6.9Hz, 3H,), 1.333 (m, 4H), 1.388 (m, 2H), 1.682 (m, 2H), 3.388 (s, 3H), 3.405(s, 3H), 2.407 (s, 3H), 3.424 (s, 3H), 4.083 (t, J = 8.4Hz, 2H,), 4.371(s, 2H), 4.440 (s, 2H), 4.477 (s, 2H), 4.563 (s, 2H); ^{13}CNMR (300M, $CDCl_3$) δ14.210, 22.774, 27.107, 28.998, 31.569, 45.860, 58.484, 58.620, 58.632, 58.849, 65.905, 66.687, 67.367, 67.944, 116.590, 128.021, 144.188, 147.291, 162.725; HRMS (Fab, M^+): $C_{19}H_{33}NO_5$ calcd 356.3437, found 356.2441; IR (neat) 2927, 1647, 1459, 1097 cm^{-1}; UV (CH_2Cl_2) λ_{max} = 327 nm (ε_{max} = 2957), 246 nm (ε_{max} = 2690).

4c: colorless oil. Yield: 93.2 %. ^{1}HNMR (400M, $CDCl_3$) δ1.607 (d, J = 6.8Hz, 6H), 1.706 (m, 2H), 3.373 (m, 1H), 3.396 (s, 3H), 3.415 (s, 6H), 3.421(s, 3H), 4.352 (s, 2H), 4.440 (s, 2H), 4.456 (s, 2H), 4.528 (s, 2H); ^{13}CNMR (400M, $CDCl_3$) δ19.766, 29.912, 58.439, 58.538, 58.636, 58.887, 65.696, 66.788, 67.744, 68.062, 116.556, 129.303, 144.613, 146.789,

163.343 HRMS (Fab, M^+): $C_{16}H_{27}NO_5$ calcd 314.1967, found 314.1982; IR (neat) 2928, 1647, 1548, 1097 cm^{-1}; UV (CH_2Cl_2) λ_{max} = 328 nm (ε_{max} = 1192), 248 nm (ε_{max} = 1010).

4d: 4d decomposed on the alumina column while trying to separation.

4e: light yellow oil. Yield: 86.2%. ^{1}HNMR (400M, $CDCl_3$) δ2.983 (s, 3H), 3.381 (s, 3H), 3.425(s, 3H), 3.454 (s, 3H), 3.991 (s, 2H), 4.429 (s, 2H), 4.560 (s, 4H), 4.558, 7.229 (m, 2H), 7.468 (m, 3H); ^{13}CNMR (400M, $CDCl_3$) δ58.492, 58.583, 58.644, 58.932, 65.613, 67.008, 67.198, 67.827, 116.381, 128.545, 128.833, 129.277, 137.864, 138.296, 144.416, 148.647, 163.192; HRMS (Fab, M^+): $C_{19}H_{25}NO_5$ calcd 348.1811, found 348.1824; IR (neat) 3064, 2928, 1656, 1394, 1097 cm^{-1}; UV (CH_2Cl_2) λ_{max} = 317 nm (ε_{max} = 2156), 240 nm (ε_{max} = 2493).

4f: white solid. Yield: 83.3%. ^{1}HNMR (300M, $CDCl_3$) δ3.060 (s, 3H), 3.404 (s, 3H), 3.421 (s, 3H), 3.449 (s, 3H), 3.473(s, 3H), 3.833 (s, 4H), 4.043 (s, 2H), 4.444 (s, 2H), 6.992 (d, J = 8.7Hz, 2H), 7,145 (d, J = 8.4Hz, 2H); ^{13}CNMR (300M, $CDCl_3$) δ58.606, 58.708, 58.784, 59.034, 65.814, 67.252, 67.400, 67.973, 68.219, 114.475, 116.315, 128.877, 129.548, 130.952, 137.868, 144.804, 148.476, 159.581. HRMS (Fab, M^+): $C_{20}H_{27}NO_6$ calcd 378.1917, found 378.1941; IR (neat) 2926, 1654, 1511, 1248, 1097 cm^{-1}; UV (CH_2Cl_2) λ_{max} = 327 nm (ε_{max} = 1686), 234 nm (ε_{max} = 3625).

4g: white solid. Yield: 83.7%. ^{1}HNMR (400M, $CDCl_3$) δ3.032 (s, 3H), 3.385 (s, 3H), 3.439 (s, 3H), 3.465(s, 3H), 4.003 (s, 2H), 4.436 (s, 2H), 4.429 (s, 2H), 4.556 (s, 4H), 7.158 (m, 2H), 7.204 (m, 2H); ^{13}CNMR (300M, $CDCl_3$) δ58.682, 58.742, 58.848, 59.095, 65.769, 67.081, 67.301, 67.935, 115.298, 115.594, 116.630, 128.983, 130.364, 130.478, 144.318, 148.738, 160.837, 163.212, 164.122; ^{19}FNMR (400M, Toluene-d_8) δ-160.162; HRMS (Fab,

M^+): $C_{19}H_{24}NO_5F$ calcd 366.1717, found 366.1711; IR (neat) 3072, 2929, 1656, 1509, 1097 cm^{-1}; UV (CH_2Cl_2) λ_{max} = 325 nm (ε_{max} = 2095), 239 nm (ε_{max} = 2711).

4h: white solid. Yield: 84.9%. ^{1}HNMR (400M, $CDCl_3$) δ0.938 (t, J = 7.6Hz, 3H), 1.706 (m, 2H), 3.796 (s, 3H), 3.846 (t, J = 8Hz, 2H), 3.877 (s, 3H), 3.886 (s, 3H), 3.991(s, 3H); ^{13}CNMR (400M, $CDCl_3$) δ11.401, 22.177, 50.416, 53.260, 53.321, 53.351, 54.041, 105.189, 122.175, 144.067, 147.851, 157.747, 161.948, 162.964, 164.170, 165.277; HRMS (Fab, M^+): $C_{16}H_{27}NO_5$ calcd 370.1138, found 370.1137; IR (neat) 2960, 1750, 1675, 1444, 1240 cm^{-1}; UV (CH_2Cl_2) λ_{max} = 330 nm (ε_{max} = 2588), 267 nm (ε_{max} = 4504), 230 nm (ε_{max} = 2631).

2.2 General cocyclotrimerization procedure for 6a and 6d.

0.25mmol isocyanate, 0.05mmol dialkyne, and 50μL 100mM Cp^{CF3}CoCOD solution (in toluene-d8) were combined in a NMR tube and added toluene-d8 to make total volume to 500μL. Freeze-pump-thawed the tube three cycles, and sealed the tube by using propane torch. Took initial NMR. Heated the tube in 85^{o}C heating bath. Used the NMR technique to monitor the reaction and recorded the reaction time. After the reaction finished, the tube was cooled to ambient temperature and volatiles were removed under vacuum. The remaining residue was subjects to alumina column chromatography with 50% CH_2Cl_2/hexanes, followed by 100% CH_2Cl_2.

6a: white solid. Yield: 77.5%. ^{1}HNMR (400M, $CDCl_3$) δ0.961 (t, J = 7.6Hz, 3H), 1.771 (m, 2H), 3.886 (t, J = 7.6Hz, 2H), 4.859 (s, 2H), 4.868 (s, 2H), 6.413 (s, 1H), 7.187(s, 1H); ^{13}CNMR (400M, $CDCl_3$) δ11.310, 22.837, 51.994, 70.155, 71.854, 111.687, 118.770,

129.348, 154.410, 162.562; HRMS (Fab, M^+): $C_{10}H_{13}NO_2$ calcd 180.1025, found 180.1017; IR (neat) 3037, 2961, 1677, 1599, 1306 cm^{-1}; UV (CH_2Cl_2) λ_{max} = 319 nm (ε_{max} = 1236), 235 nm (ε_{max} = 1291).

6b: light yellow oil. Yield: 89.2%. ^{1}HNMR (300M, $CDCl_3$) δ0.937 (t, J = 7.5Hz, 3H), 1.734 (m, 2H), 3.338 (s, 2H), 3.406 (s, 2H), 3.752 (s, 6H), 3.819 (t, J = 7.5Hz, 2H), 6.397 (s, 1H), 7.095(s, 1H); ^{13}CNMR (300M, $CDCl_3$) δ11.455, 22.928, 36.885, 40.046, 51.765, 53.419, 60.871, 114.862, 118.971, 131.472, 154.823, 162.438, 171.130; HRMS (Fab, M^+): $C_{15}H_{19}NO_5$ calcd 294.1341, found 294.1347; IR (neat) 2961, 1737, 1676, 1594, 1265 cm^{-1}; UV (CH_2Cl_2) λ_{max} = 321 nm (ε_{max} = 1414), 238 nm (ε_{max} = 1763).

6c: white solid. Yield: 65.0%. ^{1}HNMR (300M, $CDCl_3$) δ2.034 (p, J = 7.2Hz, 2H), 2.689 (t, J = 7.2Hz, 2H), 2.780 (t, J = 7.2Hz, 2H), 6.473 (s, 1H), 7.120 (s, 1H), 7.344 (m, 3H), 7.431 (m, 2H); ^{13}CNMR (300M, $CDCl_3$) δ26.227, 28.912, 32.823, 115.021, 123.281, 126.893, 128.199, 129.342, 131.165, 141.848, 149.861, 160.442; HRMS (Fab, M^+): $C_{14}H_{13}NO$ calcd 212.1075, found 212.1064.

6d: slight yellow solid. Yield: 34.0%. ^{1}HNMR (300M, $CDCl_3$) δ1.750 (p, J = 3.6Hz, 4H), 2.536 (t, J = 3.6Hz, 2H), 2.686 (t, J = 3.6Hz, 2H), 6.400 (s, 1H), 7.063 (s, 1H), 7.377 (m, 3H), 7.476 (m, 2H); ^{13}CNMR (400M, $CDCl_3$) δ22.352, 22.949, 25.448, 29.154, 116.601, 118.846, 126.764, 128.363, 129.369, 135.100, 141.184, 152.836, 161.958; HRMS (Fab, M^+): $C_{15}H_{15}NO$ calcd 226.1232, found 226.1230.

2.3 Kinetics.

Experiments were conducted in silanized 5 mm NMR tubes that were sealed under vacuum using a propane torch. In a typical experiment, 0.25mmol propyl isocyanate (**3a**),

0.10mmol 1,4-dimethoxyl-2-butyne (**2a**), and 50μL 100mM Cp^{CF3}CoCOD solution (in toluene-d8) were combined in a NMR tube and added toluene-d8 to make total volume to 500μL. Freeze-pump-thawed the tube three cycles, and sealed the tube using propane torch. Took initial NMR. Heated the tube in 85^{o}C heating bath. Used the NMR technique to monitor the reaction for at least 7 data points over three half lives.

3. General Experimental for Chapter Three

All reactions and manipulation were conducted under a dry argon atmosphere using standard Schlenk techniques. Tris(dibenzyleneacetone) dipalladium(0) was purchased from Alfa Aesar. All other chemicals were obtained from Aldrich Chemical Company and used without further purification except other mention. Acetonitrile was distilled from CaH, CH_2Cl_2 came from the Mraun dry-solvent system. Milli-Q water was treated with diethylpyrocarbonate (depc) prior to use. ^{1}H, ^{13}CNMR and ^{31}PNMR data were recorded on either a Varian Mercury 300 or 400 MHz spectrometer. Chemical shifts were reported in parts per million (ppm) referenced to the ^{1}H resonance of the residual solvent proton signal or ^{13}C resonance of the deuterated solvent or with 85% aqueous phosphoric acid as external standard. Varian HPLC system was used for purification. Scintillation counting data was recorded on Beckman Coulter LS 6500 multi-purpose scintillation counter

Scanning electron Microscopy (SEM) was performed at Duke University with a Philips FEI XL 30 Thermal Field Emitter SEM operating at 5 kV accelerating voltage. A Zeiss Axioplan 2 upright microscope equipped with high-resolution optics (50X/0.9NA Epiplan-Apochromat, 100x/0.9NA Epiplan-Neofluar), Sutter Lambda LS Senon light source, Ludl Biopoint 2 motorized stage, Hamamatsu Orca ER CCD camera, Andor Ixon 8285 EMCCD cameram CRI MicroColor tunable color LCD filter, and IQ software from Andor Bioimaging was used for control of microscope and accessories, image analysis, 3D-rendering, and deconvolution.

3.1 Synthesis of 12-thioacetic 3,6,9-trioxadodecane-1-maleimide, 11

Tetra (ethylene glycol) monotosylate 8. 20mL (0.116mol) tetra (ethylene glycol), 8mL (0.5mol) anhydrous pyridine were dissolved in 40mL anhydrous CH_2Cl_2. The solution was added dropwise with a p-toluene sulfonyl chloride solution (3.82g (0.02mol) a p-toluene sulfonyl chloride dissolved in 20 mL CH_2Cl_2) for 2 hours. The mixture was stirred at room temperature for 20 hours. The reaction solution was washed with 2x 20mL cold water and 2x20mL brine. The aqueous solution was reextracted with 2x20mL CH_2Cl_2. And the combined organic layers were dried over magnesium sulfate. Evaporate solvent under vacuum. The residue was put on high vacuum line overnight. The crude product was used to the next step without further purification. 6.83g clear oil was obtained as final product with 98.1% yield. NMR data was consistent with reported data.

Tetra (ethylene glycol) monothioacetate 10. 2.18g (0.019mol) potassium thioacetate was dissolved into 60 mL anhydrous DMF. The solution was added dropwise a solution of Ts-PEG-4 (3.3273g $9.56*10^{-3}$ mol) in 20 mL anhydrous DMF. The mixture was stirred at room temperature for 1 hour and then heated at 85 °C for 6 hours. Cooled the mixture to ambient temperature. The DMF was pulled out through high vacuum line. The residue was dissolved with CH_2Cl_2 30 mL. The organic layer was washed with 2x 10mL cold water and 2x10mL brine. The aqueous layers were reextracted with 2x15mL CH_2Cl_2. The combined organic layers were dried over magnesium sulfate. Evaporate the solvent under reduced pressure. The residue was dried on high vacuum line overnight again. The residue was applied on a short silica gel column (2x15cm). First eluted with 200 mL CH_2Cl_2. Followed by 200 mL 3% CH_2 Cl_2 / CH_3OH to elute the desired pale brown band down. The solvent was evaporated under vacuum to give the pure compound as the organic oil. NMR showed

the product is fine. 1.514g red oil products were obtained to give 62.8% yield. NMR data was consistent with reported data.

12-Thioacetic-3,6,9,12-tetraoxadodecan-1-maleimide 11. 1.9g triphenyl phosphine (7.3 mmol) were dissolved in 50 mL anhydrous THF. The clear solution was cooled to -78°C with dry ice/acetone bath. 1.47g DIAD (1.41mL, 7.3 mmol) were added over 5 minutes. The resulting mixture was stirred for another 5 minutes. After that, 10 mL 0.8 M 12-Thioacetic-3,6,9,12-tetraoxadodecan-1-ol THF solution (2.0g 12-Thioacetic-3, 6,9,12-tetraoxadodecan-1-ol was dissolved in 10 mL anhydrous THF) was added dropwise. The wine-color mixture was stirred for 5 minutes and then 0.32g neopehtyl alcohol (3.7 mmol), and 0.71g maleimide (7.3 mmol) were added sequentially as solids. The final mixture was remained under -78°C for 10 minutes, and then the cooling bath was removed. The reaction was stirred overnight at room temperature. The resulting clear solution was concentrated to approximately 10 mL under vacuum, and then was applied to a silica gel column. The column was firstly eluted with 200 mL 75% diethyl ether/hexanes. After that, the wanted band was eluted down by 200 mL diethyl ether. Removed the diethyl ether in vacuo. 1.27g products were recovered as yellow oil with 54.1% yield. ^{1}HNMR (300M, $CDCl_3$): δ 2.332 (s, 3H), 3.083 (t, J = 6.6 Hz, 2H), 3.57-3.652 (m, 12H), 3.724 (t, J = 5.7, 2H), 6.698 (s, 2H). ^{13}CNMR (300M, $CDCl_3$): δ

3.2 Synthesis of *O*- [ω-Thioacetyl tetra (ethylene glycol)]-*O*- (5'-Guanosine) Monophosphate (TA-PEG$_4$-GMP) 17.

2-N,N-Dimethylaminomethylene-2',3'- O,O-isopropylene Guanosine 13. A solution of **12** (0.45g, 1.39 mmol) and dimethyl formamide diethyl acetal (0.75mL, 5.5 mmol) in anhydrous DMF (10mL)was stirred under Ar at 55 °C for 24 hours. The clear light yellow

solution was evaporated under reduced pressure. The remaining solid was stirred in 8 mL methol. The white solid precipitate was filtered and dry on the vacuum line for 5 hours. The white solid was used for next step with further purification. The 0.331g final products were obtained as white solid with 63% yield. NMR data was consistent with reported data.

2-Cyanoethyl-N,N-diisopropylamino-5'-(2-N,N-Dimethylaminomethylene-2',3'-O,O-isopropylene Guanosine) phosphoramidite 14. 250mg Compound **13** (0.66mmol) was suspended in 5 mL dry CH_2Cl_2. 0.5g dry diisopropylethylamine was added. The mixture was stirred in ice bath for 10 minutes. 253mg 2-Cyanoethyl-N,N-diisopropylamino chlorophosphoramidite (1.07mmol) was dissolved in 5 mL dry CH_2Cl_2 and cooled to 0 °C. Then the solution of 2 was added to the suspension of 1 dropwise through a syringe about 5 minutes. The mixture was stirred at 0 °C for 10 minutes and stirred at room temperature for another 2 hours. Make sure all solid was dissolved to get clear solution. After reaction was completed, the CH_2Cl_2 solution was diluted with 40 mL CH_2Cl_2 solution. The clear solution was extracted with cold water (2x 10mL) and 2x10mL brine. The combined aqueous solution was reextracted with 2x15mL CH_2Cl_2. The combined organic layers were dried over magnesium sulfate and filtered. Removing the solvent to get the slightly yellow residue. The residue was applied to column chromatography (silica gel). Wanted band was eluted with CH_2Cl_2 / TEA (95:5) to CH_2Cl_2 / MeOH/ TEA (90:5:5). The solvent was removed under vacuum to yield 282 mg white form solid with 73.9% yield. NMR data was consistent with reported data.

2-Cyanoethyl 5'-(2-N-dimethylaminomethylene-2'-O,3'-O-isopropylidend-guanosine) [ω-Thioacetyl tetra (ethylene glycol)] phosphate 15. In a 100mL round flask, 6 mL tetrazole solution (0.45M in dry ACN) was added. 139.6 mg Compound **10** was

dissolved in 5 mL anhydrous ACN, 187.3 mg Compound **14** was dissolved in 5 mL ACN. 4 mL Compound **10** solution was transfer into tetrazole solution. The mixture was stirred at room temperature. 5 mL Compound **14** solution was added to the mixture dropwise by using a syringe during 10 minutes. After the mixture was stirred at room temperature for about 2 hours. The remaining 1 mL compound **10** solution was added to the flask. Stirred another hour to finish the reaction. (Monitored the reaction by TLC) 0.66mL T-HYDRO® was added, the reaction was stirred at room temperature for 2 hours. After removing solvent, the residue was dissolved in 20 mL CH_2Cl_2. The white precipitate was filtered. The clear solution was washed with cold water (2x 5mL) and 2x5mL brine. The combined aqueous solution was reextracted with 2x10mL CH_2Cl_2. The combined organic layers were dried over magnesium sulfate. After removing the solvent, the residue was applied to column chromatography (silica gel) and eluted with CH_2Cl_2 / MeOH (95:5) to CH_2Cl_2 (90:10). Wanted bands were collected. The solvent was removed under vacuum to yield the product as clear stick oil. 183 mg final products were obtained with 76% yield. NMR data was consistent with reported data.

2-Cyanoethyl 5'-guanosine [ω-Thioacetyl tetra (ethylene glycol)] phosphate 16. 183 mg Compound **15** was dissolved in 10 mL 60% aqueous formic acid solution. The mixture was stirred at R.T. for 3 days. After evaporation of solvent under reduced pressure, the residue was coevaporated with methanol twice and then dried on the high vacuum line overnight. 163 mg clear sticky oil products were obtained as final products with 98% yield. The crude products were used for the next step without further purification. NMR data was consistent with reported data.

***O*- [ω-Thioacetyl tetra (ethylene glycol)]-*O*- (5'-Guanosine) Monophosphate (TA-PEG$_4$-GMP) 17.** 2-cyanoethyl 5'-Guanosine [ω-thioacetyl tetra(ethylene glycol)] Phosphate (160 mg, 0.25 mmol) was dissolved in 10 mL 1.0 M 1,8-diazabicyclo[5.4.0]undec-7-ene/dry acetonitrile solution. The mixture was stirred at room temperature for 2 hours. Then, the solvent was removed under vacuum. The residue was saturated in 0.1 M triethylammonium acetate solution, loaded onto a Hamilton PRP-3 HPLC column and eluted with [A: 0.1M triethylammonium acetate (PH = 7), B: Methanol] gradient from 0 to 70% over 60 minutes. The appropriate band was collected and evaporated to obtain the white foam solid (67 mg, 44.8%). ^{1}HNMR (300M, D_2O): δ 2.82 (m, 3H), 3.43 (s, 3H), 3.57-3.69 (m, 12H), 3.91 (m, 2H), 4.08 (m, 2H), 4.30 (s, 1H), 4.47 (t, J = 3.3, 1H), 5.90 (d, J = 5.7 Hz, 1H), 8.04 (s, 1H). ^{31}PNMR (300M, D_2O): δ1.33, 1.34.

3.3 Preparation of various modified PdRNA017

5'-Phosphorothioate-modified PdRNA017. 5'-Phosphorothioate-modified PdRNA017 was prepared by *in vitro* transcription. This transcription was carried out by combining 40 μL of 5X T7 Buffer, 8 μL of 5 mM ATP and CTP, 6 μL of 5 mM GTP, 2 μL of 20 mM pyridyl-modified UTP, 12 μL of 12.5 mM GMPS, 15 pmole dsPdDNA017 template, 2.5 μL of 10 μM T7 RNA polymerase and 4 μL RNAsin (40 u/λ). DEPC water was added to bring the total volume to 200 μL. The reaction mixture was incubated at 37 ˚C for 6 hours. The RNA product was purified using Microcon 10 with centrifuge technology.

TA-PEG$_4$-GMP-PdRNA017. TA-PEG$_4$-GMP-PdRNA017 was prepared by *in vitro* transcription. This transcription was carried out by combining 40 μL of 5X T7 Buffer, 8 μL of 5 mM ATP and CTP, 6 μL of 5 mM GTP, 2 μL of 20 mM pyridyl-modified UTP, 52.6 μL

of 5.7 mM TA-PEG_4-GMP, 15 pmole dsPdDNA017 template, 2.5 μL of 10 μM T7 RNA polymerase and 4 μL RNAsin (40 u/λ). DEPC water was added to bring the total volume to 200 μL. The reaction mixture was incubated at 37 ˚C for 6 hours. The RNA product was purified using Microcon 10 with centrifuge technology.

Radiolabeled TA-PEG_4-GMP-PdRNA017. Radiolabeled TA-PEG_4-GMP-PdRNA017 was prepared with the same transcription procedure. This transcription was carried out by combining 40 μL of 5X T7 Buffer, 8 μL of 5 mM ATP and CTP, 6 μL of 5 mM GTP, 2 μL of 20 mM pyridyl-modified UTP, 52.6 μL of 5.7 mM TA-PEG_4-GMP, 15 pmole dsPdDNA017 template, 2.5 μL of 10 μM T7 RNA polymerase, 4 μL RNAsin (40 u/λ) and 30 μCi α-[^{32}P]-ATP. DEPC water was added to bring the total volume to 200 μL. The reaction mixture was incubated at 37 ˚C for 6 hours. The RNA product was purified using Microcon 10 with centrifuge technology.

3.4 Preparation of gold slides for SEM and scintillation counting

Gold slides were treated with UV-ozonolysis for 20 minutes, and then stored in 100% ethanol waiting for next step.

For Compound 11 and 5'-phosphorothioate-modified PdRNA017: The cleaned gold slides were incubated in 1mM aqueous Compound **11** solution overnight at 4 ˚C, and then rinsed in 100% ethanol for 10 minutes. The slides were air-dried and soaked into 1μM 5'-phosphorothioate-modified PdRNA017 solution for 2-4 hour. The slides were then rinsed with depc water for 30 minutes before next step. The prepared slides was incubated with 400 μM $Pd_2(DBA)_3$ for 40 minutes. After that the slides were took out and rinsed with 50%

aqueous ethanol overnight. Then, the gold Slides were air-dried and ready for SEM examination.

For TA-PEG$_4$-GMP-PdRNA017: The aqueous solutions of 0.55 μM mercaptoethanol and various amount of TA-PEG$_4$-GMP-PdRNA017 (depend on the mol ratio required) were made firstly. The cleaned gold slides were incubated in these solutions overnight at 4 ˚C. The slides were then rinsed with depc water for 30 minutes before next step. The prepared slides was incubated with 400 μM $Pd_2(DBA)_3$ for 40 minutes. After that, the slides were took out and rinsed with 50% aqueous ethanol overnight. Then, the gold Slides were air-dried and ready for SEM examination.

For scintillation counting experiments: The aqueous solutions of 0.55 μM mercaptoethanol and various amount of radiolabeled TA-PEG$_4$-GMP-PdRNA017 (depend on the mol ratio required) were made firstly. Cleaned gold slides were put into petri dish, and then the different solutions were sprayed on the gold surface. After 30 minutes, the remaining solutions were wiped off carefully and the slides were rinsed three times for 30 minutes each time with depc water. Then, the gold Slides were air-dried and ready for scintillation counting experiments.

4. References

1) Eaton, E. B.; Fatland, A. W.; Sigman, M. S. *J. Am. Chem. Soc.* **1998**, *120*, 5130.

2) Robert S. Atikinson; Michael J. Grimshire *J. Chem. Soc. Perkin Trans. I* **1986,** *6,* 1215